



저작자표시-비영리-변경금지 2.0 대한민국

이용자는 아래의 조건을 따르는 경우에 한하여 자유롭게

- 이 저작물을 복제, 배포, 전송, 전시, 공연 및 방송할 수 있습니다.

다음과 같은 조건을 따라야 합니다:



저작자표시. 귀하는 원저작자를 표시하여야 합니다.



비영리. 귀하는 이 저작물을 영리 목적으로 이용할 수 없습니다.



변경금지. 귀하는 이 저작물을 개작, 변형 또는 가공할 수 없습니다.

- 귀하는, 이 저작물의 재이용이나 배포의 경우, 이 저작물에 적용된 이용허락조건을 명확하게 나타내어야 합니다.
- 저작권자로부터 별도의 허가를 받으면 이러한 조건들은 적용되지 않습니다.

저작권법에 따른 이용자의 권리는 위의 내용에 의하여 영향을 받지 않습니다.

이것은 [이용허락규약\(Legal Code\)](#)을 이해하기 쉽게 요약한 것입니다.

[Disclaimer](#)

Doctoral Thesis

Effective Cross-layer Designs for Stable Video
Streaming Service over Wireless Networks

Wan Kim (김 완)

Department of Computer Science and Engineering

Pohang University of Science and Technology

2015



무선 망에서 안정적인 영상 스트리밍
서비스를 위한 효과적인 크로스레이어
설계

**Effective Cross-layer Designs for Stable Video
Streaming Service over Wireless Networks**



Effective Cross-layer Designs for Stable Video Streaming Service over Wireless Networks

by

Wan Kim

Department of Computer Science and Engineering

Pohang University of Science and Technology

A thesis submitted to the faculty of the Pohang University of Science
and Technology in partial fulfillment of the requirements for the degree
of Doctor of Philosophy(Doctoral) in the Computer Science and
Engineering

Pohang, Korea

12. 04. 2014

Approved by

Hwangjun Song (Signature)

Academic Advisor



Effective Cross-layer Designs for Stable Video Streaming Service over Wireless Networks

Wan Kim

The undersigned have examined this thesis and hereby certify
that it is worthy of acceptance for a doctoral degree from
POSTECH

12. 04. 2014

Committee Chair	Hwangjun Song	(Seal)
Member	Sung Je Hong	(Seal)
Member	Young Joo Suh	(Seal)
Member	Joon Ho Cho	(Seal)
Member	Jangwoo Kim	(Seal)



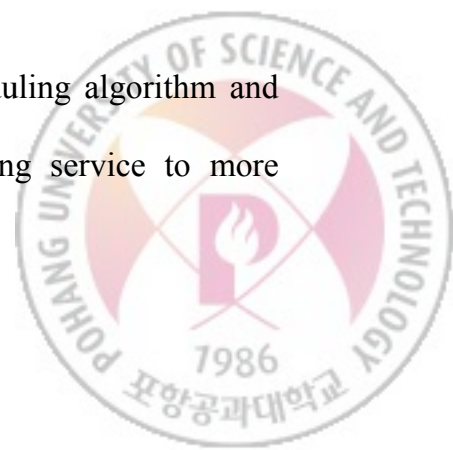
DCSE 김완, Wan Kim

200080322 Effective Cross-layer Designs for Stable Video Streaming Service over Wireless Networks, 무선 망에서 안정적인 영상 스트리밍 서비스를 위한 효과적인 크로스레이어 설계, Department of Computer Science and Engineering, 2015, 113p, Advisor: Hwangjun Song. Text in English

ABSTRACT

In this dissertation, we propose three cross-layer designs for stable video steaming service over wireless networks. First, we present an urgency-based packet scheduling and routing algorithms to effectively deliver delay-sensitive data over a multi-hop mobile ad hoc networks supporting IEEE 802.11b multi-rate service. In the proposed cross-layer design, packet urgency, node urgency, and route urgency are defined on the basis of the end-to-end delay requirement. Based on these urgency metrics and the estimated transmission delay of each packet by Kalman filter, the proposed packet scheduling algorithm determines the transmission order and drop policy to minimize the node urgency without unnecessary packet drop, and the proposed routing algorithm establishes a route to minimize the derivative of route urgency in order to maximize the number of packets delivered within the required end-to-end delay.

Second, we present a QoS-aware joint working packet scheduling algorithm and call admission control algorithm to support stable video streaming service to more



subscribers over WiMAX network. The proposed call admission control algorithm estimates the network throughput by using a local linear model in terms of a control parameter of the proposed scheduling algorithm, and performs its own functions based on the information. The proposed scheduling algorithm continuously updates the control parameter to pursue an effective tradeoff between the quality-of-service of video streaming and the network throughput.

Third, we propose a QoE-based interworking packet scheduling, call admission control, and handover system to provide a seamless video streaming services over LTE network. The proposed packet scheduling algorithm allocates wireless resources to admitted UEs while considering the QoE states of UEs and cell and wireless link states of UEs simultaneously. The proposed call admission control algorithm estimates the cell availability at the next call arriving time based on the current QoE states of UEs to determine the admission of a new UE. The proposed handover algorithm determines the appropriate handover trigger timing to keep a balance of the QoE states among immediately adjacent cells on the basis of both the cell availability and wireless link states.



Contents

I. Introduction	1
II. Background	4
II.1. IEEE 802.11b Multi-rate Service	4
II.2. WiMAX (IEEE 802.16e) Network	5
II.2.1 Scheduling Service Class	6
II.2.2 Physical Layer	7
II.2.3 MAC Layer	8
II.3. LTE (Long Term Evolution) Network	10
II.3.1 Radio Bearer Management	11
II.3.2 Physical and MAC Layers	12
II.3.3 Radio Resource Management	14
II.4. Related Works	14
III. Urgency-based Packet Scheduling and Routing Algorithms for Delay-sensitive Data over MANETs	22
III.1. Proposed Urgency and Link Condition-based Packet Scheduling Algorithm	25
III.1.1 Transmission Delay Estimation over IEEE 802.11b Multi-rate Service	26
III.1.2 Proposed Packet Transmission Order Determination	28
III.2. Proposed Urgency-based Routing Algorithm	31
III.2.1 Route Construction Mechanism	32
III.2.2 Dynamic Route Maintenance Mechanism	35
III.3. Performance Evaluation	37
III.3.1 Test of Urgency Mapping Functions	38



III.3.2	Performance Comparison with respect to End-to-End QoS Metrics	41
III.3.3	Performance Comparison with respect to Proposed Urgency Metrics	45
III.3.4	Performance Comparison with respect to Achievable Video Quality	48
IV.	QoS-aware Joint Working Packet Scheduling and Call Admission Control for Video Streaming Services over WiMAX network	52
IV.1.	Video Metadata Structure	54
IV.2.	Proposed λ -based Call Admission Control Algorithm	56
IV.3.	Proposed Video Metadata and Link Condition-aware Packet Scheduling Algorithm	59
IV.4.	Performance Evaluation	62
IV.4.1	Performance Verification of Network Throughput Estimation Model	64
IV.4.2	Performance Verification of λ Adjustment Algorithm	68
IV.4.3	Performance Comparison with Existing Algorithms	71
V.	QoE-based Interworking Packet Scheduling, Call Admission Control, and Handover System for Video Streaming Services over LTE network	73
V.1.	Proposed Packet Scheduling Algorithm	77
V.2.	Proposed Call Admission Control Algorithm	79
V.3.	Proposed Handover Algorithm	81
V.4.	Performance Evaluation	84
V.4.1	Performance Verification of the Proposed Packet Scheduling Algorithm and Comparison with Existing Algorithms in Single Cell	85
V.4.2	Performance Verification of the Proposed Call Admission	



Control and Handover Algorithms	90
V.4.3 Performance Comparison with Existing Algorithms in Multiple Cells	94
VI. Conclusions	99
REFERENCES	104



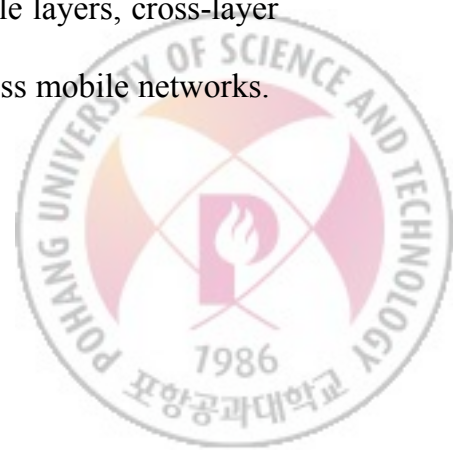
I. Introduction

Wireless network access technologies have been quickly developed to support various mobile data service requirements. The cellular link speed has increased to approximately 2 Mbps for 3G network, and 100 Mbps for 4G including LTE (Long Term Evolution) [1,2] and WiMAX (IEEE 802.16e) [3] networks by taking advantage of wideband dynamic spectrum allocation [4], now B4G (beyond 4G) and 5G networks are currently under development. Similarly, short-range WiFi (IEEE 802.11) radio speed has increased from 11 Mbps to 300 Mbps. Mobile data services are already widely deployed over internet and currently increasing growth due to popularity of application on smart device OS (Operating System) including iOS, Android, and Window Phone OS. According to a forecast of the authoritative industry report [5], mobile video streaming services will account for approximately 66.5 % of network traffic by 2017. Although the state of the art technologies are capable of supporting high data rates, it is still a challenging problem to provide diverse mobile data service of high quality over wireless network. In particular, it is difficult to support seamless high-quality mobile video



streaming services through wireless network because a large amount of data is required compared to data required by other mobile data services including text and images. Video streaming services are also strictly time-constrained whereas wireless channels are inherently time-varying. Furthermore, bit rates of video data are generally more variable due to generic characteristics of the entropy coder, scene changes, and inconsistent motion changes of the underlying video. These facts make the problem extremely challenging.

To make effective use of limited wireless resources with supporting seamless high-quality video streaming services, resource management algorithms such as routing, packet scheduling, call admission control, and handover algorithms play an instrumental role in wireless network. The routing algorithm establishes a route between a source node and a destination node via other participating nodes. In the packet scheduling algorithm, the scheduler determines which packets will be transmitted to the next scheduling interval. The call admission control algorithm decides whether to accept or not the new service requests by considering a wireless network capacity in a cell. Finally, the handover algorithm ensures the user is freely transferred among adjacent cells while remaining connected. Nowadays, cross-layer designed video streaming technology has been widely studied to provide seamless video streaming services and enhance streaming video quality with minimal redundancy over time-varying wireless networks. By sharing information among layers and/or jointly determining control parameters at multiple layers, cross-layer technology can efficiently deal with the uncertainty inherent in wireless mobile networks.



In this dissertation, we propose three cross-layer designs to provide stable video streaming service over wireless networks. First, we propose urgency-based joint working packet scheduling and routing algorithms for delay-sensitive data transmission over multi-rate MANETs. A unique feature of the proposed joint working algorithms is that the packet scheduling algorithm at the MAC layer and the routing algorithm at the network layer are tightly coupled on the basis of the urgency metrics to effectively deliver delay-sensitive data over multi-rate MANETs. Second, we propose a joint working packet scheduling algorithm and call admission control algorithm for stable video streaming service with a high network efficiency over WiMAX network. One of the unique features of the proposed system is that the proposed call admission control algorithm estimates the network throughput based on a control parameter of the proposed scheduling algorithm. It is constantly adjusted to achieve an effective tradeoff between the video quality of subscribers and the network throughput. Third, we propose a highly efficient interworking packet scheduling, call admission control, and handover system for seamless video streaming service over LTE network. The proposed packet scheduling, call admission control, and handover algorithms are tightly coupled on the QoE (Quality of Experience) state information to effectively improve QoE of all admitted UEs and utilize the limited and time-varying wireless network resources in multiple cells over LTE network.

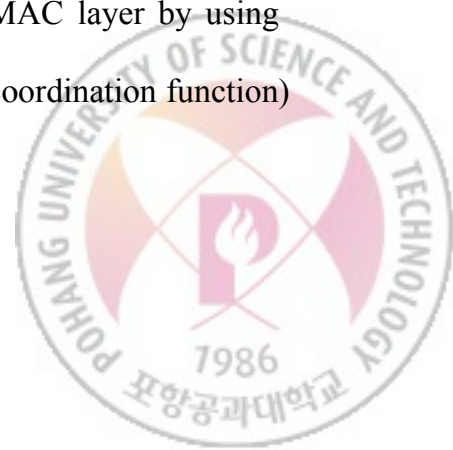


II. Background

We give a brief review of wireless network access technologies and the research literature about resource management algorithms over wireless networks. IEEE 802.11b multi-rate service, WiMAX (IEEE 802.16e) network, LTE network, and related works are presented in Section 2.1, 2.2, 2.3 and 2.4, respectively.

2.1 IEEE 802.11b Multi-rate Service

WLAN is becoming increasingly popular and IEEE 802.11 standards are widely employed as the wireless MAC protocol. IEEE 802.11 standard series are classified into several categories such as IEEE 802.11a/b/g/e/n. IEEE 802.11a/g [6,7] are developed to increase the maximum raw data rate. IEEE 802.11e [8] defines QoS (Quality of Service) enhancements for WLAN application through modifications to the MAC layer by using EDCA (Enhanced Distributed Channel Access) and HCCA ((Hybrid coordination function)

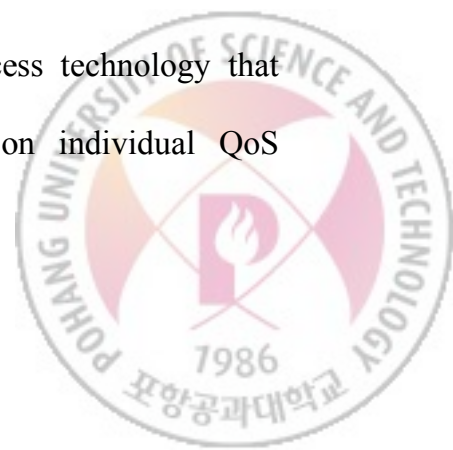


Controlled Channel Access) mechanisms, and IEEE 802.11n [9] employs MIMO (Multiple-Input Multiple-Output) technique to improve network throughput.

In this section, we briefly study IEEE 802.11b multi-rate wireless channel model. In the case of IEEE 802.11b, multi-rate service is provided by changing the modulation scheme based on the RSS (Received Signal Strength) at the receiver. That is, nodes select their modulation scheme according to the observed RSS, which must be higher than threshold RSS required for each modulation scheme. For example, the IEEE 802.11b standard provides data rates of up to 11 Mbps [10,11]: CCK (Complementary Code Keying) for 11 and 5.5 Mbps, DQPSK (Differential Quaternary Phase Shift Keying) for 2 Mbps, and DBPSK (Differential Binary Phase Shift Keying) for 1 Mbps. In mobile wireless networks, large-scale path loss, small-scale fading and multi-path, and interference cause random variations in the RSS. Generally, a node can increase the RSS by boosting the transmission power strength. And, IEEE 802.11b standard includes the carrier sensing mechanism to avoid interference; the PHY layer samples the received energy over the medium transmitting data and uses a clear channel assessment algorithm to determine if the channel is clear or not based on the RSS.

2.2 WiMAX (IEEE 802.16e) Network

WiMAX network are an emerging standard for wireless access technology that provides high data rates and differentiated services depending on individual QoS



requirements over a wide area. It supports not only all IP-based architecture, but also scalable bandwidth using AMC (Adaptive Modulation and Coding). Now, we give a brief introduction to the scheduling service classes, physical layer and MAC layer of WiMAX network.

2.2.1 Scheduling Service Class

WiMAX network define five scheduling service class types to support different applications with a wide range of QoS requirements. Every flow over WiMAX network should be mapped to a scheduling service class based on its QoS parameters. The scheduling service classes in the WiMAX standard are described below.

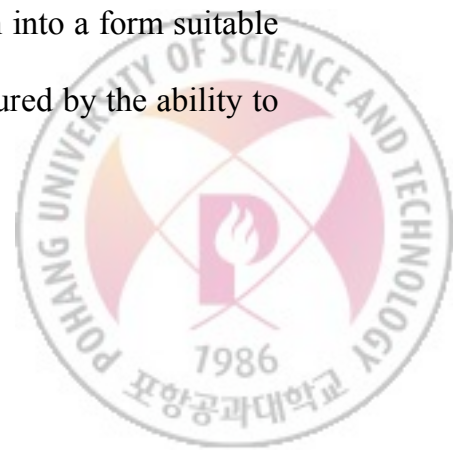
- (1) UGS (Unsolicited Grant Service): This class is suitable for real-time applications with stringent delay constraints which transmit fixed size data packets periodically. T1/E1 and VoIP without silence suppression are typical examples of this class.
- (2) ertPS (Extended real-time Polling Service): This class supports real-time applications which generate variable size data packets and need to guarantee strict delay requirements. VoIP with silence suppression belongs to this class, which is a combination of UGS and rtPS classes.
- (3) rtPS (Real-time Polling Service): Real-time applications which have low delay requirements and generate variable size data packets periodically best fit in this class. A typical application in this class is the MPEG video service.



- (4) nrtPS (Non-real-time Polling Service): This class is proper for applications which require tolerant delay constraints and a minimum data rate and generate variable size data packets. FTP service belongs to this nrtPS service class.
- (5) BE (Best Effort): This class is suitable for applications without special QoS requirements. Web services such as HTTP service, belong to this class.

2.2.2 Physical Layer

WiMAX network support several transmission modes at the physical layer, i.e. SC (Single Carrier) mode, OFDM (Orthogonal Frequency Division Multiplex) mode, and OFDMA (Orthogonal Frequency Division Multiple Access) mode. In the OFDM system, FEC (Forward Error Correction) coding is applied to the transmitted data stream to increase error resilience (i.e. more robust FEC coding provides stronger error protection). RS (Reed Solomon) concatenated with CC (Convolutional Code) coding is mandatory for all WiMAX network implementations. The standard optionally supports CTC (Convolutional Turbo Code) and LDPC (Low-Density Parity Check) codes. Then the resulting data stream is divided into multiple parallel low rate data streams. Each low rate data stream is mapped to an individual data subcarrier and modulated using some sort of PSK (Phase Shift Keying) or QAM (Quadrature Amplitude Modulation) such as BPSK (Binary Phase Shift Keying), QPSK (Quadrature Phase Shift Keying), 16QAM, and 64QAM. In fact, modulation is the process of translating a data stream into a form suitable for transmission on the physical medium, and its performance is measured by the ability to



preserve the accuracy of the encoded data. Modulation and coding rate combinations of WiMAX OFDMA are given in Table 2-1.

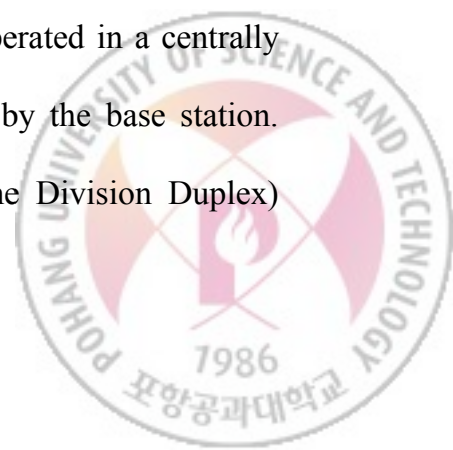
Subcarriers are distributed into several groups, which are called sub-channels. Sub-channels may be configured by using adjacent subcarriers or pseudo-randomly distributed subcarriers over the frequency spectrum. Sub-channels formed by using pseudo-randomly distributed subcarriers provide improved frequency diversity and are particularly useful for mobile applications.

Table 2-1 Modulation and coding rate combinations of WiMAX OFDMA.

<i>Modulation</i>	<i>Overall Coding Rate</i>	<i>CC Code Rate</i>	<i>RS Code</i>
64QAM	3/4	5/6	(90, 82, 4)
64QAM	2/3	3/4	(81, 72, 4)
16QAM	3/4	5/6	(60, 54, 3)
16QAM	1/2	2/3	(48, 36, 6)
QPSK	3/4	5/6	(30, 26, 2)
QPSK	1/2	2/3	(24, 18, 3)

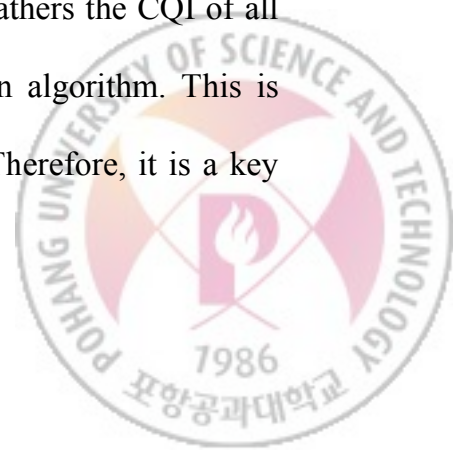
2.2.3 MAC Layer

In general, MAC, which is a sub-layer of the Data Link layer, supports the addressing and channel access control mechanisms for network nodes or terminals to communicate within a network. The MAC of WiMAX network is operated in a centrally controlled manner, i.e. resource allocation is dynamically managed by the base station. Figure 2-1 illustrates the OFDMA frame structure in a TDD (Time Division Duplex)



implementation. The medium is divided into continuous MAC frames in time and sub-channels. Each MAC frame is configured by DL (DownLink) and UL (UpLink) sub-frames. At the beginning of each MAC frame, the base station transmits the DL Map and the UL Map into the DL sub-frame. These maps provide resource allocation and other control information for the DL and UL sub-frames, respectively. And the subscriber periodically reports CQI (Channel Quality Indicator) information, which contains its wireless channel status into the CQICH in the UL sub-frame. In each frame, the TTG (Tx/Rx Transmission Gap) and the RTG (Rx/Tx Transmission Gap) are inserted between the DL and UL sub-frames, which are time gaps between transmission and reception.

The minimum resource allocation unit is called a slot, which is configured by one sub-channel over one, two, or three OFDM symbols depending on the subcarrier permutation scheme. A burst is a contiguous series of slots assigned to a given subscriber and different MCSs (Modulation and Coding Schemes) can be applied to it. The slot transmission rate is dependent on the associated MCS and a tradeoff exists between link robustness and throughput. In other words, the BER (Bit Error Rate) performance is improved at the cost of network throughput efficiency as the modulation becomes sparser and the coding rate becomes lower. In contrast, denser modulation and a higher coding rate provide higher data rates on the slot and increase sensibility against wireless channel error. WiMAX system is able to control the MCS of each subscriber according to the wireless channel status in order to improve resource utilization. Base station gathers the CQI of all subscribers, then decides on an MCS for each subscriber using own algorithm. This is critical to improve the overall performance of the WiMAX system. Therefore, it is a key



issue how many slots are allocated to each user based on the determined MCS. This means that the need for efficient call admission control algorithm and packet scheduling algorithm is essential.

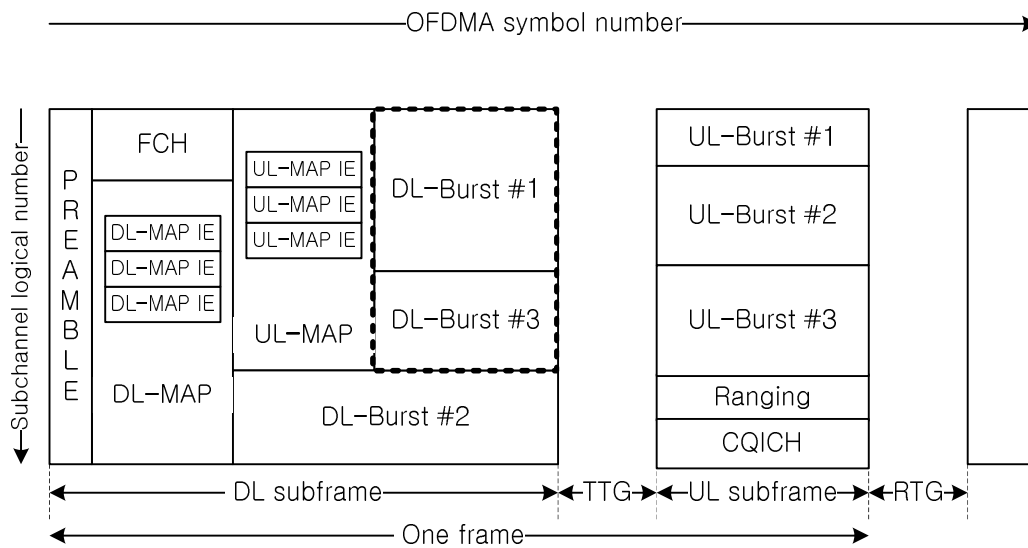
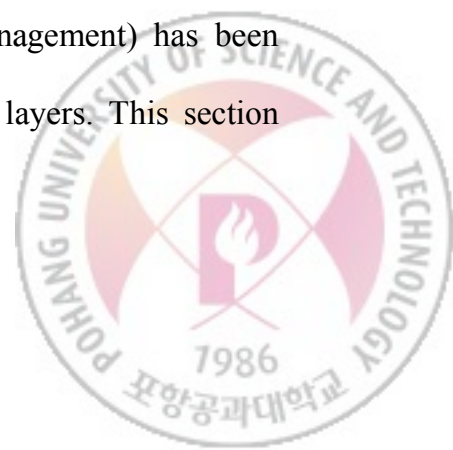


Figure 2-1 OFDMA frame structure in TDD implementation.

2.3 LTE (Long Term Evolution) Network

LTE network provide high peak data rates, support for high user mobility, improved cell edge throughput, enhanced support for end-to-end QoS, meaningful reduction of control plane latency, less than 5 ms user plane latency, and scalable bandwidth from 1.25 to 20 MHz. To fulfill these goals, the RRM (Radio Resource Management) has been designed to support advanced functionalities of MAC and physical layers. This section gives overview of the main LTE features.



2.3.1 Radio Bearer Management

LTE specifications introduce a bearer which is a logical flow established between UE (User Equipment) and eNodeB. The bearer is responsible for managing QoS provision. Depending on QoS requirements, it can be further classified as GBR (Guaranteed Bit-Rate) or Non-GBR (Non-Guaranteed Bit-Rate) bearers. To satisfy QoS requirements, several classes of QoS services have been identified through QCI (QoS Class Identifiers). As comprehensively shown in Table 2-2, each QoS class is characterized by its resource type, a priority level, the maximum packet delay budget, and the packet loss rate. The RRM (Radio Resource Management) interprets the QoS parameters into packet scheduling parameter, admission criterion, handover decision criterion, bearer queue management parameter, and so on.

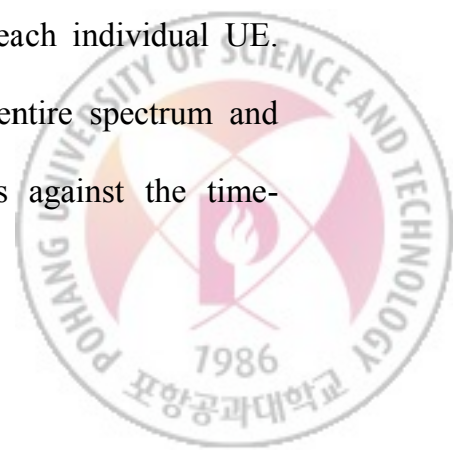


Table 2-2 Standardized QoS Class Identifiers for LTE.

<i>QCI</i>	<i>Resource Type</i>	<i>Priority Level</i>	<i>Packet Delay Budget [ms]</i>	<i>Packet Loss Rate</i>	<i>Example Service</i>
1	GBR	2	100	10^{-2}	Conversational Voice
2	GBR	4	150	10^{-3}	Conversational Video (live streaming)
3	GBR	5	300	10^{-6}	Non-Conversational Video (buffered streaming)
4	GBR	3	50	10^{-3}	Real Time Gaming
5	Non-GBR	1	100	10^{-6}	IMS Signalling
6	Non-GBR	7	100	10^{-3}	Voice, Video (live streaming), Interactive Gaming
7	Non-GBR	6	300	10^{-6}	Video (buffered streaming)
8	Non-GBR	8	300	10^{-6}	FTP, P2P File Sharing
9	Non-GBR	9	300	10^{-6}	

2.3.2 Physical and MAC Layers

The physical layer of LTE network has been designed as a flexible radio access technology so as to support several system bandwidth configurations from 1.4 MHz up to 20 MHz. In the radio spectrum access, OFDMA and SC-FDMA (Single Carrier Frequency Division Multiple Access) are used in downlink and uplink directions, respectively. These scheme allow multiple access by assigning sets of sub-carriers to each individual UE. OFDMA is able to use several sub-carriers distributed inside the entire spectrum and provide high scalability, simple equalization, and high robustness against the time-



frequency selective nature of radio channel fading. On the other hand, SC-FDMA can exploit only adjacent sub-carriers and increase the power efficiency of UEs.

The RB (Resource Block) which is the minimum resource allocation unit to be assigned to an UE for data transmission in the LTE network. It is comprised of a time/frequency radio resource spanning over two time slots in the time domain and over one sub-channel in the frequency domain. In the time domain, it is distributed every TTI (Transmission Time Interval), each one lasting 1 ms. Each TTI is made of two time slots with length 0.5 ms, corresponding to 7 OFDM symbols in the default configuration with short cyclic prefix. The frame composed of 10 consecutive TTIs. In the frequency domain, the whole bandwidth is divided in sub-channels, each one with 12 consecutive OFDM sub-carriers. When the sub-channel size is fixed, the number of RBs varies according to the total bandwidth configuration.

The two types of frame structure are supported LTE radio interface according to different duplexing schemes that are TDD and FDD (Frequency Division Duplex). Under TDD, the LTE frame is divided into two consecutive half-frames. Several frame configurations allow different ratio of resources dedicated for downlink or uplink transmission. For FDD, instead, the whole bandwidth is divided in two parts for allowing simultaneous downlink and uplink data transmissions. In this case, the LTE frame is composed of 10 consecutive identical sub-frames.

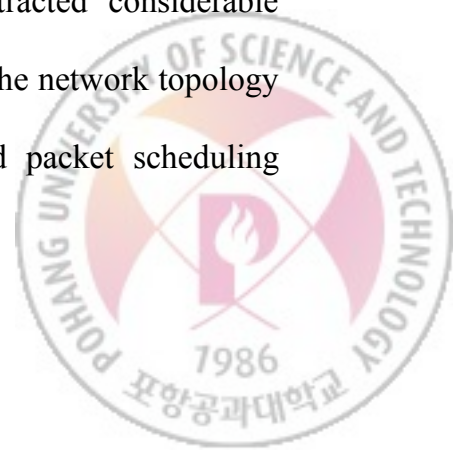


2.3.3 Radio Resource Management

LTE provide RRM procedures such as the CQI reporting, link adaptation through AMC, and HARQ to improve the usage of available radio resources. The CQI reporting is a fundamental feature of LTE network because it is able to estimate the quality of the downlink channel between a UE and the eNodeB. Each CQI is calculated by using the experienced SINR (Signal to Interference plus Noise Ratio). The CQI reporting is strictly connected with the AMC module, which selects the proper MCS trying to maximize the supported throughput with a given target BLER (Block Error Rate). The HARQ (Hybrid Automatic Repeat reQuest) is the retransmission procedure at MAC layer, based on the use of the well-known stop-and-wait algorithm. This retransmission procedure is simply performed by UE and eNodeB through the exchange of ACK (ACKnowledge) and NACK (Negative ACKnowledge) messages. When a packet transmitted by the eNodeB is not successfully decoded at the UE, a NACK is transferred over the PUCCH (Physical Uplink Control Channel). In this case, the eNodeB will conduct a previous packet retransmission. Then, the UE will send an ACK message to the eNodeB upon a successfully decoding.

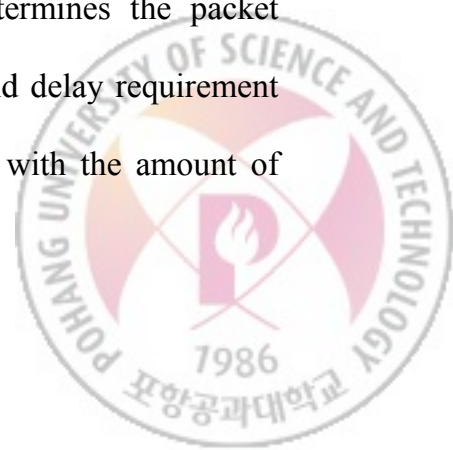
2.4 Related Works

MANETs (Mobile Ad hoc NETWORKs) technology has attracted considerable interest because nodes can self-configure and dynamically maintain the network topology without the infrastructural support. Some remarkable routing and packet scheduling



algorithms have been proposed to support seamless multimedia services over MANETs. In general, ad hoc routing protocols are categorized into three types: table-driven, on-demand, and hybrid. Table-driven protocols are essentially proactive because each node maintains an up-to-date routing table by periodically exchanging routing information. Therefore, the delay in constructing a route is negligible because the route is already known when data packets are forwarded. However, a large amount of network resources is required to maintain the latest routing information. DSDV (Destination-Sequenced Distance-Vector) [12], OLSR (Optimized Link State Routing) [13], CGSR (Cluster-head Gateway Switch Routing) [14], and WRP (Wireless Routing Protocol) [15] are examples of table-driven protocols. In contrast, on-demand protocols are fundamentally reactive, because nodes invoke the route construction mechanism only when a route is needed. Thus, the delay until the route is established may be slightly longer. Examples of on-demand protocols include DSR (Dynamic Source Routing) [16], AODV (Ad hoc On-demand Distance Vector) [17], TORA (Temporally-Ordered Routing Algorithm) [18], and CBRP (Cluster-Based Routing Protocol) [19]. Hybrid protocols combine the advantages of table-driven and on-demand protocols. For example, ZRP (Zone Routing Protocol) [20] proactively maintains topology and link state information within the routing zone and reactively searches for routes beyond the routing zone.

A packet scheduling algorithm determines the transmission order and drop policy at each node. An EDF (Earliest Deadline First) scheduler [21] determines the packet transmission order by considering the arrival time and the end-to-end delay requirement of each packet. The transmission priority of each packet increases with the amount of

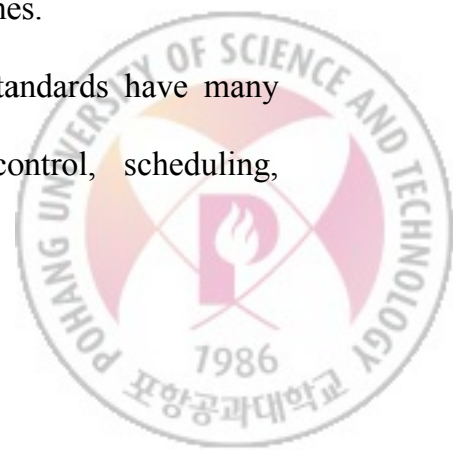


time consumed over the network. In a CMS (Coordinated Multi-hop Scheduling) scheduler [22], the transmission priority of a packet at each node is recursively expressed using the transmission priority of the same packet at the previous node along the route. A node will increase the transmission priority of a packet if an excessive delay occurs. Conversely, if a small delay occurs, the node will decrease the transmission priority of a packet in order to serve more urgent packets. In [23], the proposed scheduler is designed to mitigate interference and improve network capacity over wireless mesh networks. The scheduler determines the sets of flows along which transmissions can take place with the least inter-flow interference based on received signal strength. In the drop-tail policy [24], nodes simply drop newly arriving packets if the buffer is full. However, the drop-tail policy leads to a high packet loss rate, a long queuing delay, low utilization of network resources, and long-lasting congestion under a heavy traffic load. Active packet drop policies such as RED (Random Early Detection) [25], BLUE [26], SRED (Stabilized Random Early Drop) [27], and DRED (Dynamic Random Early Detection) [28] have been proposed to solve these problems. Typically, they operate by maintaining drop/mark probabilities and probabilistically dropping or marking packets before the buffer becomes full. The RED algorithm detects congestion and measures the traffic load level in the buffer using the average buffer size. BLUE uses the instantaneous buffer length and link utilization as indicators of traffic load and congestion. SRED and DRED are more effective in stabilizing the buffer size and controlling the packet loss rate while maintaining high link utilization.



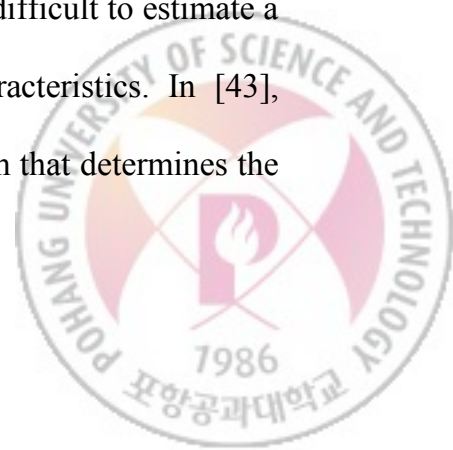
In recent years, many considerable efforts have been focused on a cross-layer approach to effectively utilize the limited and time-varying wireless network resources. In [29], joint scheduling and power control algorithms are proposed to limit multi-user interference and reduce the power consumption over a single hop. QAR (QoS-Aware Routing) [30] incorporates the admission control scheme and the feedback scheme to determine a route satisfying the bandwidth requirement. In [31], Liang et al. optimizes a lifetime-distance factor that represents the relative weights assigned to the remaining distance and the remaining lifetime of a packet in order to determine its transmission priority over multi-hop wireless networks. A novel software solution between the 802.11 MAC and network layers (Layer 2.5 SoftMAC [32]) is proposed for coordinating the real-time and best-effort packet transmission among neighbouring nodes over multi-hop wireless networks. Several effective rate control algorithms at the MAC (Medium Access Control) layer are proposed by considering the time-varying wireless link states [33,34,35]. Recently, multi-rate based routing algorithms have been proposed in [36,37]. These routing algorithms determine a route with a higher throughput and lower delay although hop count increases. IEEE 802.11 standards are widely employed as the wireless MAC protocol, which supports multi-rate service by changing the modulation scheme and coding rate based on the received signal strength at the receiver. IEEE 802.11b and IEEE 802.11g provide data rates of up to 11 Mbps and 54 Mbps, respectively. Higher data rates are commonly achieved by selecting more efficient modulation schemes.

WiMAX (IEEE 802.16e) and LTE (Long Term Evolution) standards have many advanced functions including traffic classification, admission control, scheduling,



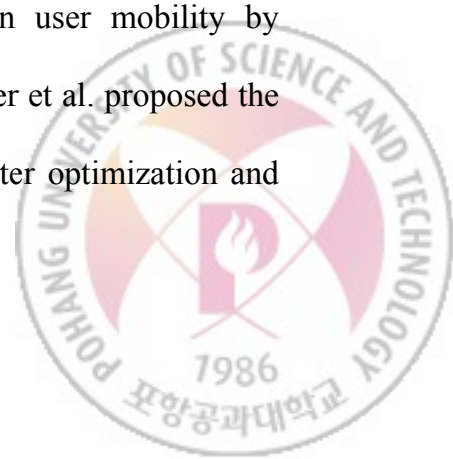
handover, and MCS (Modulation and Coding Scheme) decision to meet QoS requirements. Various packet scheduling, call admission control, and handover algorithms have been proposed to effectively handle time-varying wireless channel/network conditions. In packet scheduling algorithms, the MAX SNR (Signal-to-Noise Ratio) selects the user with the best wireless link state so that it can maximize the instant network throughput. The PF (Proportional Fair) [38] approach not only takes the instantaneous wireless link states into account, but also looks at the long-term average wireless link states to maximize long-term throughput. However, neither the MAX SNR nor PF guarantee QoS. On the other hand, some packet scheduling algorithms have been presented that focus on QoS problems. In the MLWDF (Modified Largest Weighted Delay First) [39] and EXP (Exponential rule) [40], they consider the wireless link states of users, and in addition they analyze the tolerable maximum queueing delay at the base station to support a QoS. The EXP provides a stricter QoS than the MLWDF by using an exponential function to keep the queueing delay below a pre-determined maximum delay. In A-DTPQ (Adaptive Delay Threshold-based Priority Queueing) [41], it adaptively controls the tolerable maximum delay; wireless network resources are not allocated to real-time services when their delay is even less than the maximum delay.

To simultaneously account for QoS and network utilization in a cell, a call admission control algorithm need to consider not only the traffic characteristics, but also the time-varying wireless network capacity [42]. However, it is very difficult to estimate a wireless network capacity due to time-varying wireless link characteristics. In [43], Niyato et al. proposed a queue-aware call admission control algorithm that determines the



connection acceptance probability based on a queueing model. In [44], Jeong et al. presented a call admission control algorithm considering the network capacity in a cell and the current network load simultaneously. In [45], Sohn et al. proposed an adaptive admission control algorithm that estimates the number of supporting users per OFDM frame based on bit error rate, average channel gain, and data rate requirements of every user. In [46], the admission control algorithm is proposed based on the characteristics of data delivery services to support adaptive multimedia service. In [47], Lee et al. proposed a statistical connection admission control for mobile WiMAX systems that works based on the SNR values of users and traffic parameters. In [48], Qian et al. proposed a novel radio admission control to optimize system capacity with supporting QoS of each service class by combining complete sharing and virtual partitioning resource allocation model.

Efficient handover algorithms have also been researched. In [49], Aziz et al. proposed a simple ICIC (Inter Cell Interference Coordination) scheme for determining an optimized handover parameter to avoid the radio link failure while maintaining low handover rates. In [50], Jansen et al. proposed the handover optimization algorithm to automatically control the values of the handover parameters such as hysteresis and time-to-trigger for improving overall network utilization. In [51], Legg et al. proposed an intra-frequency handover by analyzing the influence of handover parameters according to different user mobility. In [52], Kitagawa et al. proposed a self-optimization algorithm for handover parameters to support robustness against the change in user mobility by adjusting handover margin according to user speeds. In [53], Lobinger et al. proposed the coordination system for self-optimization between handover parameter optimization and



load balancing to improve system performance. In [54], Munoz et al. proposed the optimization system of the handover procedure which pursues an effective tradeoff between QoS of users in the cell and the amount of signaling load as a result of handovers.

A large number of cross-layer optimization techniques have been studied in the research literature to provide a seamless video streaming service over wireless network. In [55], Haghan et al. proposed a multilevel service classification based on video frame type information in order to enhance the QoS of video streaming service. In [56], Deb et al. proposed a scheduling algorithm for video multicast that combines adaptive modulation and coding with scalable video effectively to improve video quality. The proposed algorithm ensures the efficient, fair, and timely delivery of video streaming service considering wireless channel state of subscribers and video codec information. In [57], Jeon et al. proposed a combined packet scheduling algorithm and CAC algorithm based on a statistical approach to handle both real-time service and non-real-time service. The proposed packet scheduler gives higher priority to only the real-time service packets that are close to the deadline. CAC algorithm controls the network input load based on the network congestion level. The empty ratio of video buffer is adopted as the quality measure of video streaming services and the condition of network congestion. In [58], Navarro-Ortiz et al. proposed a QoE-aware packet scheduling algorithm to avoid playback interruptions using estimation of the amount of video data stored in the player buffer by video encoding rate of the application layer. In [59], Karachontzitis et al. proposed a novel cross-layer scheme for packet scheduler to support video transmission



constraints requirement obtained from video data structure information of application layer.



III. Urgency-based Packet Scheduling and Routing Algorithms for Delay- sensitive Data over MANETs

Our objective is to deliver delay-sensitive data packets as many as possible within the end-to-end delay requirement and to distribute the traffic load across the entire network simultaneously over a multi-hop MANETs supporting IEEE 802.11b multi-rate service. To achieve this objective, urgency metrics are defined by considering the end-to-end delay requirement.

Definition of Packet Urgency: The packet urgency ($u_{pkt}(t)$) at the j_{th} node along a route (\vec{R}) at time t is defined as

$$u_{pkt}(t) = f_{urg} \left(\frac{d_{residual}(t)}{D_{max}} \right),$$

(3-1)



where $d_{residual}(t) = D_{max} - d_{acc}^j(t)$,

where D_{max} is the maximum tolerable end-to-end delay, $d_{acc}^j(t)$ is the cumulative delay from the source node to the j_{th} node, $d_{residual}(t)$ is the residual delay to satisfy the end-to-end delay requirement over the remaining hops, and $f_{urg}\left(\frac{d_{residual}(t)}{D_{max}}\right)$ is the urgency mapping function between $d_{residual}(t)$ and $u_{pkt}(t)$. In general, $u_{pkt}(t)$ should be inversely proportional to $d_{residual}(t)$ (i.e., a packet with a smaller $d_{residual}(t)$ should be transmitted more urgently for delivery to the destination node in time) [60].

Definition of Node Urgency: The node urgency ($u_{node}(t)$) is defined as the sum of packet urgency of all the packets in the buffer, i.e.,

$$u_{node}(t) = \sum_{i=1}^{n_{pkt}} u_{pkt(i)}(t), \quad (3-2)$$

where n_{pkt} is the number of packets in the buffer and $u_{pkt(i)}(t)$ is the packet urgency of the i_{th} packet in the buffer. A larger node urgency implies that more urgent packets are in the buffer.

Definition of Route Urgency: The route urgency ($u_{route}(t)$) is defined as the sum of node urgency of all the nodes along \vec{R} , i.e.,



$$u_{route}(t) = \sum_{j \in \vec{R}} u_{node(j)}(t), \quad (3-3)$$

where \vec{R} denotes the route including all intermediate nodes and $u_{node(j)}(t)$ is the node urgency of the j_{th} node along the route. As the route urgency increases, it may become a congestion route.

The overall architecture of the proposed cross-layer design is shown in Figure 3-1. As shown in the figure, the packet scheduling algorithm at the MAC layer and the routing algorithm at the network layer are tightly coupled on the basis of the urgency metrics to effectively deliver delay-sensitive data over multi-rate MANETs. In the proposed system, the packet scheduling algorithm determines the packet transmission order and the packet drop policy to minimize the node urgency at each node without unnecessarily dropped packets, and the routing algorithm constructs a route to deliver data packets in time with the given node urgency information.

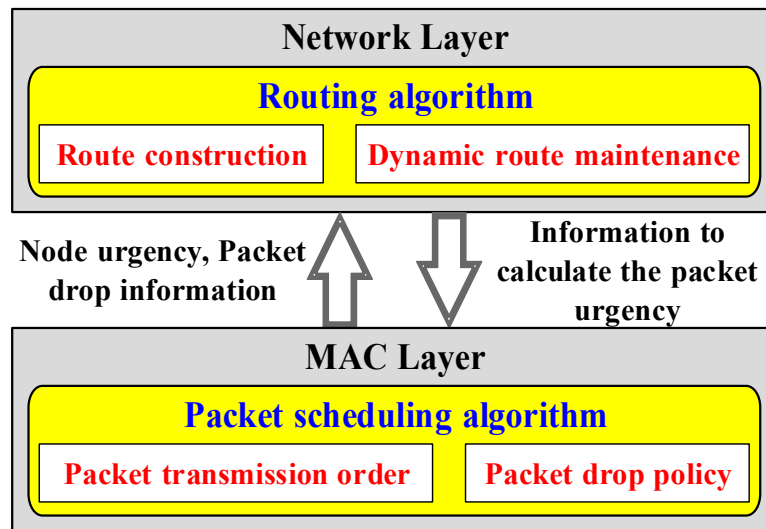


Figure 3-1 Overall architecture of proposed cross-layer design.



3.1 Proposed Urgency and Link Condition-based Packet Scheduling Algorithm

First, we describe the additional information required in the data packet header to successfully implement the proposed packet scheduling algorithm. In the proposed algorithms, it is assumed that one-hop neighbour nodes are already time synchronized by periodically exchanging beacons including time stamps [61,62,63]. An example is shown in Figure 3-2. Each node can estimate the delay over the previous hop using the timestamp (ts^{pre}) at the previous node. Then, the cumulative delay from the source node to the current node ($d_{acc}^{cur}(t)$) is calculated by adding the delay over the previous hop ($ts^{cur} - ts^{pre}$) to the cumulative delay from the source node to the previous node ($d_{acc}^{pre}(t)$).

D_{max}	$d_{acc}(t)$	ts
End-to-end delay requirement (4 bytes)	Accumulated delay from the source node to the previous node (4 bytes)	Timestamp at the previous node (4 bytes)

Figure 3-2 Additional information in data packet header.



3.1.1 Transmission Delay Estimation over IEEE 802.11b Multi-rate Service

It is assumed that the transmission power and the carrier-sensing threshold are the same at every node, and a modulation scheme is automatically selected on the basis of the received signal strength by RBAR (Receiver-Based Auto-Rate) [64]. In other words, a transmitter selects the adequate modulation scheme based on the observed received signal strength and determines the transmission rate. However, instantaneous observed received signal strength is not proper for representing the future wireless link status because the wireless link changes dynamically. Kalman filter [65,66] is adopted to estimate the received signal strength for the next interval because this filter is a linear dynamic system to effectively remove the non-stationary white Gaussian noise from the measured data. First of all, wireless channel is modeled by

$$rss(t + \Delta) = A \cdot rss(t) + w(t), \quad (3-4)$$

$$rss_{obs}(t) = H \cdot rss_{est}(t) + v(t), \quad (3-5)$$

where $rss(t)$ is the state variable of the received signal strength value in the system model at time t , $rss_{obs}(t)$ is the observed received signal strength value at time t , Δ is the updating interval, A is the state transition matrix, H is the matrix for observation model, $w(t)$ is the process white noise, and $v(t)$ is the measurement white noise. A indicates how wireless channel conditions are changing at the next state and H represents the relationship between the measurement sample rss_{obs} and the estimated



wireless channel state rss_{est} at time t as shown in Eq. 3-5. After the system model of Kalman filter is determined, the estimated received signal strength value at the node is calculated by

$$\widetilde{rss}_{est}(t + \Delta) = A \cdot \widetilde{rss}_{est}(t) + K(t) \cdot \left(rss_{obs}(t) - H \cdot A \cdot \widetilde{rss}_{est}(t) \right), \quad (3-6)$$

where $\widetilde{rss}_{est}(t)$ is the estimated received signal strength value at time t and $K(t)$ is the Kalman gain that is determined by considering the stochastic nature of the process and measurement dynamics. It is calculated by

$$K(t) = \left(A \cdot \tilde{P}(t) \cdot A^T + Q \right) \cdot H^T \cdot \left(H \cdot \left(A \cdot \tilde{P}(t) \cdot A^T + Q \right) \cdot H^T + R \right)^{-1}, \quad (3-7)$$

where Q is the covariance matrix of the process white noise, R is the covariance matrix of the measurement white noise, and $\tilde{P}(t)$ is the covariance of the prediction error.

Those are obtained by

$$Q = E \left(w(t) \cdot w(t)^T \right), \quad (3-8)$$

$$R = E \left(v(t) \cdot v(t)^T \right), \quad (3-9)$$

$$\tilde{P}(t) = \left(A \cdot \tilde{P}(t - \Delta) \cdot A^T + Q \right) - K(t - \Delta) \cdot H \cdot \left(A \cdot \tilde{P}(t - \Delta) \cdot A^T + Q \right). \quad (3-10)$$

Now, we can estimate the transmission delay $\tilde{d}_{trans}(t)$ at the current node over IEEE 802.11b multi-rate service as follows [67].



$$\begin{aligned}
\tilde{d}_{trans}(t) &= \left(DIFS + 3SIFS + BO + T_{RTS} + T_{CTS} + T_{DATA}(\widetilde{rss}_{est}(t)) + T_{ACK} \right) \cdot 10^{-6} \\
&= \left(1542 + \frac{8 \cdot L_{DATA_MAC}}{R_{tr}(\widetilde{rss}_{est}(t))} \right) \cdot 10^{-6},
\end{aligned} \tag{3-11}$$

where $DIFS$ is the distributed inter-frame space, $SIFS$ is the short inter-frame space, BO is the average back-off time, T_{RTS} , T_{CTS} , $T_{DATA}(\widetilde{rss}_{est}(t))$, and T_{ACK} are the transmission time of RTS (Request-To-Send), CTS (Clear-To-Send), data when $\widetilde{rss}_{est}(t)$ was given, and ACK (ACKnowledgment) packets at the node, respectively, L_{DATA_MAC} is the data length at the MAC layer, and $R_{tr}(\widetilde{rss}_{est}(t))$ is the transmission rate over the wireless link at the node.

3.1.2 Proposed Packet Transmission Order Determination

The transmission priority of each packet is determined on the basis of its packet urgency and wireless link condition. A packet with a high transmission priority is transmitted earlier than a packet with a low transmission priority to minimize the node urgency. In the proposed packet scheduling algorithm, the transmission priority of a data packet is determined according to the variation of node urgency after the packet transmission. The node urgency after the k_{th} data packet transmission can be expressed by

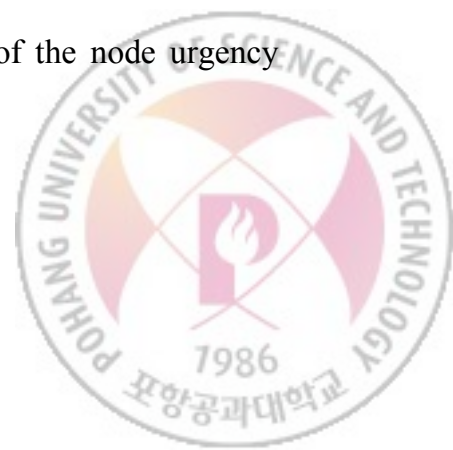


$$\begin{aligned}
u_{node} \left(t + \Delta \tilde{T}_{pkt(k)} \right) &= u_{node} (t) + \Delta u_{node} (t, k) \\
&= u_{node} (t) + \sum_{\substack{i=1 \\ i \neq k}}^{n_{pkt}} \left\{ u_{pkt(i)} \left(t + \Delta \tilde{T}_{pkt(k)} \right) - u_{pkt(i)} (t) \right\} - u_{pkt(k)} (t),
\end{aligned} \tag{3-12}$$

where $\Delta u_{node} (t, k)$ is the increasing amount of the node urgency when the k_{th} data packet is transmitted at time t , and $\Delta \tilde{T}_{pkt(i)}$ is the transmission delay of the i_{th} data packet estimated by using Kalman filter. Now, the increasing amount of the node urgency after the transmission of the k_{th} data packet at time t is represented as follows. The equation is simplified by using the first order Taylor series expansion under the assumption of $|\Delta \tilde{T}_{pkt(k)}| < \varepsilon$, where ε is a small real number.

$$\begin{aligned}
\Delta u_{node} (t, k) &= u_{node} \left(t + \Delta \tilde{T}_{pkt(k)} \right) - u_{node} (t) \\
&\cong \sum_{\substack{i=1 \\ i \neq k}}^{n_{pkt}} \left\{ u_{pkt(i)} (t) + \Delta \tilde{T}_{pkt(k)} \cdot \frac{du_{pkt(i)} (t)}{dt} \right\} - \sum_{\substack{i=1 \\ i \neq k}}^{n_{pkt}} u_{pkt(i)} (t) - u_{pkt(k)} (t) \\
&= \sum_{\substack{i=1 \\ i \neq k}}^{n_{pkt}} \left\{ \Delta \tilde{T}_{pkt(k)} \cdot \frac{du_{pkt(i)} (t)}{dt} \right\} - u_{pkt(k)} (t) \\
&\cong \Delta \tilde{T}_{pkt(k)} \cdot \sum_{\substack{i=1 \\ i \neq k}}^{n_{pkt}} \left\{ \frac{\Delta u_{pkt(i)} (t)}{\Delta \tilde{T}_{pkt(i)}} \right\} - u_{pkt(k)} (t),
\end{aligned} \tag{3-13}$$

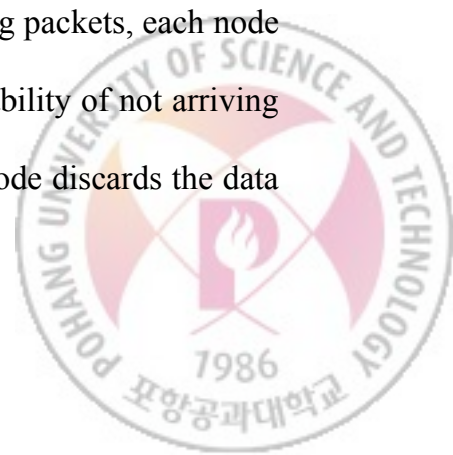
where $\Delta u_{pkt(i)} (t)$ is the decreasing amount of the packet urgency when the i_{th} data packet is transmitted. Therefore, the proposed packet scheduling algorithm selects a packet from the packets in the buffer to maximize the decreasing amount of the node urgency normalized by its transmission time, i.e.,



$$\begin{aligned}
k^* &= \arg \min_{1 \leq k \leq n_{pkt}} \frac{\Delta u_{node}(t, k)}{\Delta \tilde{T}_{pkt(k)}} \\
&= \arg \min_{1 \leq k \leq n_{pkt}} \sum_{\substack{i=1 \\ i \neq k}}^{n_{pkt}} \left\{ \frac{\Delta u_{pkt(i)}(t)}{\Delta \tilde{T}_{pkt(i)}} \right\} - \frac{u_{pkt(k)}(t)}{\Delta \tilde{T}_{pkt(k)}}.
\end{aligned} \tag{3-14}$$

If $\Delta \tilde{T}_{pkt(i)} \neq \Delta \tilde{T}_{pkt(j)}$ for $i \neq j$, a sequence of packets should be considered simultaneously to obtain the optimal solution. In this case, the wireless link condition in the relatively far future is required to transmit multiple packets. However, it is non-causal and very difficult to predict the condition accurately. As a feasible solution, we select only a packet with the steepest decreasing rate (i.e. the smallest derivative of the packet urgency) of the node urgency at time t . Because routing control packets such as RREQ (Route REQuest), RREP (Route REPLY), and RERR (Route ERRor) play a critical role in route construction and maintenance, the proposed packet scheduling algorithm assigns the highest transmission priority (maximum packet urgency) to them in the implemented system.

Since the buffer size at each node is limited, a packet drop policy is required when the buffer overflows. In this dissertation, packets are dropped in the following two cases: (I) To avoid unnecessary packet transmission, delay-sensitive packets are immediately dropped when the sum of their accumulated delay and estimated transmission delay is larger than the required end-to-end delay regardless of buffer occupancy and network congestion level. (II) When buffer overflow is caused by newly arriving packets, each node in the proposed system drops the data packet having the highest probability of not arriving at its destination node in time. That is, when the buffer overflows, a node discards the data



packet having the maximum packet urgency in the buffer. Figure 3-3 shows a flowchart for the proposed packet drop policy.

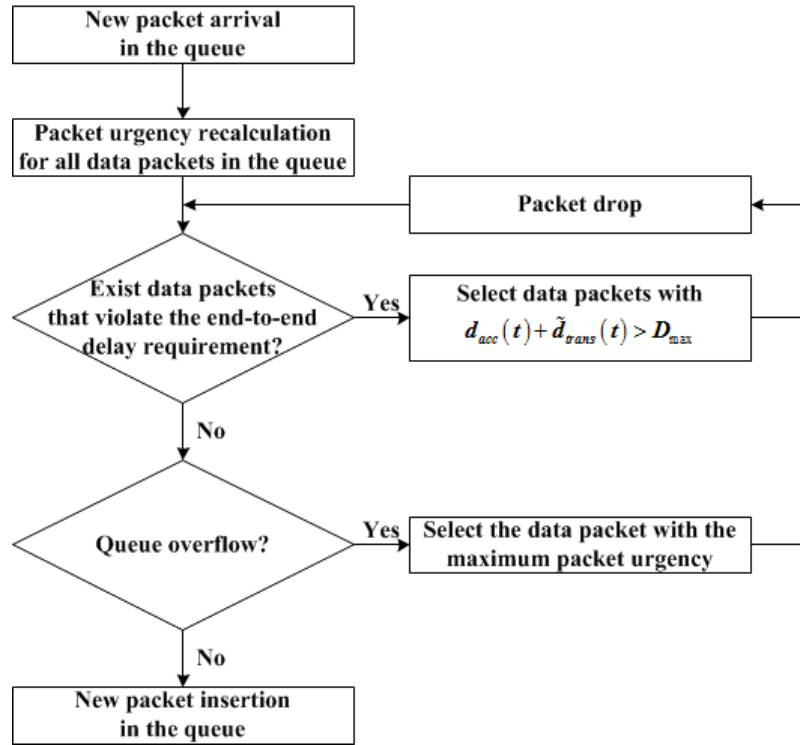
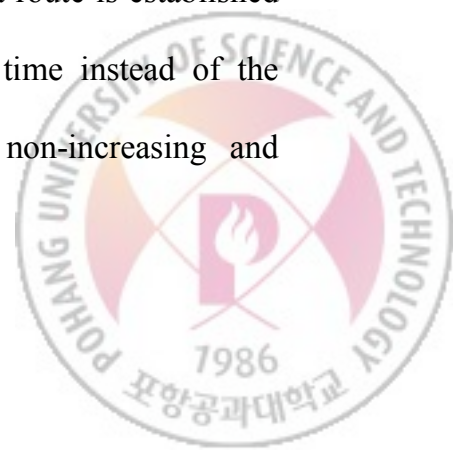


Figure 3-3 Flowchart for proposed packet drop policy.

3.2 Proposed Urgency-based Routing Algorithm

As compared to existing routing algorithms, one of the most significant and distinctive features of the proposed routing algorithm is the fact that a route is established to maximize the number of arriving packets at the destination in time instead of the shortest or fastest routes. If the urgency mapping function is non-increasing and



differentiable in $0 < \frac{d_{residual}}{D_{max}} < 1$, the route urgency increases when more packets are staying at the intermediate node buffer. Based on the phenomenon, the derivative of route urgency is selected as the cost function of the below routing problem. Now, the routing problem is formulated as follows to take into account the number of packets and their urgency over the route simultaneously.

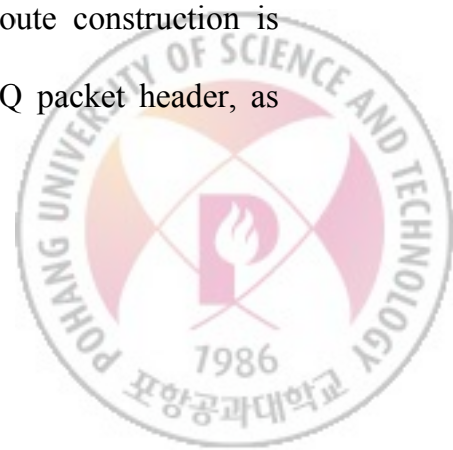
Problem Formulation for Routing Algorithm: Determine a route \vec{R} to minimize

$$\frac{du_{route(\vec{R})}(t^-)}{dt}. \quad (3-15)$$

When the urgency mapping function is convex, the established route includes the nodes holding packets with big residual delay values. When the urgency mapping function is linear, the derivative of the urgency mapping function is constant value, and thus the routing algorithm considers only numbers of packets stored in the buffer at the nodes over the constructed route. At last, if the urgency mapping function is concave, the created route consists of nodes having packets whose delay values are so big that it would be dropped shortly without arriving at the destination on time.

3.2.1 Route Construction Mechanism

In the proposed routing algorithm, the basic procedure for route construction is similar to AODV but additional information is required in the RREQ packet header, as



shown in Figure 3-4. Based on the information, the optimal route of the above problem is obtained by

$$\begin{aligned}\vec{R}^* &= \arg \min_{\vec{R} \in R_{avail}} \frac{du_{route(\vec{R})}(t^-)}{dt} \\ &= \arg \min_{\vec{R} \in R_{avail}} \left\{ \sum_{j \in \vec{R}} \frac{du_{node(j)}(t^-)}{dt} \right\},\end{aligned}\tag{3-16}$$

where R_{avail} is the set of all available routes between the source node and the destination node. A source node floods an RREQ packet only when a route is needed. When an intermediate node receives the RREQ packet, it recalculates the derivative of the interim route urgency over the interim route by adding its node urgency derivative, and then updates the RREQ packet. The intermediate node rebroadcasts only the updated RREQ packet to its neighbour nodes for an interim route with the minimum derivative of the route urgency in order to reduce the number of RREQ packets. These steps are repeated until the RREQ packet arrives at the destination node. When RREQ packets arrive at the destination node, the route with the minimum derivative of route urgency is selected, and then, an RREP packet for the selected route is sent back to the source node. The obtained route is optimal in terms of derivative of route urgency without loss of generality. Figure 3-5 shows a flowchart for the proposed route construction mechanism.



$$\sum_{j \in R_{interim}} \frac{du_{node(j)}(t)}{dt}$$

Derivative of the interim route urgency
(4 bytes)

Figure 3-4 Additional information in RREQ packet header.

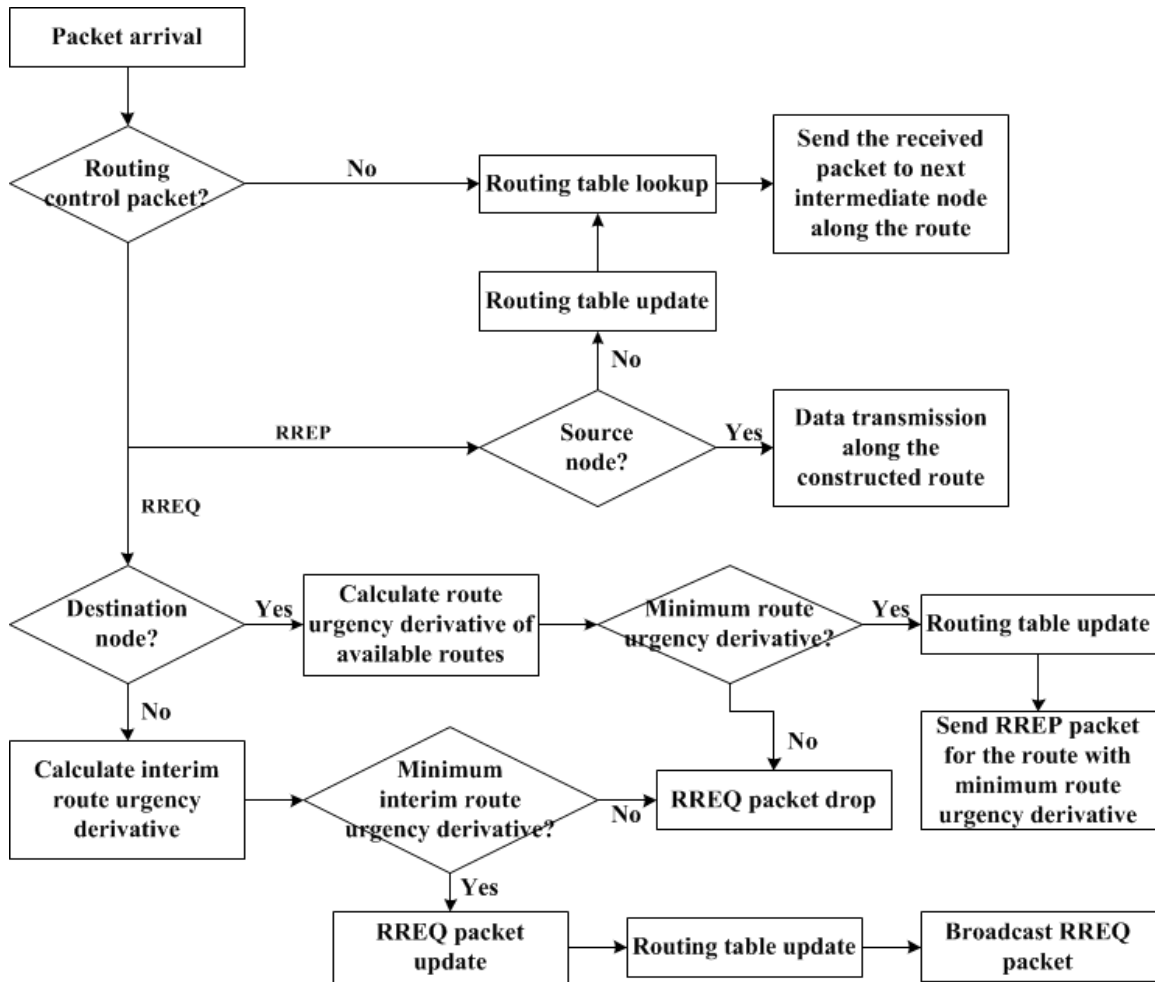


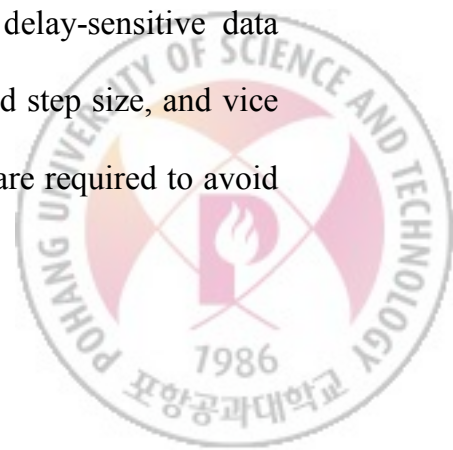
Figure 3-5 Flowchart for proposed route construction mechanism.



3.2.2 Dynamic Route Maintenance Mechanism

The service satisfaction of users may deteriorate drastically if there are frequent packet drops along an unstable route. Therefore, dynamic route maintenance must be considered in order to effectively transmit delay-sensitive data. In this dissertation, the route maintenance mechanism considers the following two factors: (I) the estimated signal strength of each flow and (II) the packet drop rate of each flow. When the estimated signal strength obtained from Eq. 3-6 is less than the pre-determined threshold, the intermediate node notifies the source node by sending an RERR packet and a new route is established before the actual link failure occurs. As a result, the delay jitter is decreased because it effectively reduces the link failures associated with the node mobility. Meanwhile, the nodes record the number of dropped packets within a packet drop counting interval and the corresponding flows. Then, the nodes select the flow whose packets are dropped with the highest frequency. If the number of dropped packets for the selected flow is larger than a pre-determined threshold, an RERR packet is transmitted to the source node to request a new route, even though the current route is still available. If the source node desires a new route after receiving the RERR packet, it can reinitiate the route construction mechanism.

The packet drop counting interval is dynamically adjusted on the basis of observed packet drop information in order to reduce the route maintenance overhead. If the number of dropped packets for the selected flow is below a pre-determined threshold, a node realizes that the current routes passing through it are suitable for delay-sensitive data transmission and increases the packet drop counting interval by a fixed step size, and vice versa. Lower and upper bounds for the packet drop counting interval are required to avoid



unnecessary route reconstructions and to effectively reflect the current network state, respectively. To reduce the unnecessary routing overhead, the node with a large node urgency value does not broadcast RREQ and RREP packets to its neighbour nodes since it may not deliver the delay-sensitive data on time. It is called RREQ/RREP packet forwarding control mechanism in the followings. Figure 3-6 shows a flowchart for the proposed dynamic route maintenance mechanism.

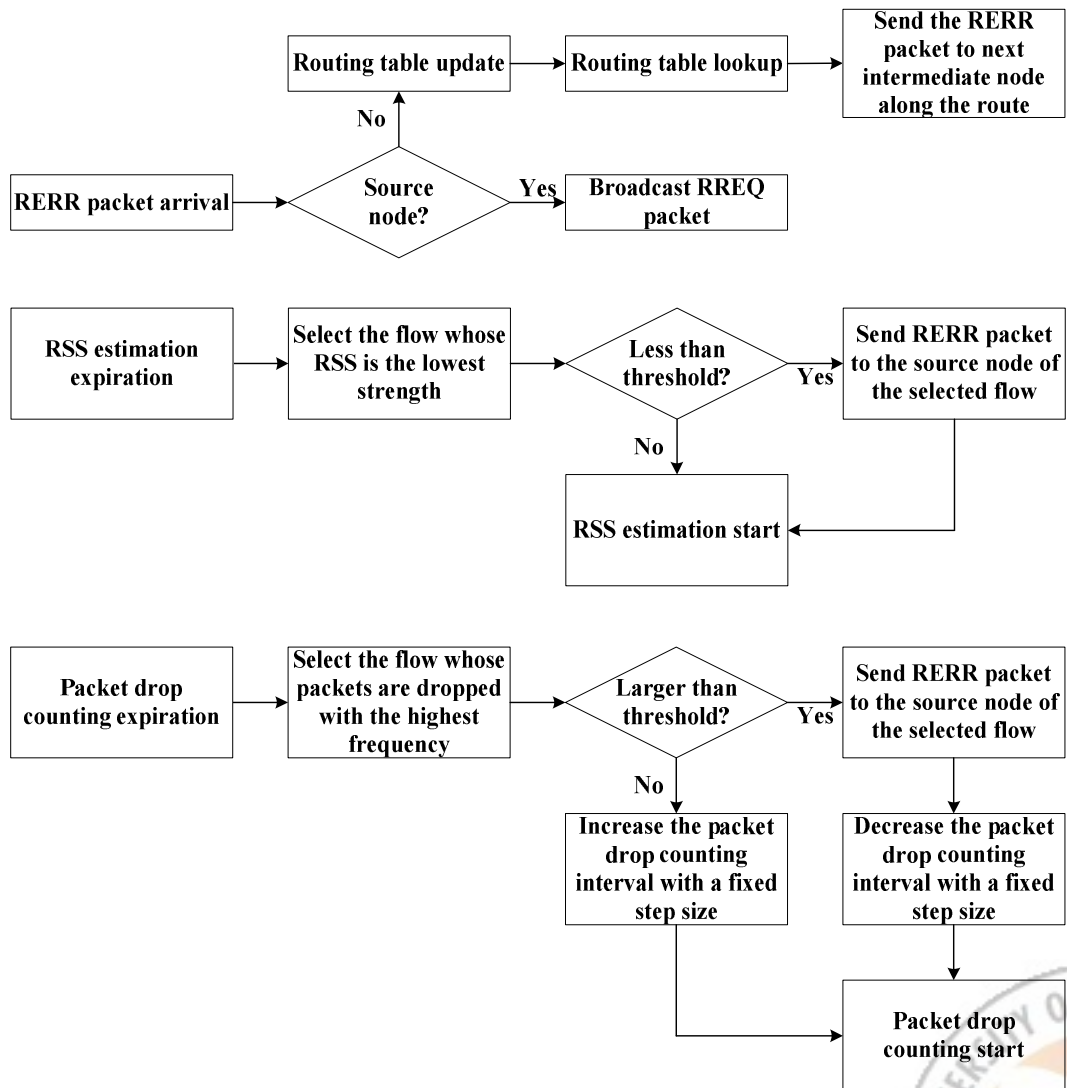
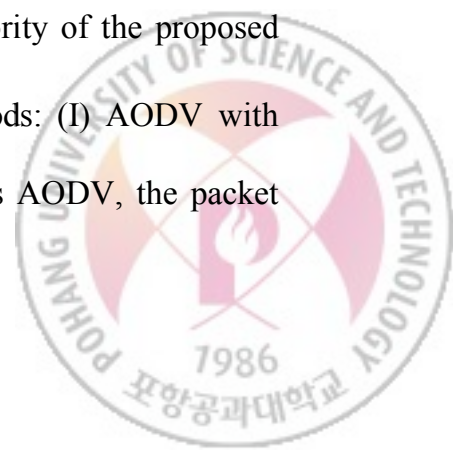


Figure 3-6 Flowchart for proposed dynamic route maintenance mechanism.



3.3 Performance Evaluation

Experimental results are provided to demonstrate the performance of the proposed joint working algorithms. During the experiment, the NS-2 simulator [68] is employed. Thirty nodes are randomly located in a 400 m \times 400 m rectangular area and seventy nodes are randomly located in a 600 m \times 600 m rectangular area. All nodes move at a speed of 1 ~ 5 m/s according to a random waypoint model. The number of connections is 1 ~ 20. Pairs of source and destination nodes are arbitrarily determined. A two-ray ground model is adopted for the wireless channel, and nodes try to access the medium according to the IEEE 802.11 MAC protocol. The target bandwidth of each data flow is set to 40.96 Kbps. That is, all source nodes generate 10 packets/s, and the packet size is 512 bytes. The buffer size is fixed to 50 packets at every node. The packet drop counting interval is dynamically adjusted in the range of 1.0 ~ 5.0 s with a fixed step size of 1.0 s. The threshold for dynamic route maintenance is set to a 20 % packet drop rate. D_{max} is set to 1.0 s. The transmission power is set to 0.0127 W. The carrier sense threshold and receptions threshold are 2.25×10^{-11} W and 3.652×10^{-10} W, respectively. The transmission rates according to the distance are determined as shown in Figure 3-7. A , H , Q , and R of Kalman filter are set to 1, 1, 10, and 0.5, respectively. The initial values of $\widetilde{r_{ss_{est}}}(0)$ and $\widetilde{P}(0)$ are fixed to 0. To verify the superiority of the proposed joint working algorithms, they are compared with four other methods: (I) AODV with FCFS/Drop-tail/RBAR (the routing algorithm at the network layer is AODV, the packet



scheduling algorithm at the MAC layer is FCFS (First-Come, First-Served) service discipline and drop-tail policy, and the MAC layer adopts RBAR (Receiver-Based Auto-Rate)), (II) DSR with FCFS/Drop-tail/RBAR, (III) QAR with FCFS/Drop-tail/RBAR, and (IV) the proposed routing algorithm with FCFS/Drop-tail/RBAR. The total simulation time is set to 500 s.

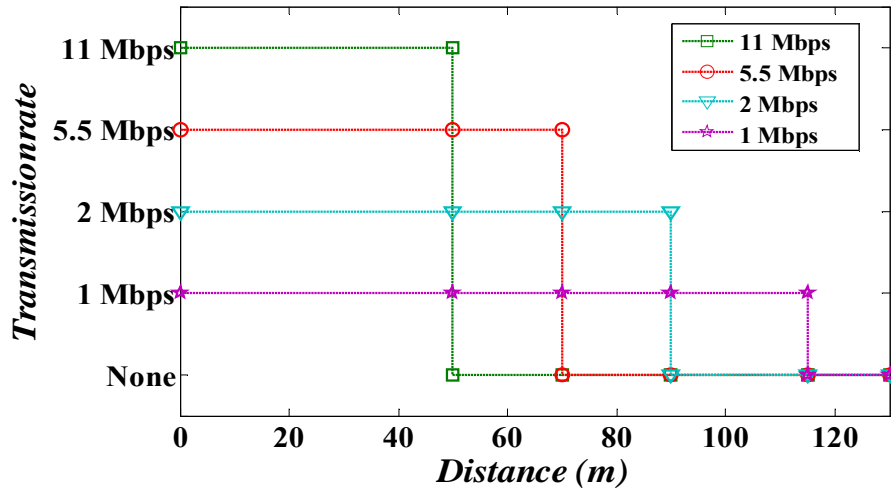
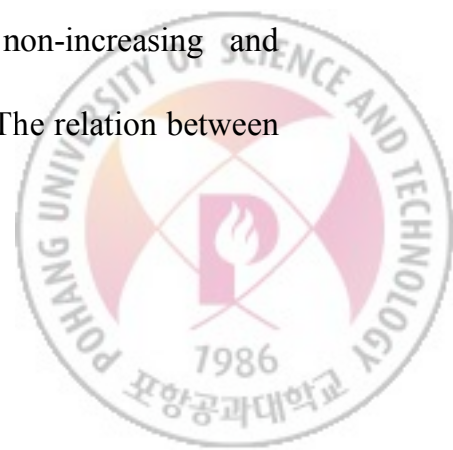


Figure 3-7 The transmission rates according to distance in IEEE 802.11b multi-rate service.

3.3.1 Test of Urgency Mapping Functions

To verify the performance of the proposed joint working algorithms, we preformed experiment with a variety of non-increasing functions. As shown in Figure 3-8, we examined three types (e.g. convex, linear, and, concave) of non-increasing and differentiable urgency mapping functions in $0 < d_{residual}(t)/D_{max} < 1$. The relation between



the mapping functions and the corresponding routes is presented in Figure 3-9, and the histograms of accumulated packet urgency values over the routes are shown in Figure 3-10. It is obviously shown in Figure 3-10 that the route contains more packets with large packet urgency values as the urgency mapping function becomes more concave, vice versa. Based on the observation, the convex mapping function with $s=2$ is selected as the urgency mapping function of the proposed joint working algorithms in the followings.

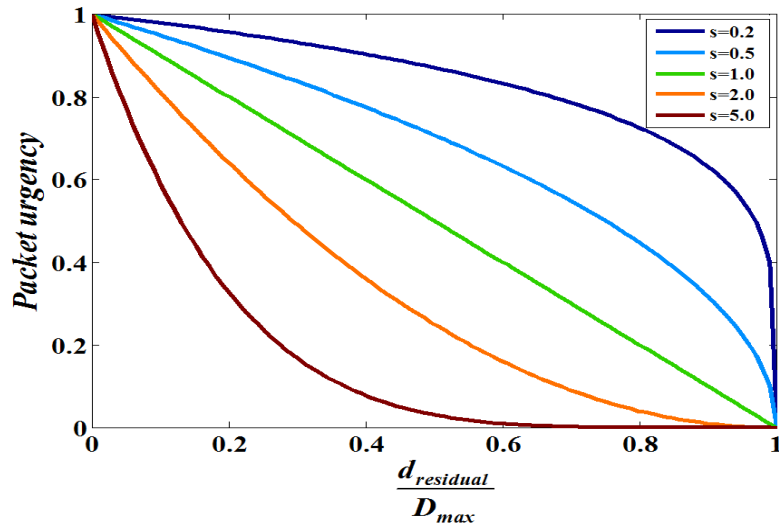


Figure 3-8 The packet urgency mapping function: $u_{pkt} = f_{urg} \left(\frac{d_{residual}}{D_{max}} \right) = \left(1 - \frac{d_{residual}}{D_{max}} \right)^s$.



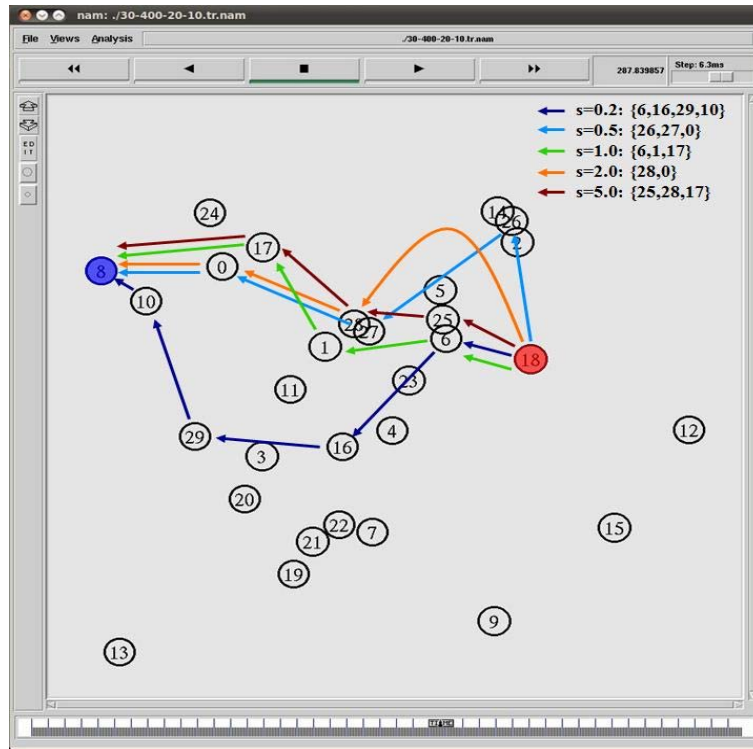


Figure 3-9 Snapshot of routing paths at about 287 s.

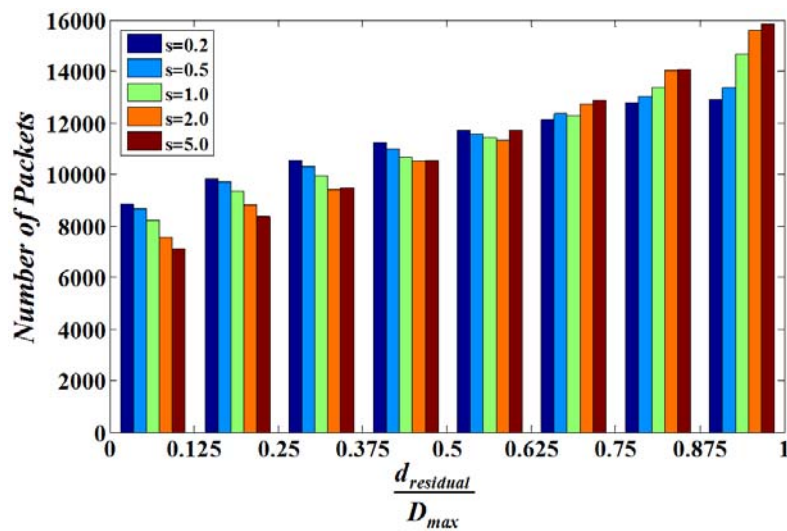
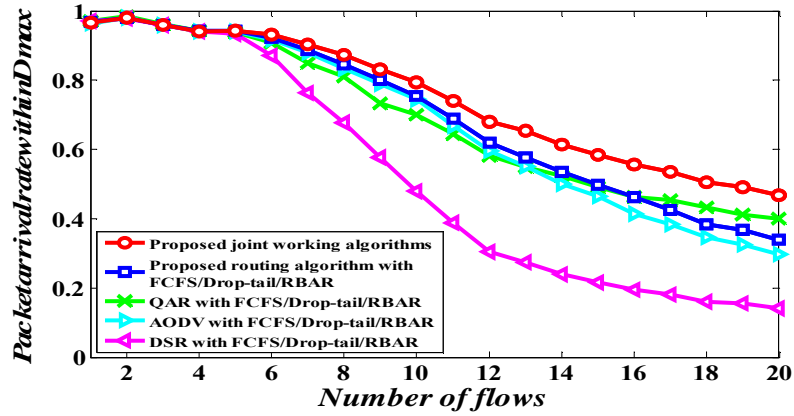


Figure 3-10 Histograms of accumulated packet urgency values over the routes.

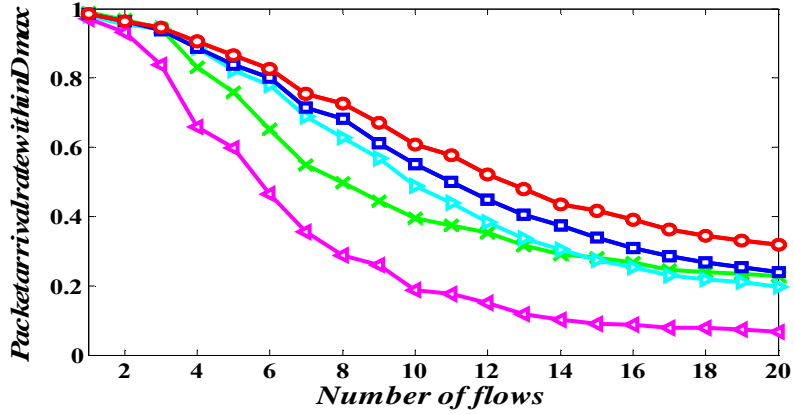
3.3.2 Performance Comparison with respect to End-to-End QoS Metrics

In this section, the packet arrival rate within D_{max} , end-to-end delay, and routing overhead are adopted as end-to-end QoS performance metrics. The packet arrival rate within D_{max} is given in Figure 3-11. It is observed that DSR with FCFS/Drop-tail/RBAR has significantly decreasing packet arrival rates within D_{max} as the number of flows increases. Actually, DSR with FCFS/Drop-tail/RBAR shows the worst performance because intermediate nodes may transmit RREP packets through stale cached routes, and then pollute local caches at the other nodes over MANETs. Consequently, the packet arrival rate within D_{max} decreases. QAR with FCFS/Drop-tail/RBAR also exhibits worse performance than the proposed joint working algorithms because it accounts for only the available bandwidth of a new route without considering existing routes. Thus, it may degrade the QoS of the existing routes by accepting a new route. Under a heavy traffic load, the proposed routing algorithm with FCFS/Drop-tail/RBAR presents worse performance than QAR with FCFS/Drop-tail/RBAR, as shown in Figure 3-11 (a). The reason is that the proposed routing algorithm with FCFS/Drop-tail/RBAR increases the network stress by transmitting packets that violate the end-to-end delay requirement, and it does not reflect the current network state effectively during the route establishment stage. In contrast, the proposed joint working algorithms provide better performance than any other method because they distribute the traffic load over the entire network and effectively control the packets accumulated in the buffer at each node.





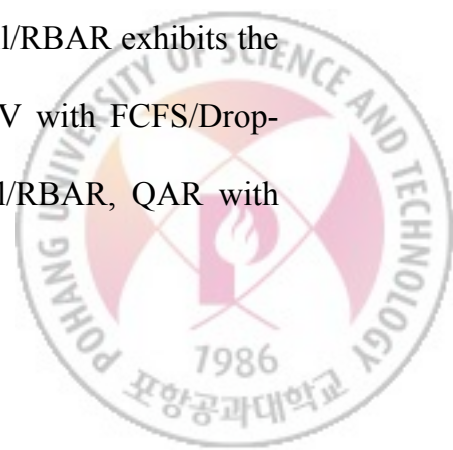
(a)



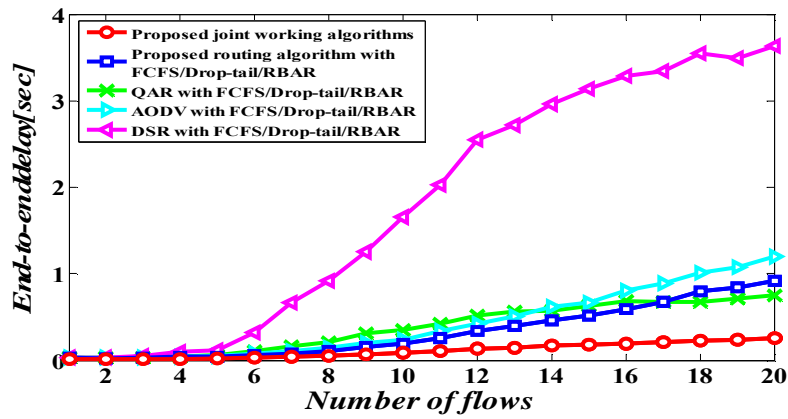
(b)

Figure 3-11 Packet arrival rate within D_{max} : (a) 400 m \times 400 m network topology with 30 nodes and (b) 600 m \times 600 m network topology with 70 nodes.

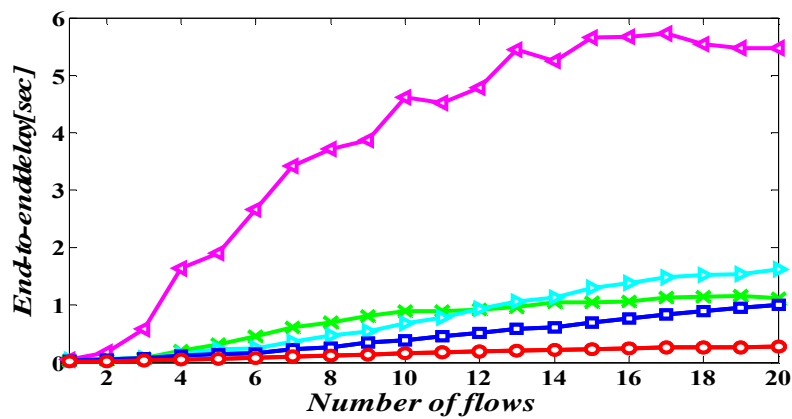
The resulting end-to-end delay is presented in Figure 3-12. As shown in the figure, the end-to-end delay curve of DSR with FCFS/Drop-tail/RBAR increases significantly when the number of flows increases. In fact, DSR with FCFS/Drop-tail/RBAR exhibits the worst performance, as observed in Figure 3-12. Compared to AODV with FCFS/Drop-tail/RBAR and the proposed routing algorithm with FCFS/Drop-tail/RBAR, QAR with



FCFS/Drop-tail/RBAR supports a low end-to-end delay under a heavy traffic load. However, the end-to-end delay of QAR with FCFS/Drop-tail/RBAR is greater than that of the proposed joint working algorithms because it does not consider the end-to-end delay requirement of each packet. The proposed joint working algorithms maintain the end-to-end delay of each packet within a tolerable range as far as possible. On the basis of these observations, the proposed joint working algorithms can provide better delivery service for delay-sensitive data transmission over multi-rate MANETs.



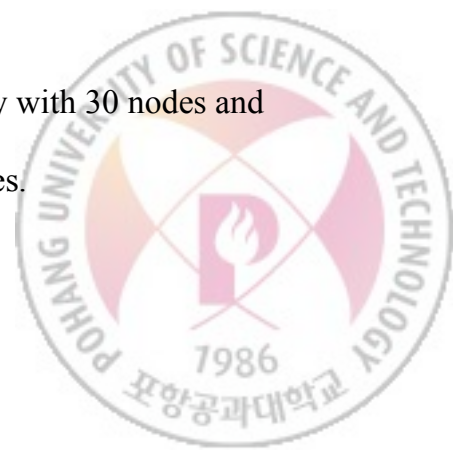
(a)



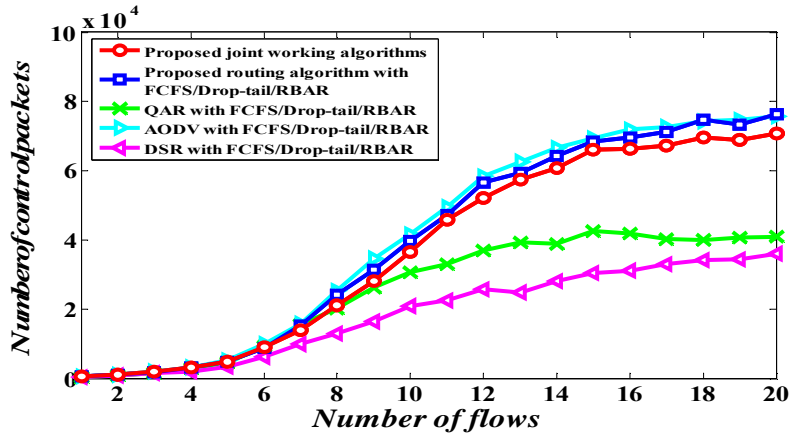
(b)

Figure 3-12 End-to-end delay: (a) 400 m \times 400 m network topology with 30 nodes and

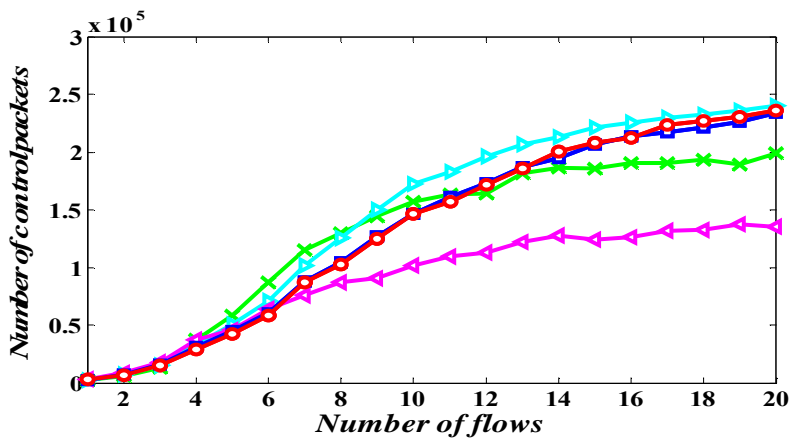
(b) 600 m \times 600 m network topology with 70 nodes.



Now, we consider the routing overhead, which it is one of the most important factors in protocol design over multi-rate MANETs. Figure 3-13 shows the number of routing control packets. DSR with FCFS/Drop-tail/RBAR has the smallest routing overhead because it uses source routing instead of relying on a routing table at each node and route caching can reduce the route discovery overhead. It is observed in Figure 3-13 that the control overhead of the proposed joint working algorithms is almost same as AODV with FCFS/Drop-tail/RBAR by adopting RREQ/RREP packet forwarding control mechanism.

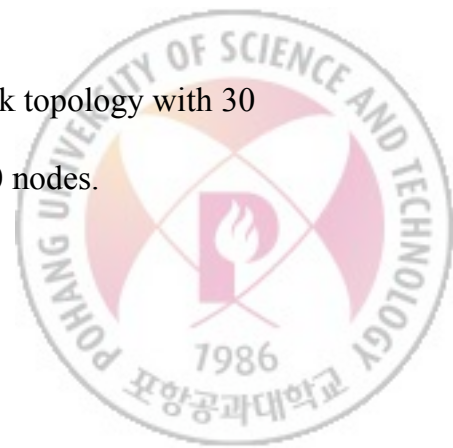


(a)



(b)

Figure 3-13 Number of control packets: (a) 400 m \times 400 m network topology with 30 nodes and (b) 600 m \times 600 m network topology with 70 nodes.



3.3.3 Performance Comparison with respect to Proposed Urgency Metrics

In this section, we compare the proposed joint working algorithms with the other four methods in terms of the proposed urgency metrics when the number of connections is 14. The sum of node urgency values is provided in Figure 3-14. It is apparently observed that DSR with FCFS/Drop-tail/RBAR has the highest sum of node urgency values among all algorithms, furthermore this curve suddenly increase when the traffic is concentrated at only some nodes and/or when network congestion occurs. AODV with FCFS/Drop-tail/RBAR, QAR with FCFS/Drop-tail/RBAR, and the proposed routing algorithm with FCFS/Drop-tail/RBAR have an even higher sum of node urgency, although their curves are considerably lower and smoother than one of DSR with FCFS/Drop-tail/RBAR. However, the proposed joint working algorithms significantly reduce the sum of node urgency values. The results are summarized statistically in Table 3-1.



Table 3-1 Statistics of node urgency sum.

<i>Methods</i>	<i>Average node urgency sum</i>	<i>Maximum node urgency sum</i>	<i>Standard deviation of node urgency sum</i>
Proposed joint working algorithms	5.163	32.159	5.955
Proposed routing algorithm with FCFS/Drop-tail/RBAR	24.318	119.997	27.288
QAR with FCFS/Drop-tail/RBAR	16.995	138.000	24.545
AODV with FCFS/Drop-tail/RBAR	28.713	162.667	33.324
DSR with FCFS/Drop-tail/RBAR	230.926	448.571	95.524

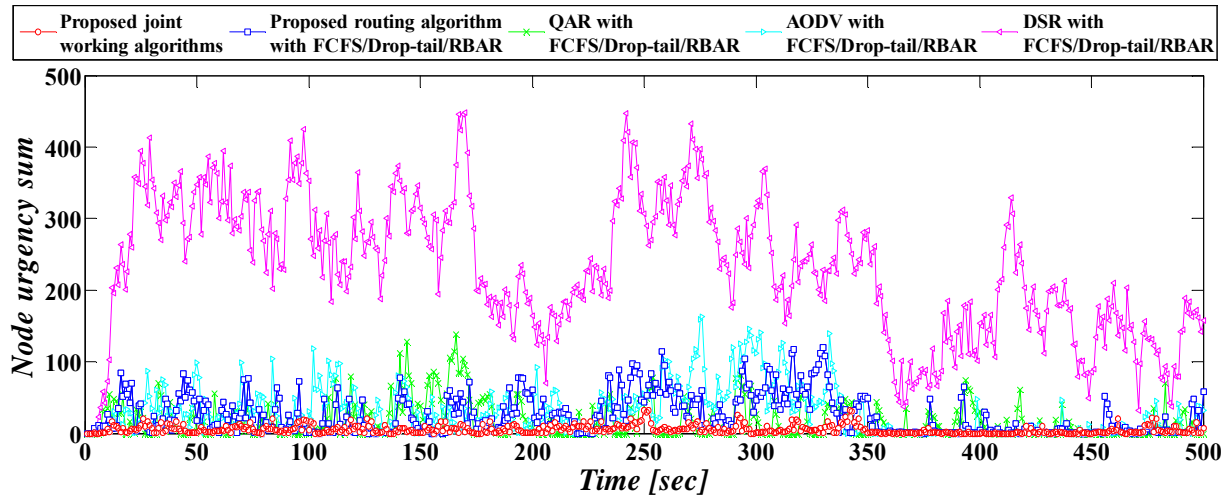


Figure 3-14 Sum of node urgency values over the entire network.



In addition, the node urgency at each individual node is presented in Figure 3-15. This shows that the proposed joint working algorithms can maintain consistently low node urgency among active nodes, whereas some active nodes participating in data forwarding obviously have high node urgency in the other methods. The statistical results in Table 3-2 indicate that the proposed joint working algorithms can significantly decrease the average, maximum, and standard deviation of node urgency by distributing traffic over the entire network.

Table 3-2 Statistics of node urgency at each node.

<i>Methods</i>	<i>Average node urgency</i>	<i>Maximum node urgency</i>	<i>Standard deviation of node urgency</i>
Proposed joint working algorithms	0.172	0.409	0.106
Proposed routing algorithm with FCFS/Drop-tail/RBAR	0.811	3.141	0.734
QAR with FCFS/Drop-tail/RBAR	0.567	1.767	0.470
AODV with FCFS/Drop-tail/RBAR	0.957	2.857	0.835
DSR with FCFS/Drop-tail/RBAR	7.698	21.021	5.218



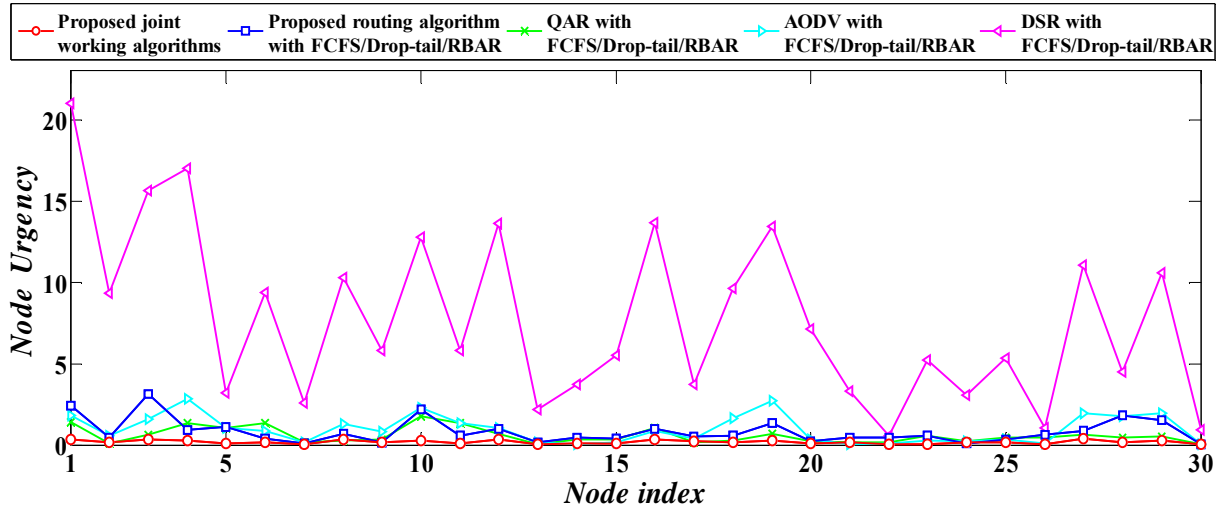
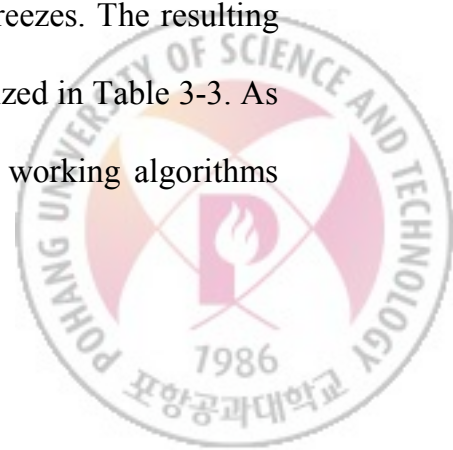


Figure 3-15 Node urgency at each node.

3.3.4 Performance Comparison with respect to Achievable Video Quality

It is well known that video traffic is very sensitive to delay and delay jitter. In this section, the achievable video quality is measured for 14 connections. During the experiment, the H.264/AVC JM 15.1 [69] video codec is employed. The test video sequences are the QCIF (Quarter Common Intermediate Format)-sized City, Crew, and Foreman. The video stream is encoded at 15 fps, and its target bandwidth is set to the value of the product of the packet size and the average number of packets received per second that satisfies the end-to-end delay requirement at the destination node. A GOP (Group of Pictures) consists of 15 frames (IPPPPPPPPPPPPPPP). The performance measure is the achievable PSNR (Peak Signal to Noise Ratio) value without scene freezes. The resulting PSNR curves are presented in Figure 3-16, and the results are summarized in Table 3-3. As shown in the table, it is obviously observed that the proposed joint working algorithms

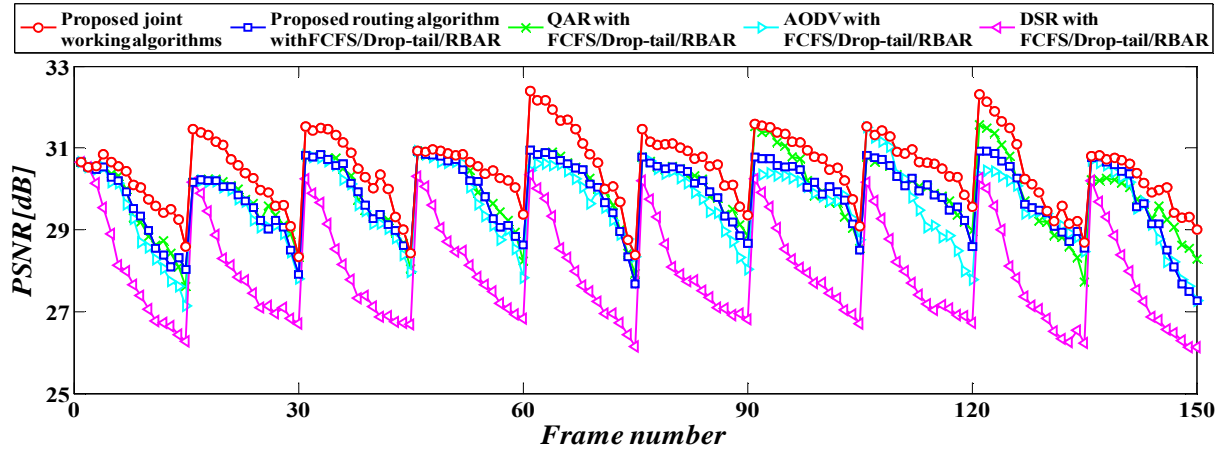


provide better PSNR values than the other methods. For the subjective quality comparison, some captured frames are presented in Figure 3-17. It is apparently observed in the figures that the proposed joint working algorithms can support much better subjective video quality than those of the existing routing algorithms.

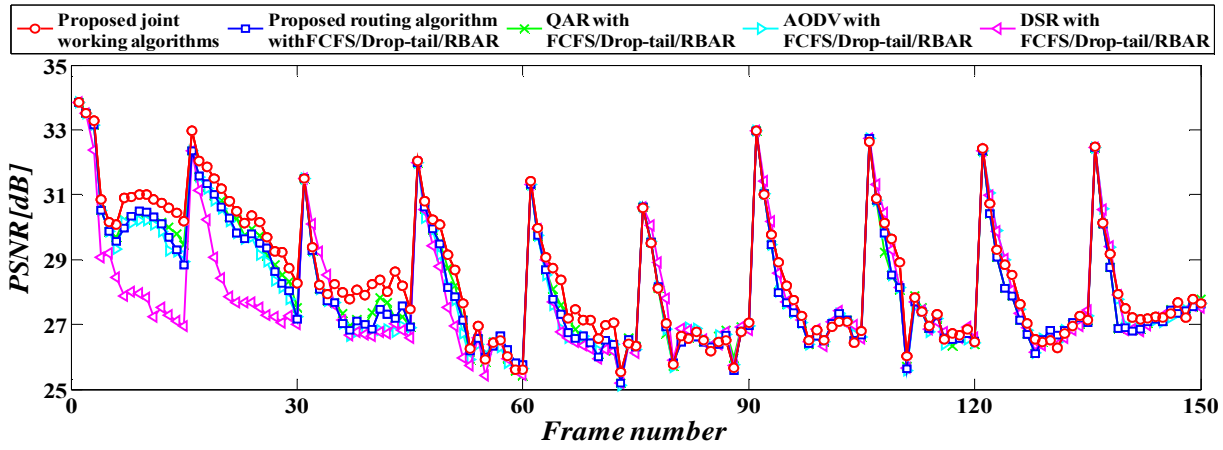
Table 3-3 Average PSNR value comparison.

<i>Methods</i>	<i>Test video sequences (dB)</i>		
	<i>City</i>	<i>Crew</i>	<i>Foreman</i>
Proposed joint working algorithms	30.490	28.469	29.713
Proposed routing algorithm with FCFS/Drop-tail/RBAR	29.807	28.137	28.859
QAR with FCFS/Drop-tail/RBAR	29.875	28.174	28.929
AODV with FCFS/Drop-tail/RBAR	29.615	28.109	28.642
DSR with FCFS/Drop-tail/RBAR	27.952	27.844	28.262

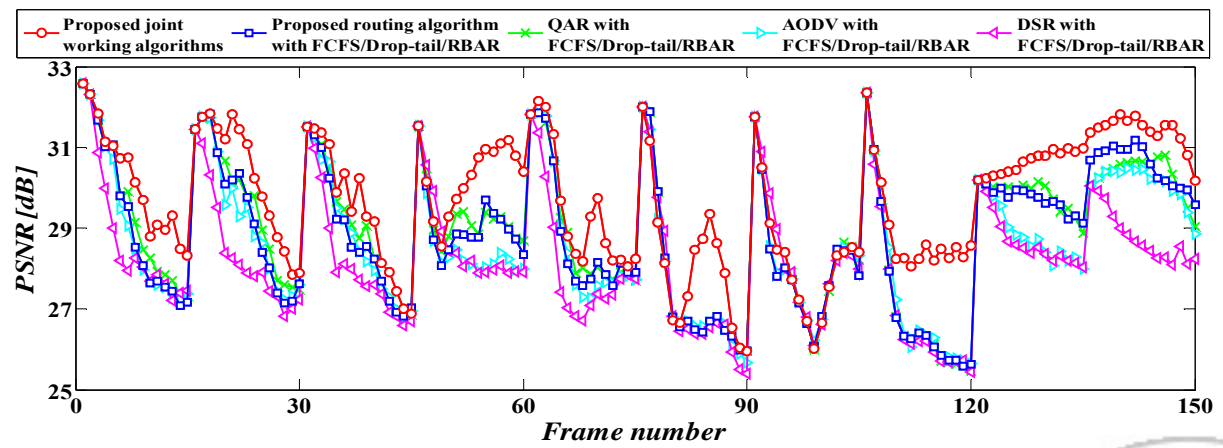




(a)

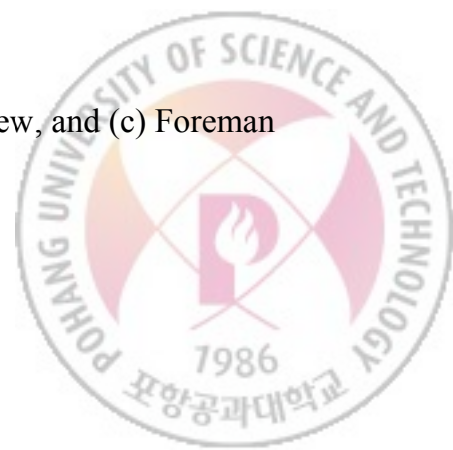


(b)



(c)

Figure 3-16 PSNR values according to frame number: (a) City, (b) Crew, and (c) Foreman video sequences.



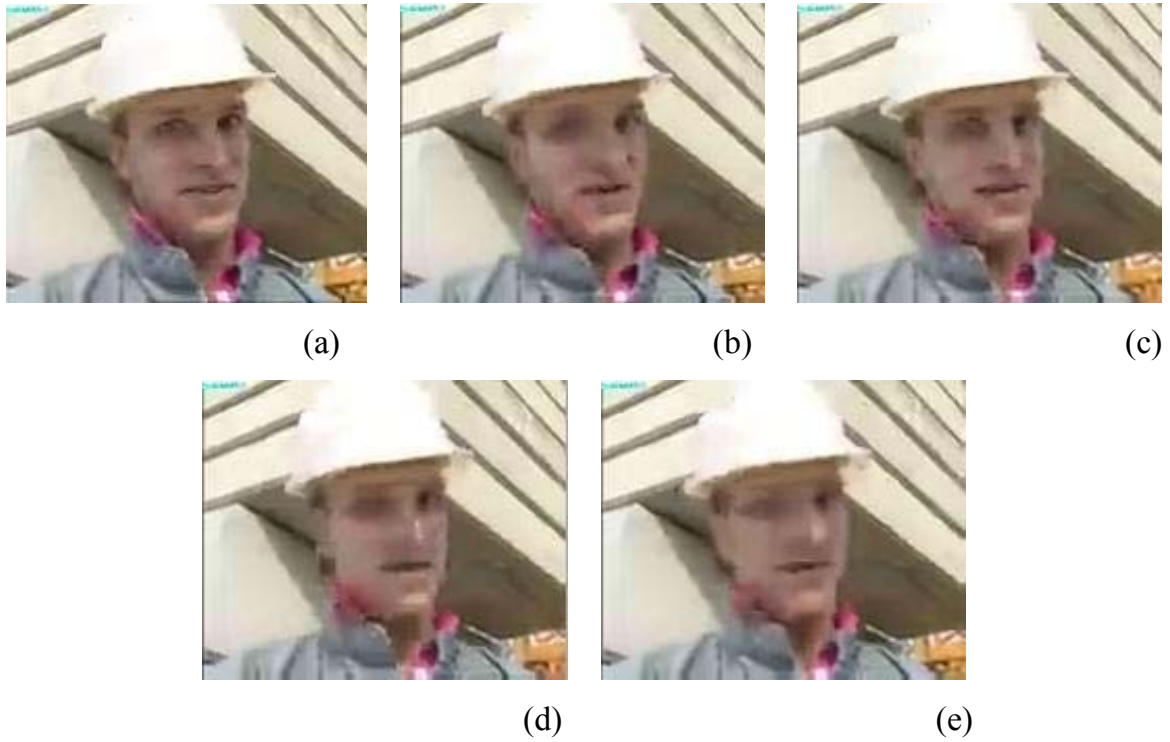
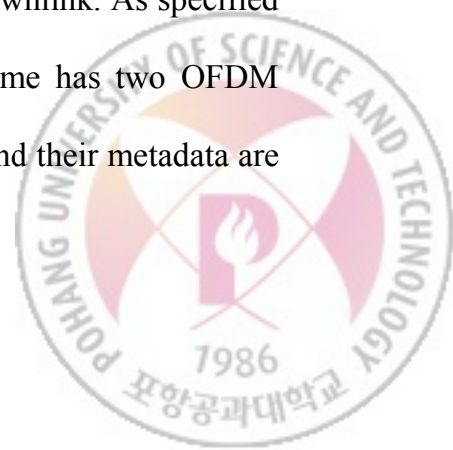


Figure 3-17 Subjective video quality comparison of the 57th frame of Foreman video sequence: (a) Proposed joint working algorithms, (b) proposed routing algorithm with FCFS/Drop-tail/RBAR, (c) QAR with FCFS/Drop-tail/RBAR, (d) AODV with FCFS/Drop-tail/RBAR, and (e) DSR with FCFS/Drop-tail/RBAR.

IV. QoS-aware Joint Working Packet Scheduling and Call Admission Control for Video Streaming Services over WiMAX network

The goal of the proposed video streaming system is to improve both the QoS of video streaming services and the network utilization over WiMAX network. The overall structure of the proposed video streaming system is presented in Figure 4-1. The target application of the proposed system is a video-on-demand streaming service which is a typical application of rtPS service class. In the proposed system, WiMAX OFDMA supports DL PUSC (Down Link Partial Usage of SubCarrier) in the downlink. As specified by the IEEE 802.16 standard, the basic allocation unit of this scheme has two OFDM symbols spread over 24 subcarriers. It is assumed that the video data and their metadata are



already available at the base station and a fixed number of slots are dedicated to the rtPS service class.

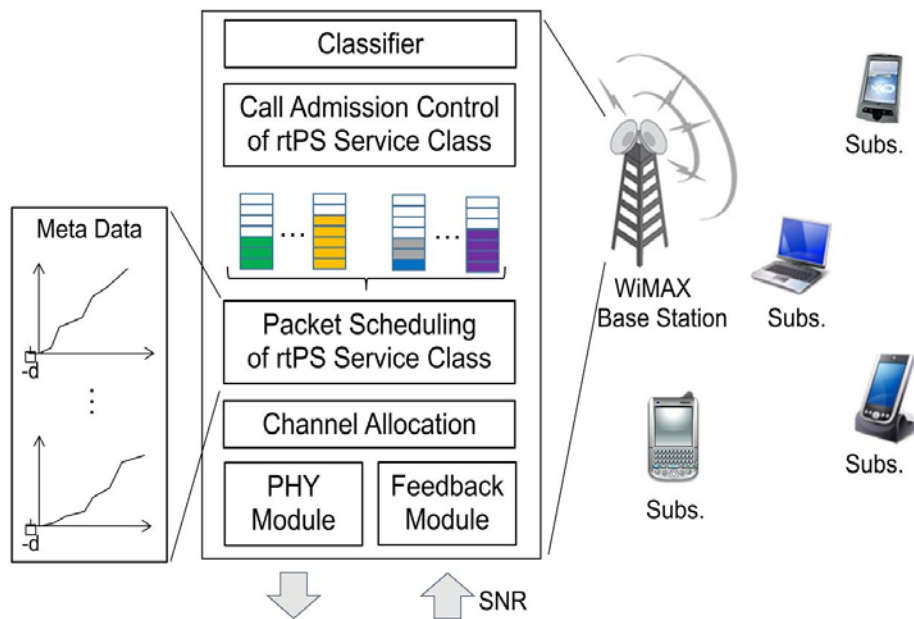
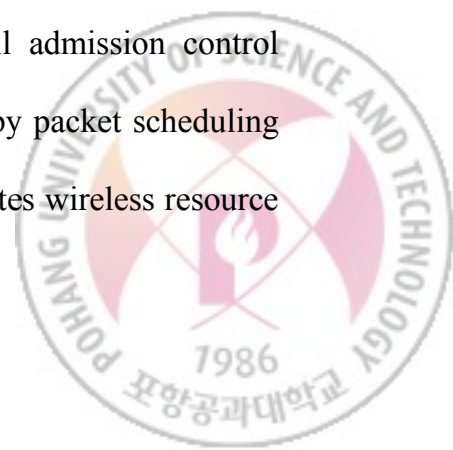


Figure 4-1 The proposed video streaming system over WiMAX network.

To achieve our goal, the cross-layer design is adopted for jointly work among admission control algorithm and packet scheduling algorithm based on video metadata at application layer. The overall architecture of the proposed cross-layer design is shown in Figure 4-2. As shown in the figure, admission control algorithm and packet scheduling algorithm are tightly coupled on the basis of the packet scheduling control variable to effectively improve network utilization in the base station and QoS satisfaction of subscribers simultaneously. In the proposed cross-layer design, call admission control algorithm conduct its function based both the control variable given by packet scheduling algorithm and video metadata, and packet scheduling algorithm allocates wireless resource



to admitted subscribers considering their video buffering picture values calculated by video metadata.

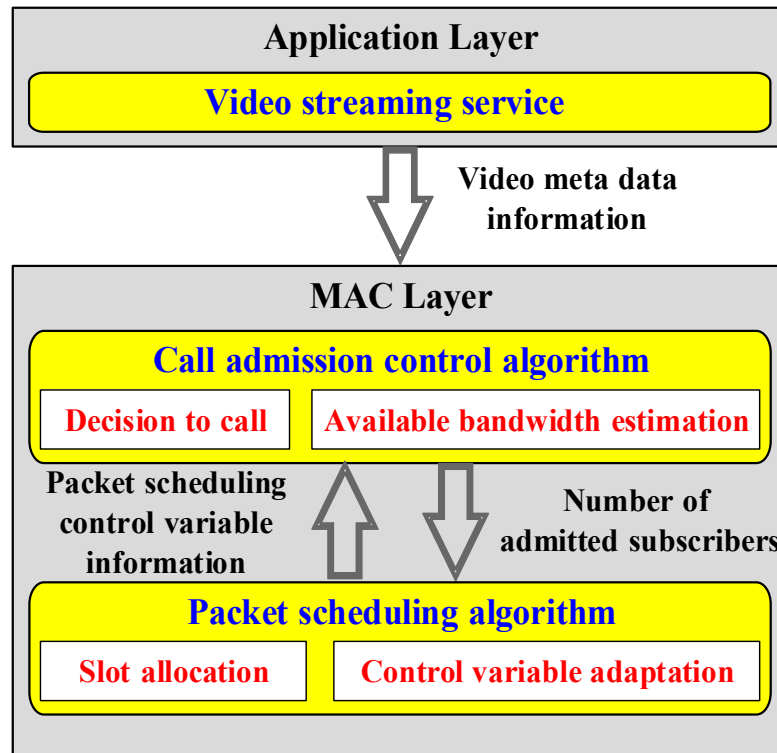
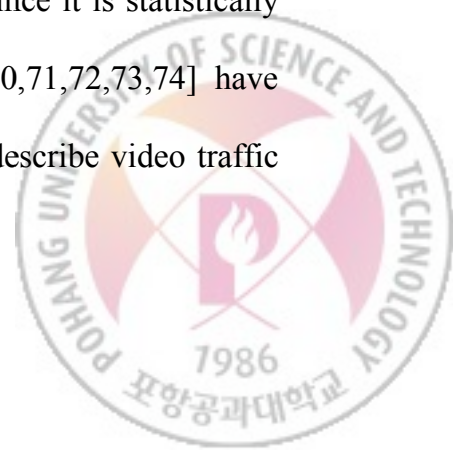


Figure 4-2 Overall architecture of proposed cross-layer design.

4.1 Video Metadata Structure

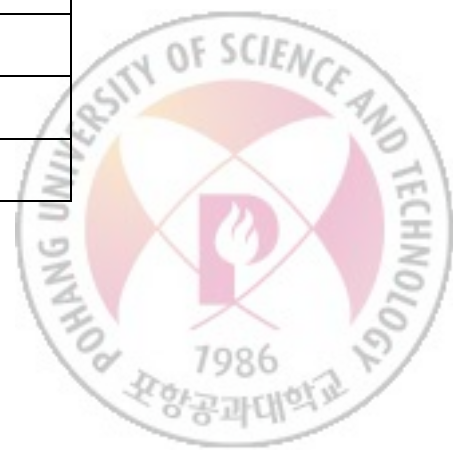
Metadata is employed to effectively describe the characteristics of video traffic. It is a very complicate task to present the characteristics of video traffic since it is statistically non-stationary although many video traffic-modeling techniques [70,71,72,73,74] have been proposed. Because it is very difficult to accurately estimate or describe video traffic



with a fixed statistical property, the proposed system adopts a measurement-based approach based on metadata. Other media-related information such as the coding information of the compressed video stored in the video DB and the video traffic characteristics are saved into metadata. The metadata are then used to enhance the effectiveness of the packet scheduling algorithm and the call admission control algorithm. Table 4-1 shows an example of the proposed metadata DB. The size of the metadata DB is however negligible compared to that of the video DB since these metadata files only contain text data. By using the metadata, we can accurately calculate the buffering urgency with a low computational complexity in the followings.

Table 4-1 The proposed video metadata DB structure (test video is Silence of the Lambs)

<i>Picture No.</i>	<i>GOP No.</i>	<i>Output Bit Rates (bytes)</i>	<i>Encoding Picture Type</i>
1	1	1470	I
2	1	510	P
3	1	540	B
4	1	510	P
...
120	8	1050	P
121	8	720	B
122	8	1320	P
...
159	10	720	B
160	11	37680	I
...



4.2 Proposed λ -based Call Admission Control Algorithm

The number of admitted subscribers is used as a network utilization measure. To achieve our goal, we can formulate call admission control algorithm by using this measure as follows.

Problem Formulation for Call Admission Control Algorithm: Determine

$\vec{U} = (u_1, u_2, \dots, u_{N_{ss}})$ to maximize

$$\sum_{i=1}^{N_{ss}} u_i, \quad (4-1)$$

$$\text{subject to } BW_{avg}^{req}(t) \leq BW_{avg}^{avail}(t, \lambda) \quad (4-2)$$

where u_i is set to 1 only if the i_{th} subscriber is admitted (otherwise it is set to 0), N_{ss} is the total number of subscribers in the cell, λ is a real value variable related to the packet scheduling algorithm, $BW_{avg}^{req}(t)$ and $BW_{avg}^{avail}(t, \lambda)$ are the required average network throughput and the available average network throughput of all subscribers for the next Δ , i.e.

$$BW_{avg}^{req}(t) = \frac{1}{\Delta} \sum_{i=1}^{N_{ss}} \left(u_i \cdot \int_t^{t+\Delta} R_i^{req}(\tau) d\tau \right), \text{ for } \forall t, \quad (4-3)$$

$$BW_{avg}^{avail}(t, \lambda) = \frac{1}{\Delta} \sum_{i=1}^{N_{ss}} \left(u_i \cdot \int_t^{t+\Delta} R_i^{sch}(\tau, \lambda) d\tau \right), \text{ for } \forall t, \quad (4-4)$$



where Δ is the basic time unit in which the packet scheduling algorithm is performed, $R_i^{req}(t)$ is the amount of data that should be transmitted during a WiMAX frame in $(t, t + \Delta)$ for the i_{th} subscriber (it is easily calculated based on the video metadata), and $R_i^{sch}(\tau, \lambda)$ is the resulting amount of transmittable data during a WiMAX frame in $(t, t + \Delta)$ of the i_{th} subscriber determined by the packet scheduling algorithm with a given λ (when the i_{th} subscriber is not selected by the packet scheduling algorithm, $R_i^{sch}(\tau, \lambda)$ is zero).

The process to calculate $BW_{avg}^{avail}(t, \lambda)$ is non-causal because it requires the future information on the wireless network as shown in Eq. 4-4, which is quite a difficult work due to the time-varying wireless network characteristics. Under the assumption that Δ is large enough to smooth out the fast fading effect of the wireless channel and simultaneously the moving distance of subscribers during the Δ interval is negligible, it is possible to say that the network throughput does not change abruptly for the next Δ interval with no change of λ , and thus it is assumed to be independent of time t for the next Δ , i.e.

$$BW_{avg}^{avail}(t, \lambda) \cong BW_{avg}^{est}(\lambda) \text{ for the next } \Delta. \quad (4-5)$$

Now, the estimated network throughput $BW_{avg}^{est}(\lambda)$ is calculated by a measurement-based local linear model of λ if λ is sufficiently close to $\bar{\lambda}_{avg}$. That is,

$$BW_{avg}^{est}(\lambda) = \alpha \cdot \lambda + \beta \text{ if } |\lambda - \bar{\lambda}_{avg}| \leq \varepsilon, \quad (4-6)$$



where α and β are model coefficients, $\bar{\lambda}_{avg}$ is the average value of λ values in the last Δ interval, and ε is a small real number. The coefficients are determined in order to minimize the following weighted error function between the estimated values and the real data set for a number of the last Δ intervals.

$$e_{WMSE} = \sum_{i=1}^{N_{win}} \sum_{j=1}^{M_i} \omega_i \cdot \left(BW_{avg}^{obs}(i, j) - \alpha \cdot \lambda_{i,j} - \beta \right)^2, \quad (4-7)$$

where N_{win} is the number of Δ intervals in a sliding window for the linear model, M_i is the number of entries in the previous i_{th} Δ interval, $BW_{avg}^{obs}(i, j)$ and $\lambda_{i,j}$ are the j_{th} observed average network throughput and the corresponding λ value for the i_{th} Δ interval, and ω_i is the weighting factor for the previous i_{th} Δ interval as shown in Figure 4-3. Since more recent information is further associated with the future channel condition, $\{\omega_i, \text{ for } 1 \leq i \leq N_{win}\}$ should be fixed to satisfy $\omega_m \leq \omega_n$ for $m \geq n$. It means that the proposed model is implicitly considering the mobility change of subscribers.

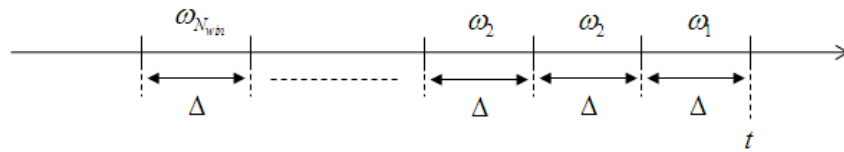


Figure 4-3 Weighting factors for the Δ intervals.

By differentiating Eq. 4-7 with respect to α and β , we can calculate two coefficients to minimize it as follows.



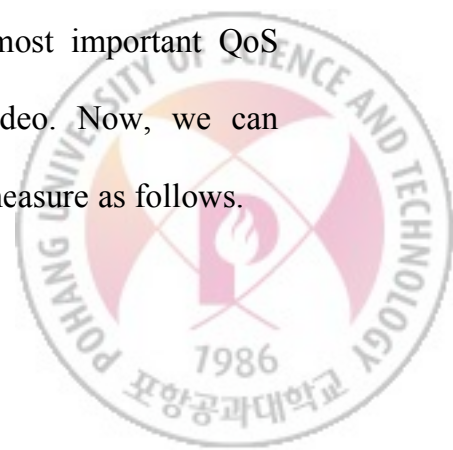
$$\alpha = \frac{\left(\sum_{i=1}^{N_{win}} \sum_{j=1}^{M_i} \omega_i \cdot BW_{avg}^{obs}(i, j) \right) \cdot \left(\sum_{i=1}^{N_{win}} \sum_{j=1}^{M_i} \omega_i \cdot \lambda_{i,j} \right) - \left(\sum_{i=1}^{N_{win}} \omega_i \cdot M_i \right) \left(\sum_{i=1}^{N_{win}} \sum_{j=1}^{M_i} \omega_i \cdot \lambda_{i,j} \cdot BW_{avg}^{obs}(i, j) \right)}{\left(\sum_{i=1}^{N_{win}} \sum_{j=1}^{M_i} \omega_i \cdot \lambda_{i,j} \right)^2 - \left(\sum_{i=1}^{N_{win}} \omega_i \cdot M_i \right) \left(\sum_{i=1}^{N_{win}} \sum_{j=1}^{M_i} \omega_i \cdot \lambda_{i,j}^2 \right)}, \quad (4-8)$$

$$\beta = \frac{\sum_{i=1}^{N_{win}} \sum_{j=1}^{M_i} \omega_i \cdot BW_{avg}^{obs}(i, j) - \alpha \cdot \sum_{i=1}^{N_{win}} \sum_{j=1}^{M_i} \omega_i \cdot \lambda_{i,j}}{\sum_{i=1}^{N_{win}} \omega_i \cdot M_i}. \quad (4-9)$$

Furthermore, we use an outlier removal process to improve the model accuracy. In other words, if the difference between an observed datum and the model-based estimated datum is greater than one standard deviation, the datum is removed. Based on the filtered data, we can derive the network throughput model again by using the same method. Actually, Δ and $\{\omega_i\}$ should be determined by considering the channel fading effect and the subscribers' mobility. Finally, if $BW_{avg}^{req}(t) \leq BW_{avg}^{est}(\lambda)$ for the next Δ interval, the new subscriber is accommodated. Otherwise the new subscriber is not admitted.

4.3 Proposed Video Metadata and Link Condition-aware Packet Scheduling Algorithm

Scene freezing, caused by buffer underflow, is one of the most important QoS factors for video streaming services since it incurs unsmooth video. Now, we can formulate our problem for packet scheduling algorithm by using this measure as follows.



Problem Formulation for Packet Scheduling Algorithm: Select u_i from admitted subscribers as the next in-service subscriber to maximize

$$\lambda \cdot \text{buffer}_i(t) + (1 - \lambda) \cdot BW(mcs_i(t)), \quad (4-10)$$

where $\text{buffer}_i(t)$, the buffer urgency, is the buffer occupancy of the i_{th} subscriber at time t and $BW(mcs_i(t))$ is the bandwidth of the i_{th} subscriber at time t when $mcs_i(t)$ is chosen based on the CQI over WiMAX network as shown in Table 4-2. As an aside from the above, it is well known that compressed video traffic is in burst pattern and is non-stationary. Therefore, the absolute size of buffered data is sometimes not a proper measure for stable video streaming quality. Instead, the number of video pictures stored at the buffer is a more reasonable measure. Thus the buffering urgency is defined by

$$\text{buffer}_i(t) = \max(T_{Th} - f_i(t), 0), \quad (4-11)$$

where T_{Th} is the threshold value required for smooth video streaming over a time-varying wireless network, and $f_i(t)$ is the number of video pictures piled up at the buffer at time t (it is also easily calculated by using video metadata). When the number of buffered video pictures is larger than T_{Th} , a subscriber starts the video play-out.



Table 4-2 Relationship among the SNR threshold values, the chosen MCSs/coding rate, and the corresponding bandwidth values of WiMAX network.

<i>SNR Threshold Value</i>		<i>MCS, Overall Coding Rate</i>	<i>BW(MCS)</i>
-	11.2 dB	QPSK, 1/2	48 bits/slot
11.2 dB	16.4 dB	QPSK, 3/4	72 bits/slot
16.4 dB	18.2 dB	16QAM, 1/2	96 bits/slot
18.2 dB	22.7 dB	16QAM, 3/4	144 bits/slot
22.7 dB	24.4 dB	64QAM, 2/3	192 bits/slot
24.4 dB	-	64QAM, 3/4	216 bits/slot

By adaptively controlling λ , the call admission control algorithm and the packet scheduling algorithm work together. As λ decreases, $BW_{avg}^{avail}(t, \lambda)$ generally increases and thus more subscribers can be admitted even though the probability of scene freezing may increase as well, vice versa. Now we study the λ adaptation algorithm; the proposed algorithm controls λ based on the observed average scene freezing rates of subscribers and the target scene freezing rate, i.e.

$$\lambda = 1 / \left(1 + \left(SF_{target} / SF_{avg} \right)^k \right), \quad (4-12)$$

$$SF_{avg} = \frac{\sum_{i=1}^{N_{ss}} SF_i \cdot u_i}{\sum_{i=1}^{N_{ss}} u_i}, \quad (4-13)$$

$$SF_i = \frac{P_i^{frozen}}{P_{win}}, \quad (4-14)$$



where SF_{target} is the pre-determined target scene freezing rate, P_{win} is the number of pictures in a sliding window of size N_{SF} , and P_i^{frozen} is the number of frozen pictures of the i_{th} subscriber in the window.

4.4 Performance Evaluation

During the simulation, NS-2 [68] and WiMAX module [75] are employed. Initially, 40 subscribers are uniformly distributed in the cell and moving by the Random Waypoint model. H.264 is adopted as the video codec and CIF-size compressed video trace files [76] at 30 pps (pictures per sec) are used as shown in Table 4-3. And, a streaming service request from 40 subscribers is generated every 2 second after the start of service, and the rejected subscribers continuously make a join request every 2 second. 300 slots per WiMAX frame are reserved for the streaming service. The parameters of OFDMA are fixed as shown in Table 4-4. Basically, AWGN (Additive White Gaussian Noise) wireless channel model is used with the shadowing effect. The total simulation time and T_{Th} are set to 1000 seconds and 150, respectively.



Table 4-3 Summary of test video sequences.

<i>Test Video</i>	<i>QP</i>	<i>Mean Rate (bps)</i>	<i>Peak Rate (bps)</i>
Silence of the Lambs	24	249959	7401120
	48	15407	437040
Star Wars IV	24	265247	3685440
	48	17165	414960
NBC News	24	848557	7438800
	48	35915	840960
Sony Demo	24	710261	9040800
	48	28612	692880
Tokyo Olympics	24	526165	8508240
	48	27106	484080



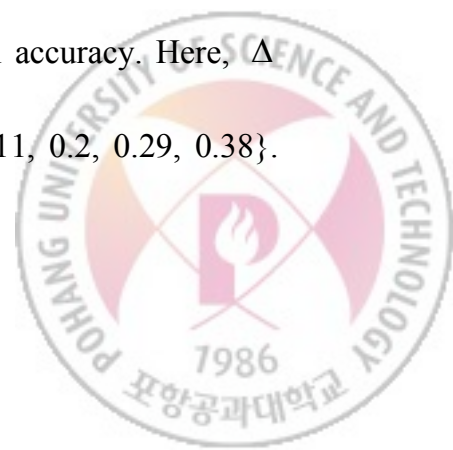
Table 4-4 OFDMA parameters during simulation.

<i>Parameter</i>	<i>Value</i>
Channel Bandwidth (MHz)	20
FFT size	2048-FFT PUSC
Number of used data subcarriers	1440
Number of subchannels	30
Number of pilot subcarriers	240
Number of null & guardband subcarriers	368
Cyclic prefix or guard time	1/8
Oversampling rate	28/25
Subcarrier frequency spacing (kHz)	10.94
Useful symbol time (μs)	91.4
Guard time (μs)	11.4
OFDM symbol duration (μs)	102.86
WiMAX frame	5 ms
Number of OFDM symbols in a WiMAX frame	48

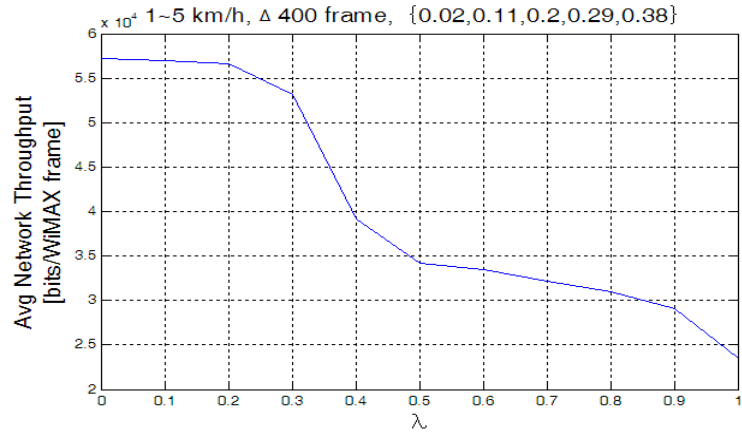
4.4.1 Performance Verification of Network Throughput Estimation

Model

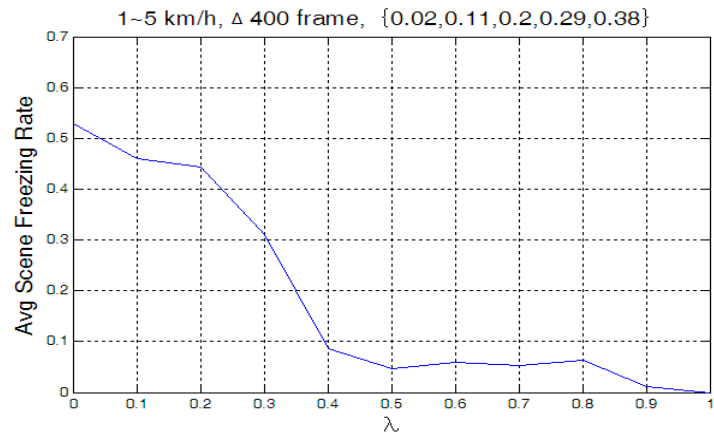
In this section, we verify the proposed network throughput estimation model and show the relationship among subscriber speed, Δ , $\{\omega_i\}$, and model accuracy. Here, Δ and $\{\omega_i\}$ are empirically set to 400 WiMAX frames and $\{0.02, 0.11, 0.2, 0.29, 0.38\}$.



First, we investigate the average scene freezing rate and the average network throughput with λ changing from 0 to 1. The result is given in Figure 4-4. It is clear in (a) of Figure 4-4 that the average network throughput almost monotonically decreases as λ increases. However, the average network throughput curve is a nonlinear function of λ . Now, a local linearization technique is adopted to obtain an approximate mathematical model with a low computational complexity.



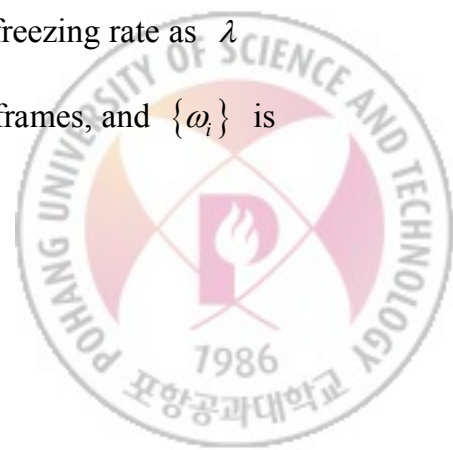
(a)



(b)

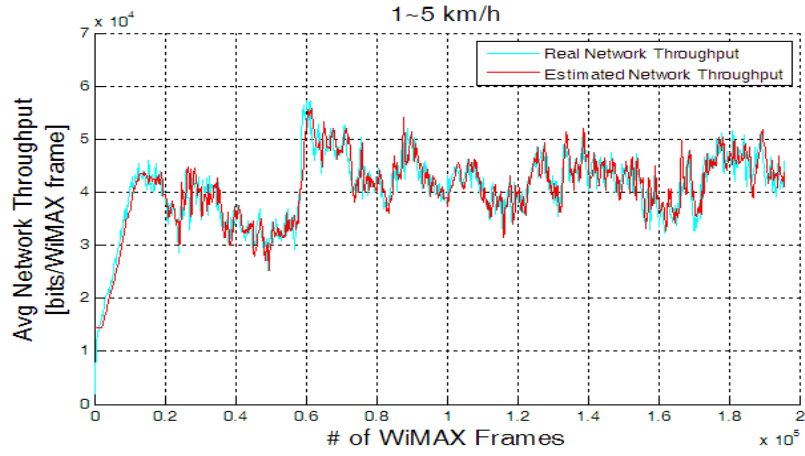
Figure 4-4 Plots of average network throughput and average scene freezing rate as λ changes from 0 to 1 when the speed is 1~5 km/h, Δ is 400 WiMAX frames, and $\{\omega_i\}$ is

$\{0.02, 0.11, 0.2, 0.29, 0.38\}$.

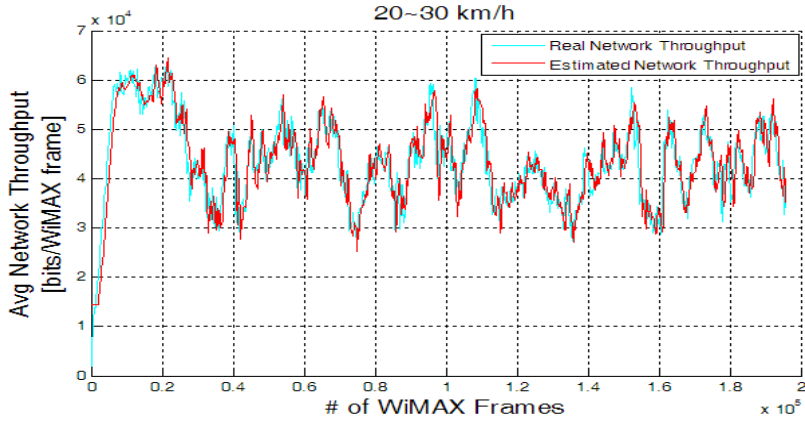


The estimated network throughput curve and the real network throughput curve are presented in Figure 4-5. It is demonstrated that the average estimation error rate, which is the average ratio of error between the real network throughput and the estimated network throughput, is 5.81058 % when the speed is 1~5 km/h as in (a) of the figure, 7.22387 % when the speed is 20~30 km/h as in (b) of the figure, and 8.88921 % when the speed is 60~70 km/h as in (c) of the figure. These results show that the proposed local linear network throughput model works reasonably well. It is also observed that the estimation error becomes slightly larger as the speed is increasing. Hence we need to adjust and according to the speed of the subscribers to improve the model accuracy.

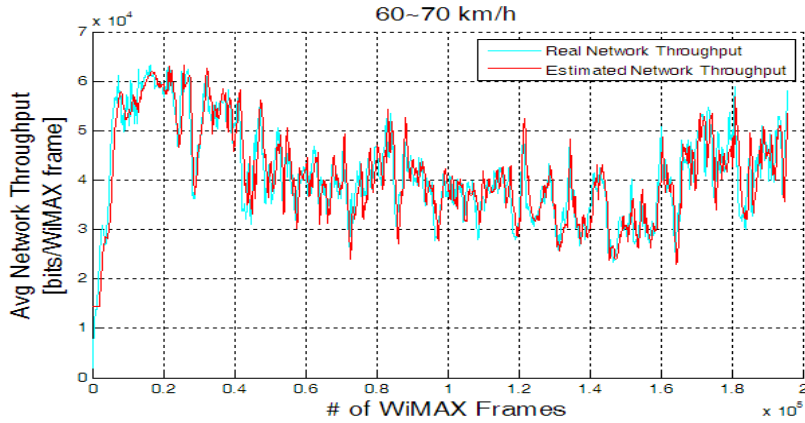




(a)

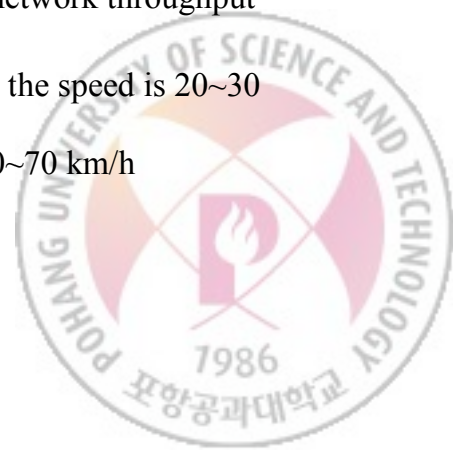


(b)



(c)

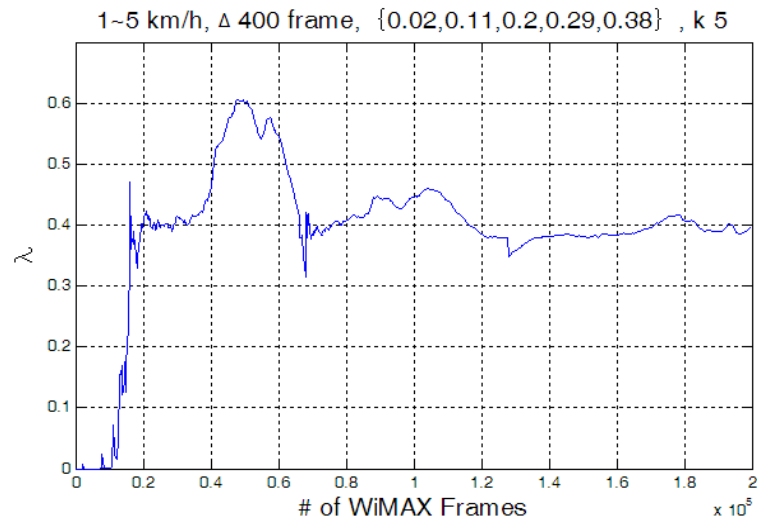
Figure 4-5 Network throughput estimation accuracy according to the speed when Δ is 400 WiMAX frames, and $\{\omega_i\}$ is $\{0.02, 0.11, 0.2, 0.29, 0.38\}$: (a) network throughput plots when the speed is 1~5 km/h, (b) network throughput plots when the speed is 20~30 km/h, and (c) network throughput plots when the speed is 60~70 km/h



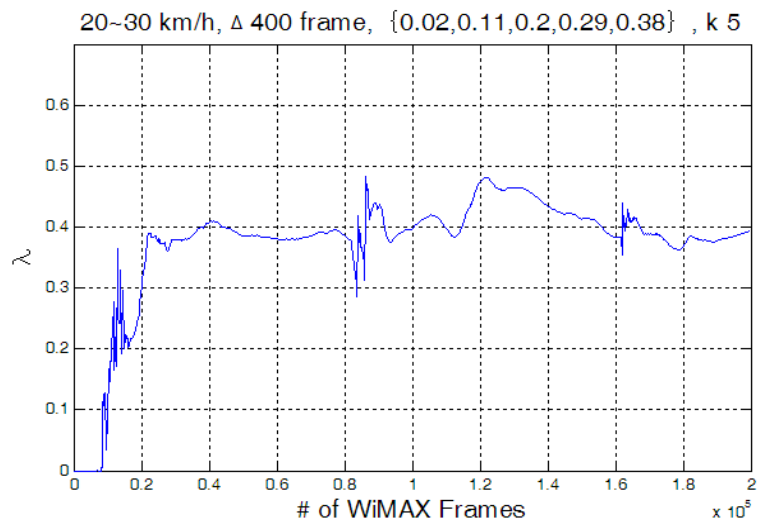
4.4.2 Performance Verification of λ Adjustment Algorithm

As is shown in (b) of Figure 4-4, the average scene freezing rate also almost monotonically decreases as λ increases. This result means that an effective tradeoff between the average scene freezing rate and the average network throughput can be attained by adjusting λ . Next, the performance of the proposed λ adjustment algorithm is presented. Initially, λ and N_{SF} are set to 0 and 21,000 pictures (700 seconds), respectively. In addition, the target scene freezing rate is fixed to 0.14 during the simulation. The simulation results are provided in Figure 4-6; (a), (c), and (e) represent the plots of time-varying λ , and (b), (d) and (f) are the corresponding plots of the average scene freezing rates when the speed of subscribers is 1~5 km/h, 20~30 km/h, or 60~70 km/h. It is clear in (a) and (b) of Figure 4-6 that λ rapidly increases when the average scene freezing rate becomes larger than the target scene freezing rate, and slowly changes when the average scene freezing rate stays around the target scene freezing rate. Furthermore, the adaptation speed of λ becomes faster as the speed of subscribers increases. The reason is that the wireless network conditions changes faster depending on the speed of subscribers. As a result of the above, it is apparent that the resulting average scene freezing rate stays around the tolerable target scene freezing rate regardless of the speed of subscribers. The summarized results are presented in Table 4-5 in the following section; the resulting average scene freezing rates of the proposed system are about 0.14 (target scene freezing rate) in spite of the speed of subscribers.

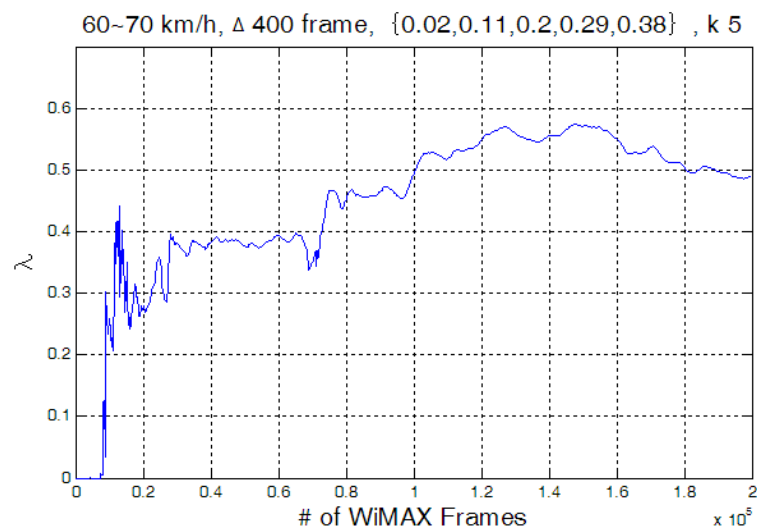




(a)

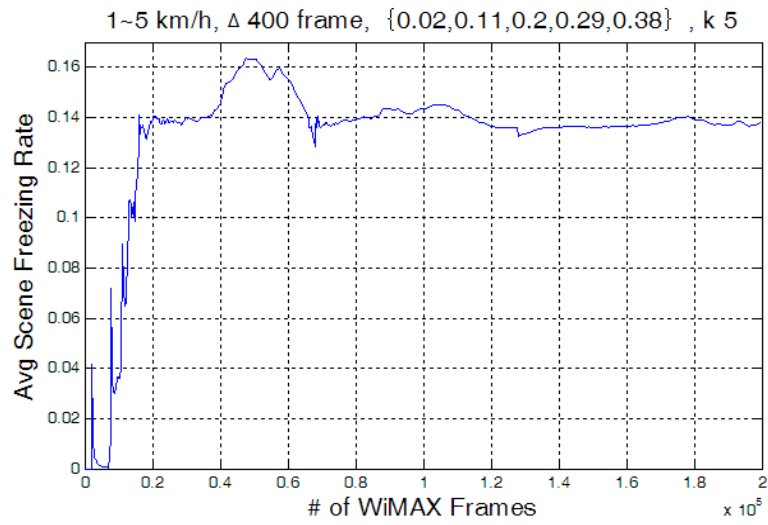


(b)

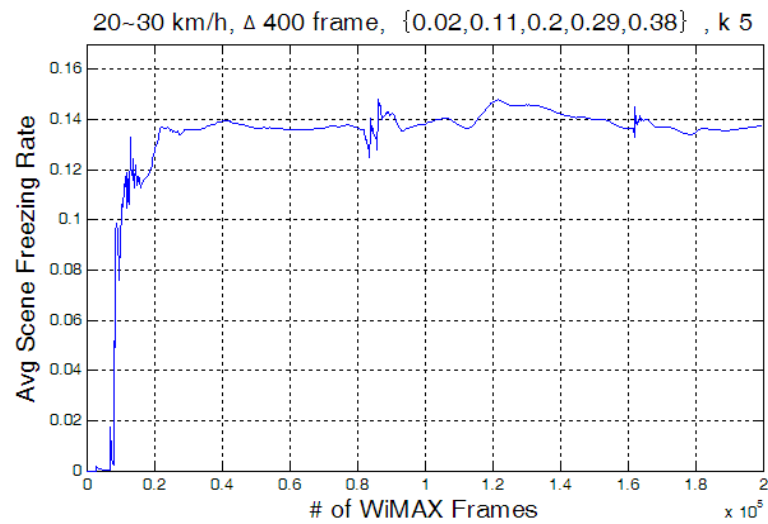


(c)

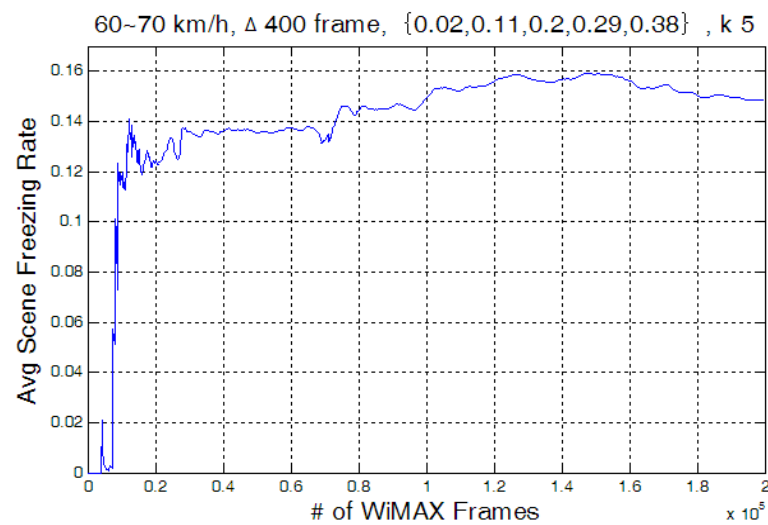




(d)



(e)



(f)



Figure 4-6 Dynamic adjustment of λ and the corresponding average scene freezing rate :

(a) λ plot when the speed is 1~5 km/h, (b) λ plot when the speed is 20~30 km/h, (c) λ plot when speed is 60~70 km/h, (d) average scene freezing rate plot when the speed is 1~5 km/h, (e) average scene freezing rate plot when the speed is 20~30 km/h, and (f) average scene freezing rate plot when the speed is 60~70 km/h.

4.4.3 Performance Comparison with Existing Algorithms

We compare the proposed joint working packet scheduling algorithm and call admission control algorithm with existing algorithms including MAX SNR, PF, MLWDF and EXP in terms of the average scene freezing rate and the average network throughput. The existing algorithms estimate the available network throughput by just averaging the observed network throughput values during the last multiple Δ intervals, and perform the admission process by the same method as the proposed algorithm. The tolerable maximum delay of MLWDF and EXP is set to 700ms. The simulation results are summarized in Table 4-5. It is observed in the table that the proposed system significantly reduces the average scene freezing rate of the admitted subscribers and accommodates more subscribers earlier after the start of streaming service in the cell while the average network throughput is a little decreased compared to existing algorithms.



Table 4-5 Performance comparison with existing scheduling algorithms: (a) when speed is 1~5 km/h, (b) when speed is 20~30 km/h, and (c) when speed is 60~70 km/h.

<i>Scheduler</i>	<i>Avg. Scene Freezing Rate</i>	<i># of Admitted Subs. (at the 1st req. / by the end)</i>	<i>Avg. Network Throughput [bits / WiMAX frame]</i>
MAX SNR	0.5132219	33 / 40	56417.52
PF	0.2027471	27 / 34	44307.98
MLWDF	0.2221635	29 / 35	41371.42
EXP	0.2666852	27 / 34	36809.89
Prop. Sys.	0.1380518	33 / 38	40386.52

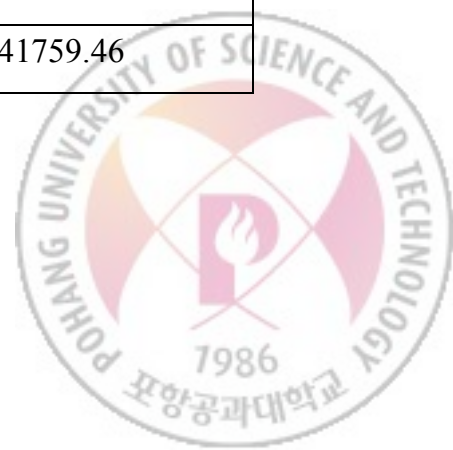
(a)

<i>Scheduler</i>	<i>Avg. Scene Freezing Rate</i>	<i># of Admitted Subs. (at the 1st req. / by the end)</i>	<i>Avg. Network Throughput [bits / WiMAX frame]</i>
MAX SNR	0.3211376	36 / 40	63356.61
PF	0.2080184	31 / 38	47167.66
MLWDF	0.2423837	30 / 38	46223.67
EXP	0.2883577	29 / 33	38391.91
Prop. Sys.	0.1374578	35 / 40	45759.81

(b)

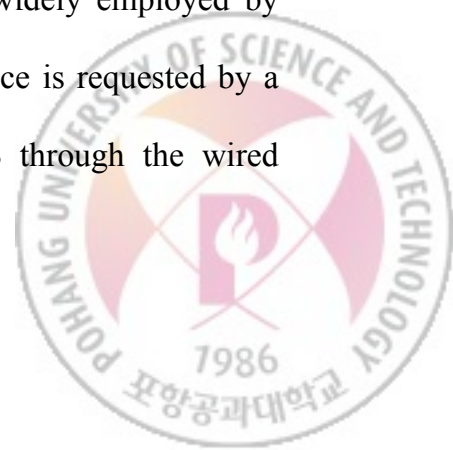
<i>Scheduler</i>	<i>Avg. Scene Freezing Rate</i>	<i># of Admitted Subs. (at the 1st req. / by the end)</i>	<i>Avg. Network Throughput [bits / WiMAX frame]</i>
MAX SNR	0.3067084	38 / 40	63209.19
PF	0.1941032	28 / 40	51411.30
MLWDF	0.2144849	27 / 40	50404.77
EXP	0.3079316	23 / 31	39465.26
Prop. Sys.	0.1487079	37 / 40	41759.46

(c)



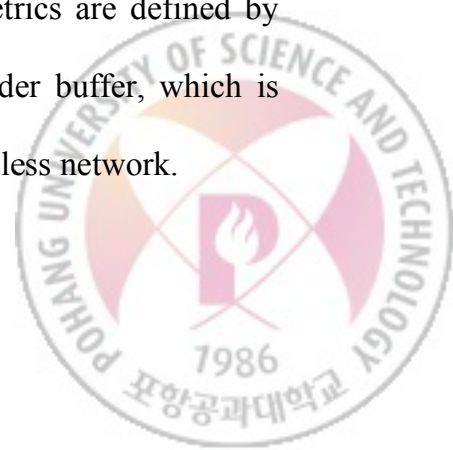
V. QoE-based Interworking Packet Scheduling, Call Admission Control, and Handover System for Video Streaming Services over LTE network

The goal of the proposed system is to effectively provide seamless video streaming services to UEs, and improve cell load balancing among immediately adjacent eNodeBs to support the fair service quality among UEs located in the other neighboring cells. The overall structure of the proposed interworking system is shown in Figure 5-1. The target application under our consideration in this dissertation is HTTP (Hyper Text Transfer Protocol) progressive download video streaming service, which is widely employed by YouTube, Vimeo, and MSN Soapbox. When a video streaming service is requested by a UE, the video content server transmits video data to the eNodeB through the wired



backbone network. In the RRC (Radio Resource Control) of the eNodeB, the connection controller establishes the link for video streaming service with the requirements such as video encoding data rate, initial latency, and frames per second, and the call admission controller determines whether the UE is accepted or not. The packet scheduler in the MAC allocates the RBs to admitted UEs according to a scheduling policy. When a UE approaches more closely other adjacent eNodeB than its serving eNodeB, a handover is triggered to switch to the target eNodeB.

To achieve our goal, an effective interworking packet scheduling, call admission control, and handover system is proposed in this dissertation. The interworking mechanism among the components of the proposed system is presented in Figure 5-2. As shown in the figure, the packet scheduling, call admission control, and handover algorithms are tightly coupled on the basis of the QoE state information of UEs and cells in order to not only enhance the QoE of admitted UEs, but also attain well-balanced traffic load among adjacent cells. In the proposed interworking system, the packet scheduling algorithm allocates RBs to all admitted UEs by considering the QoE states of UEs and wireless link states simultaneously, and the proposed call admission control algorithm is trying to stochastically guarantee the QoE states of already admitted UEs and provide video streaming services to as many UEs as possible. Finally, the proposed handover algorithm determines the proper handover trigger based on the QoE state of UE to efficiently distribute the traffic load to adjacent eNodeBs. First of all, QoE metrics are defined by considering the amount of buffered video frames at the video decoder buffer, which is associated with video streaming service quality over time-varying wireless network.



Definition of QoE state of a UE: The QoE state of the i_{th} UE ($q_{UE_i}(t)$) is defined by

$$q_{UE_i}(t) = \begin{cases} \frac{F_{FPS} \cdot T_{RB}}{r_i^{en}} \int_0^t r_i^{sch}(\tau) d\tau - F_{FPS} \cdot (t - t_0 - T_{init}), & \text{if } t \geq t_0 + T_{init}, \\ \frac{F_{FPS} \cdot T_{RB}}{r_i^{en}} \int_0^t r_i^{sch}(\tau) d\tau & \text{otherwise,} \end{cases} \quad (5-1)$$

$$r_i^{sch}(\tau) = r_i(\tau) \cdot n_i^{sch}(\tau), \quad (5-2)$$

where F_{FPS} is a frame per second of the video streaming service, T_{RB} is the time duration of the resource block, r_i^{en} is the video encoding data rate of the i_{th} UE, $r_i^{sch}(\tau)$ is the transmitted data rate of the i_{th} UE at the time τ , t_0 is the time when the video streaming service is requested by a UE, T_{init} is an initial latency of the video streaming service, $r_i(\tau)$ is the data rate of the i_{th} UE at the time τ when a modulation scheme is automatically selected by AMC (Adaptive Modulation and Coding) module of eNodeB, and $n_i^{sch}(\tau)$ is the number of RBs allocated by the packet scheduling algorithm to the i_{th} UE at the time τ .

Definition of QoE state of a cell: The QoE state of the j_{th} eNodeB ($q_{eNB_j}(t)$) is defined as a function of the variance of QoE states of UEs from the predefined target frame buffering threshold, i.e.

$$q_{eNB_j}(t) = \frac{1}{N_j} \sum_{i=1}^{N_j} \left(\max \{ B_{target}^{fr} - q_{UE_i}(t), 0 \} \right)^2, \quad (5-3)$$



where B_{target}^{fr} is the predefined target frame buffering threshold and N_j is the number of admitted UEs in the j_{th} eNodeB.

Definition of cell availability: The cell availability metric of the j_{th} eNodeB ($ca_{eNB_j}(t)$) is defined as the ratio of the number of UEs satisfying QoE (that have more buffered video frames than the predefined target frame buffering threshold) to all admitted UEs, i.e.

$$ca_{eNB_j}(t) = \frac{n(UE \text{ with } q_{UE_i}(t) \geq B_{target}^{fr})}{N_j} = 1 - \frac{n(UE \text{ with } q_{UE_i}(t) < B_{target}^{fr})}{N_j} \quad (5-4)$$

$$= 1 - \frac{1}{N_j} \sum_{i=1}^{N_j} \left\lceil \max \left\{ 0, 1 - \frac{q_{UE_i}(t)}{B_{target}^{fr}} \right\} \right\rceil,$$

where $\lceil x \rceil$ is the smallest integer that is not less than x .

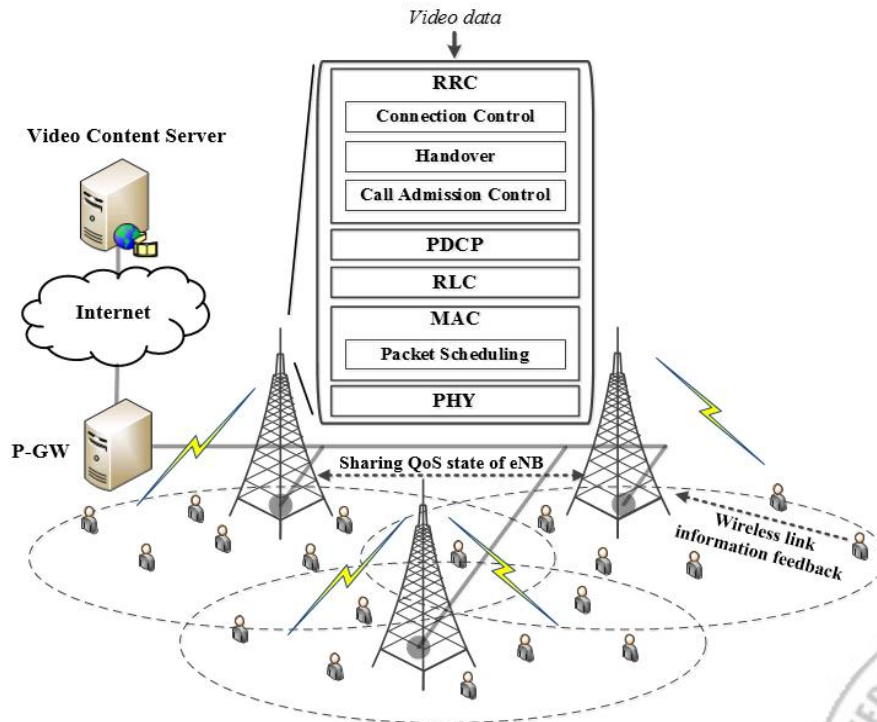


Figure 5-1 Overall structure of the proposed interworking system over LTE network.

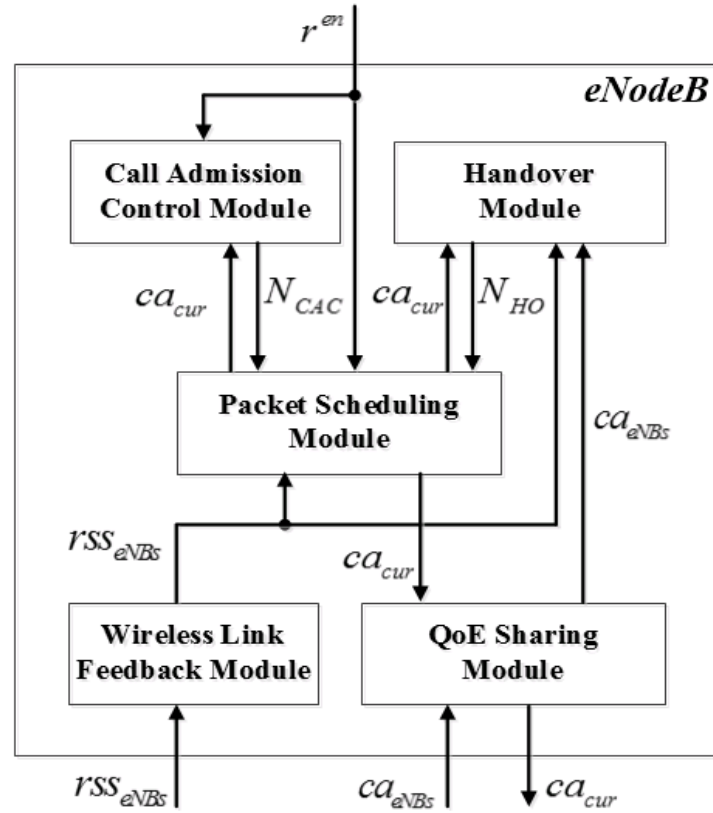


Figure 5-2 The interworking mechanism of the proposed system components.

5.1 Proposed Packet Scheduling Algorithm

The proposed scheduling algorithm is designed to avoid the receiver buffer underflow of as many admitted UEs as possible by regulating the amount of buffered video data. It is well known that the receiver buffer underflow causes unsmooth video play-out. Now, we can formulate our packet scheduling problem as follows.



Problem Formulation for Packet Scheduling Algorithm: Select UE_i among admitted UEs for each RB to maximize both the QoE improvement and the network utilization in a cell after T_{RB}

$$\alpha \cdot \frac{r_i(t)}{R_{MAX}} + (1 - \alpha) \cdot \frac{q_{eNB_j}(t) - q_{eNB_j}(t + T_{RB})|_{UE_i}}{q_{eNB_j}(t) - \min_{1 \leq k \leq N_j} q_{eNB_j}(t + T_{RB})|_{UE_k}} \quad \text{for } \forall i, \quad (5-5)$$

where α is the weighting factor between QoE states of UE and achievable data rate ($0 \leq \alpha \leq 1$), R_{MAX} is the maximum data rate when the most dense modulation scheme is selected regardless of the channel conditions, and $q_{eNB_j}(t + T_{RB})|_{UE_i}$ is the QoE state of the j_{th} eNodeB at the time $t + T_{RB}$ when the i_{th} UE is selected, which is calculated by

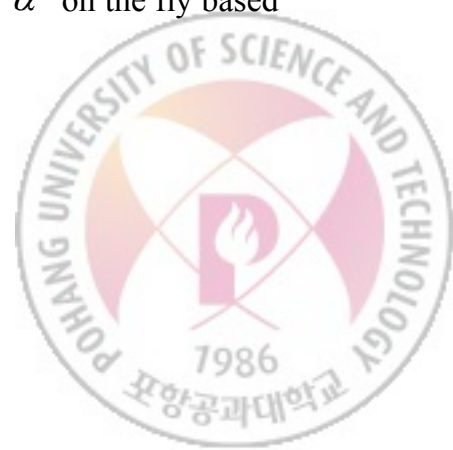
$$q_{eNB_j}(t + T_{RB})|_{UE_i} = \frac{1}{N_j} \sum_{k=1}^{N_j} \left(\delta_{ik} \cdot \max \left\{ B_{target}^{fr} - \left(q_{UE_k}(t) + \left(F_{FPS} \cdot \frac{r_k(t) \cdot T_{RB}}{r_k^{en}} \right) \right), 0 \right\} + (1 - \delta_{ik}) \cdot \max \left\{ B_{target}^{fr} - q_{UE_k}(t), 0 \right\} \right)^2, \quad (5-6)$$

$$\delta_{ik} = \begin{cases} 1, & \text{if } i = k, \\ 0, & \text{otherwise.} \end{cases} \quad (5-7)$$

Now, the optimal solution of the above problem is selected by

$$i^* = \arg \max_{1 \leq i \leq N_{UE}} \left\{ \alpha \cdot \frac{r_i(t)}{R_{MAX}} + (1 - \alpha) \cdot \frac{q_{eNB_j}(t) - q_{eNB_j}(t + T_{RB})|_{UE_i}}{q_{eNB_j}(t) - \min_{1 \leq k \leq N_j} q_{eNB_j}(t + T_{RB})|_{UE_k}} \right\}. \quad (5-8)$$

Furthermore, the proposed scheduling algorithm dynamically controls α on the fly based on the QoE states of UEs as shown in Eqs. 5-9 and 5-10.



$$\alpha = e^{\frac{-a_{adt} \left(b_{adt} \frac{q_{UE}^{MIN}(t)}{B_{target}^{fr}} \right)}{1 + e^{-a_{adt} \left(b_{adt} \frac{q_{UE}^{MIN}(t)}{B_{target}^{fr}} \right)}}}, \quad (5-9)$$

$$q_{UE}^{MIN}(t) = \min_{1 \leq k \leq N_j} \left\{ \min \left\{ B_{target}^{fr}, q_{UE_k}(t) \right\} \right\}, \quad (5-10)$$

where a_{adt} and b_{adt} are design parameters that determine the slope of the curve and location of inflection point of the curve, respectively. As α increases, the wireless network utilization can be improved at the cost of QoE states of UEs, and vice versa.

5.2 Proposed Call Admission Control Algorithm

The objective of the call admission control algorithm is to maximize the number of admitted UEs while guaranteeing smooth video streaming services. To effectively support the seamless video streaming services to all admitted UEs, the proposed call admission control algorithm determines whether new call requests are admitted or not by checking the cell availability metric. Under the assumption that new call requests are Poisson distributed [77] and the remaining time that an existing UE will stay in the cell is Pareto distributed [78], the cell availability metric can be estimated at the predicted next call arriving time. Since the inter arriving time between two adjacent new call requests is Exponential distributed when new call requests are Poisson distributed, the next call inter arriving time is stochastically represented by



$$t_{\Delta} = -\frac{1}{\lambda} \log_e (1 - F(t_{\Delta})), \quad (5-11)$$

where λ is the incoming arrival rate and $F(t_{\Delta})$ is the cumulative distribution function of Exponential distribution. Thus, the UE livability after t_{Δ} can be predicted as follows.

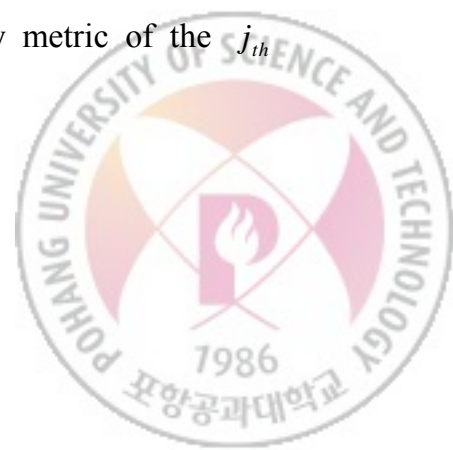
$$\begin{aligned} p_i &= \Pr(X_i > t_i^{stay} + t_{\Delta} | X_i > t_i^{stay}) \\ &= \frac{\left(1 + \frac{t_i^{stay} + t_{\Delta}}{\beta_{prt}}\right)^{-\alpha_{prt}}}{\left(1 + \frac{t_i^{stay}}{\beta_{prt}}\right)^{-\alpha_{prt}}} = \left(\frac{1 + \frac{t_i^{stay} + t_{\Delta}}{\beta_{prt}}}{1 + \frac{t_i^{stay}}{\beta_{prt}}}\right)^{-\alpha_{prt}} = \left(\frac{\beta_{prt} + t_i^{stay}}{\beta_{prt} + t_i^{stay} + t_{\Delta}}\right)^{\alpha_{prt}}, \end{aligned} \quad (5-12)$$

where X_i is the random variable representing the survival time of the i_{th} UE, t_i^{stay} is the time interval that the i_{th} UE has been staying in a cell, and α_{prt} and β_{prt} are parameters of the Pareto distribution. Now, we are able to estimate the QoE state of the i_{th} UE at the time $t + t_{\Delta}$ by

$$\tilde{q}_{UE_i}(t + t_{\Delta}) = q_{UE_i}(t) + F_{FPS} \cdot \frac{r_i^{avg}(t) \cdot t_{\Delta}}{r_i^{en}} - F_{FPS} \cdot t_{\Delta}, \quad (5-13)$$

$$r_i^{avg}(t) = \frac{1}{\Delta_{win}} \int_{t-\Delta_{win}}^t r_i^{sch}(\tau) d\tau, \quad (5-14)$$

where Δ_{win} is the time interval of a sliding window that is large enough to smooth out the fast fading effect of the wireless channel and simultaneously the moving distance of UE during the Δ_{win} interval is negligible. Finally, the cell availability metric of the j_{th} eNodeB at the time $t + t_{\Delta}$ is estimated by



$$\widetilde{ca}_{eNB_j}(t+t_\Delta) = 1 - \frac{\sum_{i=1}^{N_j} p_i \cdot \left[\max \left\{ 0, 1 - \frac{\tilde{q}_{UE_i}(t+t_\Delta)}{B_{target}^{fr}} \right\} \right]}{\sum_{i=1}^{N_j} p_i}. \quad (5-15)$$

When a new call request is arrived, the eNodeB determines its admission by checking the following criterion.

Criterion for Call Admission Control:

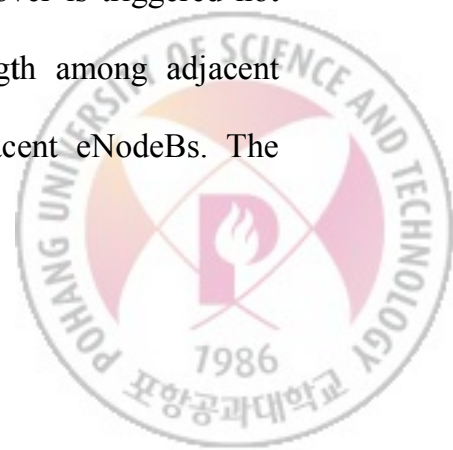
$$\text{If } \widetilde{ca}_{eNB_j}(t+t_\Delta) \geq T_{CA}, \quad \text{then accept the new call request.} \quad (5-16)$$

Otherwise, reject the new call request.

where T_{CA} is the threshold value that determines whether a cell is overloaded or not. As T_{CA} increases, the proposed call admission controller permits a new call conservatively, and thus the QoE state in a cell is enhanced even though a less number of UEs are admitted, and vice versa.

5.3 Proposed Handover Algorithm

Compared to existing handover algorithms, one of the most significant and distinctive features of the proposed handover algorithm is that handover is triggered not only to select an eNodeB with the highest received signal strength among adjacent eNodeBs, but also keep a balance of the QoE states among adjacent eNodeBs. The



handover problem is formulated as follows to take into account both the cell availability metrics of neighboring eNodeBs and the received signal strength.

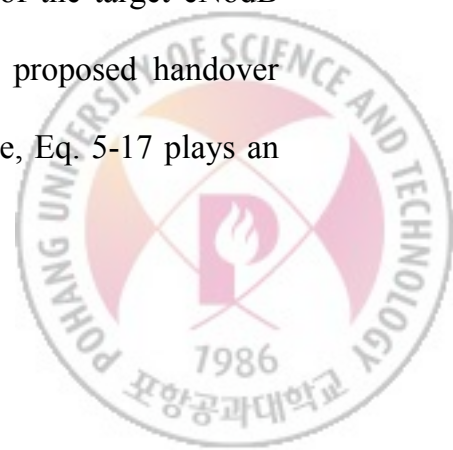
Criterion for Handover: The current eNodeB serving the handover triggered UE selects the eNB_j with the maximum cell availability metric among immediately adjacent eNodeBs

$$\text{subject to } ca_{eNB_j}(t) - ca_{eNB_{SeNB}}(t) \geq T_{HO}, \quad (5-17)$$

$$\left| r_{SS_j}(t) - r_{SS_{SeNB}}(t) \right| \leq T_{RSS}, \quad (5-18)$$

where $SeNB$ is the current serving eNodeB index of the handover triggered UE, $r_{SS_j}(t)$ is the received signal strength between the triggered UE and the j_{th} eNodeB at the time t , T_{RSS} is the maximum difference value among the received signal strength values (its physical meaning is an overlapped distance range of adjacent cells for handover triggering), and T_{HO} is the minimum difference value among the cell availability metrics.

The load balancing among adjacent cells is achieved by transferring UEs from the overloaded eNodeB with cell availability metric less than T_{CA} to the idle eNodeB with wireless resources enough for the transferred UE while satisfying Eqs. 5-17 and 5-18. In other words, when handover occurs, if the target eNodeB does not have wireless resources to support both existing UEs and the transferred UE, the QoE state of the target eNodeB may be seriously deteriorated after the handover is complete. The proposed handover checks Eqs. 5-17 and 5-18 to avoid this undesirable case. Furthermore, Eq. 5-17 plays an



important role in preventing the ping-pong effect of transferred UEs, which may incur repeated handover requests and unnecessary control signaling overhead.

Figure 5-3 illustrates the whole handover procedure. The adjacent eNodeBs periodically exchange their cell availability metrics, and the UE periodically reports its wireless link states to the current serving eNodeB. The proposed handover algorithm of the serving eNodeB makes a decision on whether a handover is triggered or not. When a handover trigger is determined, the current serving eNodeB sends the handover request message to the target eNodeB. The corresponding target eNodeB replies to the serving eNodeB by sending back the handover response message. Finally, the serving eNodeB notifies the UE handover trigger by sending the handover command message as soon as the handover response message is arrived.

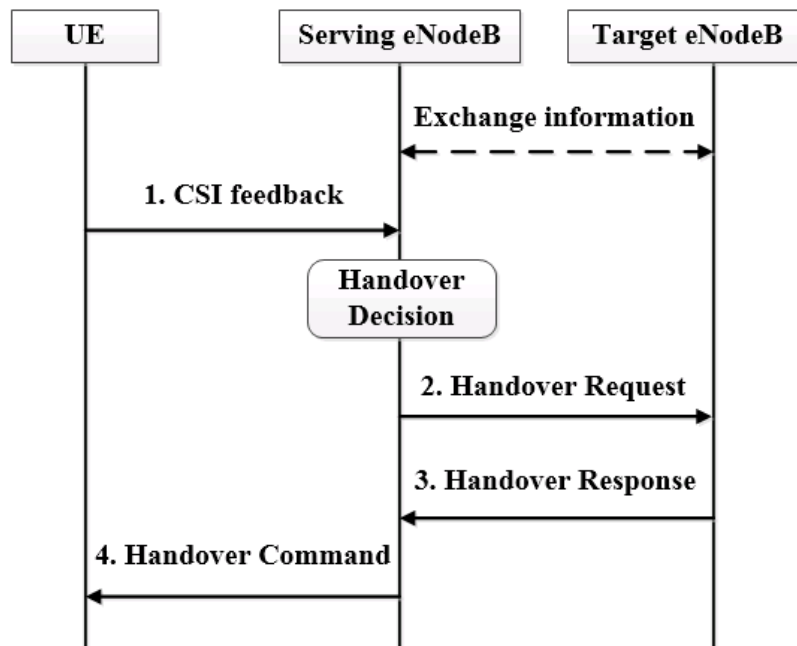
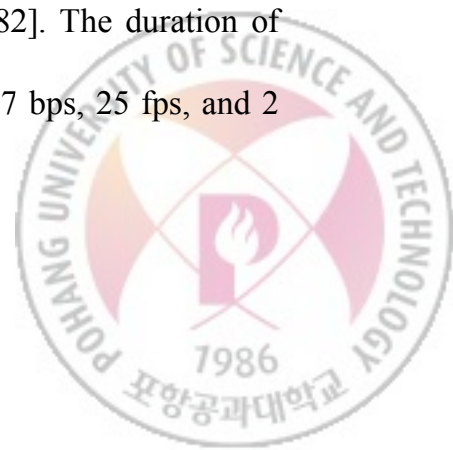


Figure 5-3 The handover preparation procedure.



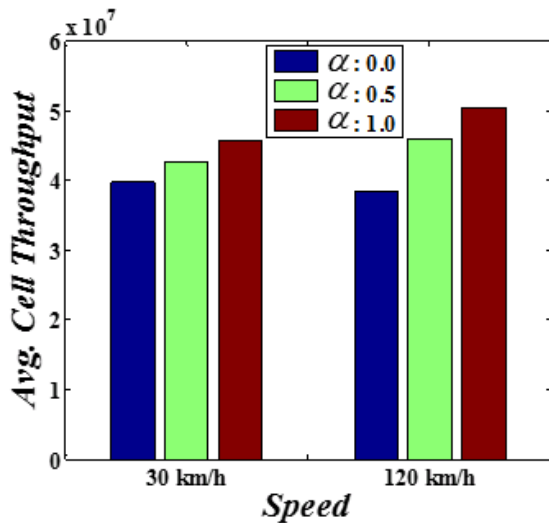
5.4 Performance Evaluation

Simulation results are provided to demonstrate the performance of the proposed interworking system. During the simulation, the LTE simulator [79] is employed, which is an open source simulator for LTE network. The radius of an eNodeB is 0.5 km and three eNodeBs are installed. The UEs are randomly located in each eNodeB, and their average moving speed are set to 30 km/h and 120 km/h according to a random waypoint model. Each UE requests only one video streaming service to video content server during the simulation. Each eNodeB allocates 100 RB per downlink for video streaming services. The carrier frequency is 2 GHz and the bandwidth for the downlink is 20 MHz. The symbol for TTI, subframe length, subcarriers per RB, and subcarrier spacing are 14, 1 ms, 12, and 15 kHz, respectively. The frame structure is FDD (Frequency Division Duplex) and wireless channel models are set to ITU Vehicular A. B_{target}^{fr} , a_{adt} , b_{adt} , $F(t_{\Delta})$, α_n , β_n , and T_{RSS} are set to 50 frame, 5, 0.5, 0.6, 5, 300, and 3.7881 dB, respectively. The scene freezing interval per video clip [80,81] is used as QoE performance metric. It is a video frame rebuffering time until certain amount of video frames when video buffer underflow occur. The average cell throughput, the number of admitted UEs, and the number of handover requests are used as QoS performance metric. The video metadata information is extracted from FLV (FLash Video) video format using FLVTool2 [82]. The duration of video clip, average data rate, F_{FPS} , and T_{Init} are 120 sec, 2,030,187 bps, 25 fps, and 2 sec, respectively. The total simulation time is fixed to 300 sec.

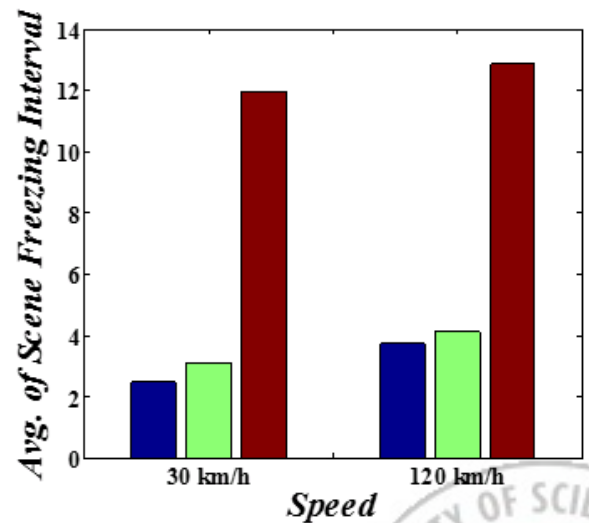


5.4.1 Performance Verification of the Proposed Packet Scheduling Algorithm and Comparison with Existing Algorithms in Single Cell

First of all, we investigate the influence of the weighting factor in Eq. 5-5 without call admission control. The total number of UEs is set to 150. It is clearly observed in Figure 5-4 (a) that the average cell throughput increases as α becomes larger because the proposed packet scheduling algorithm is more focusing on the improving network utilization by selecting UEs with better wireless link conditions. However, as α increases, the average and the variance of scene freezing interval increase as shown in Figure 5-4 (b) and (c). Although mobility speed is changing, almost similar phenomenon is observed as shown in the Figure 5-4. Overall, by adjusting the weighting factor α , the proposed scheduling algorithm can achieve an effective tradeoff between the average cell throughput and the average and variance of scene freezing interval.

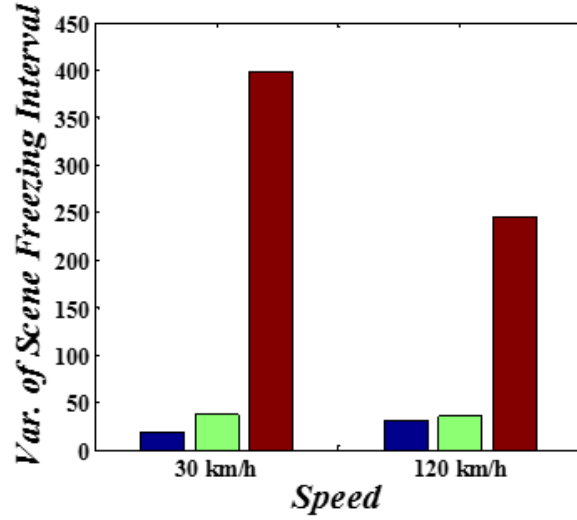


(a)



(b)

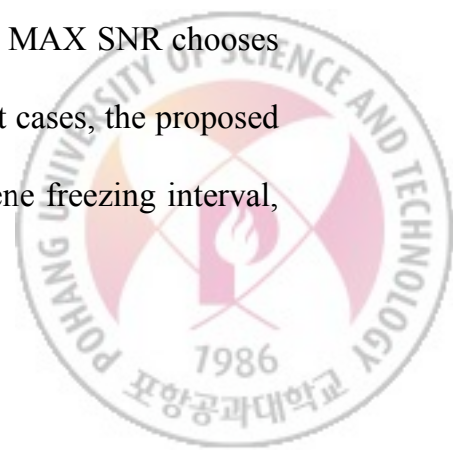




(c)

Figure 5-4 The performance comparison respect to α : (a) average cell throughput, (b) average of scene freezing interval, and (c) variance of scene freezing interval.

Table 5-1 presents the performance comparison with existing packet scheduling algorithms according to the number of UEs in single cell without call admission control: ① MAX SNR (select the UE with the strongest SNR), ② PF, ③ MLWDF, ④ EXP, and ⑤ QAS, and Figure 5-5 illustrates the corresponding bar graphs. Figure 5-5 (a), (c), and (e) present the performance when the speed is 30 km/h, and Figure 5-5 (b), (d), and (f) show the performance when the speed is 120 km/h. The proposed packet scheduling is examined when α was adjusted according to Eq. 5-9. As clearly seen in Table 5-1 and Figure 5-5, the average cell throughput of the proposed scheduling algorithm is larger than those of the existing algorithms except for the MAX SNR because the MAX SNR chooses only the UE based on the best wireless link state. Furthermore, in most cases, the proposed scheduling algorithm achieves the lowest average and variance of scene freezing interval,



which means that the proposed scheduling system provides better QoE of video streaming services. Exceptionally, the variance of scene freezing interval of the MLWDF represents the best performance when the number of UEs is 200 since the MLWDF performs in a round robin manner as a result of the drastically increasing queueing delay in the cell that does not support the required QoE. On the other hand, as the number of UEs increases, the EXP exhibits even worse performance than one of the MAX SNR since it is excessively trying to keep the queueing delay of all admitted UEs below the target delay. When the number of UEs is small, the average and variance of scene freezing interval of the QAS are smaller than those of the PF. However, as the number of UEs becomes larger, the QAS and the PF achieve approximately identical values for the average and variance of scene freezing interval because the cell is heavily overloaded. Even when there are changes in velocity, almost the same phenomena is observed in terms of average and variance of scene freezing interval.



Table 5-1 The summary of performance comparison with existing methods according to the number of UEs in single cell: (a) when speed is 30 km/h and (b) when speed is 120 km/h.

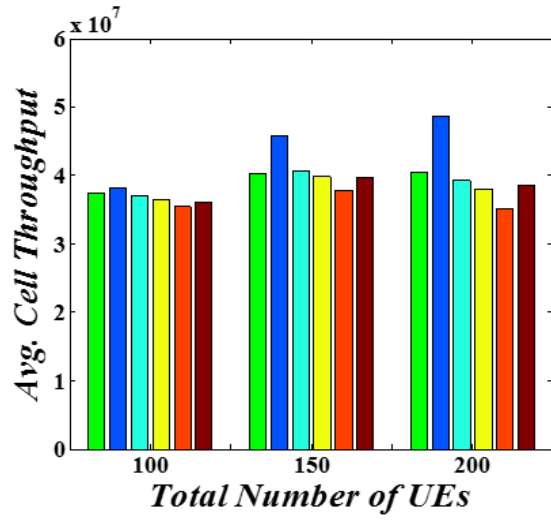
<i>Method</i>	<i>Avg. Cell Throughput [Byte/sec]</i>			<i>Avg. of Scene Freezing Interval [sec]</i>			<i>Var. of Scene Freezing Interval</i>		
	<i>100 UEs</i>	<i>150 UEs</i>	<i>200 UEs</i>	<i>100 UEs</i>	<i>150 UEs</i>	<i>200 UEs</i>	<i>100 UEs</i>	<i>150 UEs</i>	<i>200 UEs</i>
Proposed Scheduling Algorithm	37337866	40269035	40428800	0.000	2.136	10.199	0.000	15.860	238.846
MAX SNR	38116000	45698635	48633333	9.356	11.963	19.190	236.116	397.994	659.145
PF	37155733	40509458	39222400	0.448	2.967	10.959	1.704	27.230	195.323
MLWDF	36527733	39748658	38014933	2.603	5.899	12.809	12.024	25.834	103.079
EXP	35477600	37796235	35162666	6.825	12.794	21.542	58.351	144.028	331.212
QAS	36028266	39688282	38609866	0.282	2.730	10.912	0.926	22.601	189.866

(a)

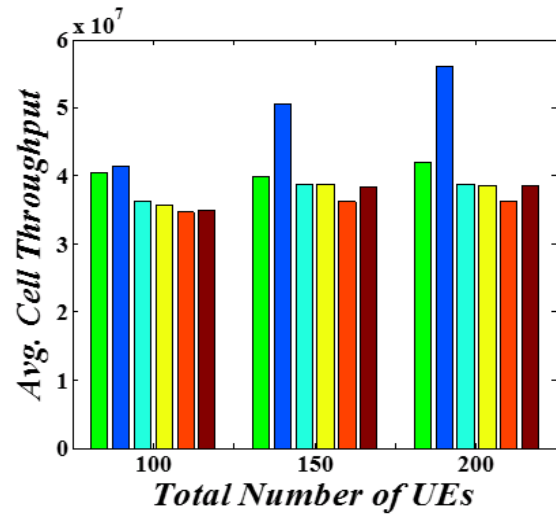
<i>Method</i>	<i>Avg. Cell Throughput [Byte/sec]</i>			<i>Avg. of Scene Freezing Interval [sec]</i>			<i>Var. of Scene Freezing Interval</i>		
	<i>100 UEs</i>	<i>150 UEs</i>	<i>200 UEs</i>	<i>100 UEs</i>	<i>150 UEs</i>	<i>200 UEs</i>	<i>100 UEs</i>	<i>150 UEs</i>	<i>200 UEs</i>
Proposed Scheduling Algorithm	40448266	39852705	41996266	0.007	2.934	13.918	0.005	21.966	364.631
MAX SNR	41390400	50451294	56144266	7.534	12.870	19.526	124.361	244.961	491.166
PF	36141600	38680235	38784800	0.198	3.624	15.684	0.630	29.725	388.001
MLWDF	35724533	38783294	38622400	3.284	7.072	15.486	11.281	39.815	169.301
EXP	34569866	36197035	36182933	8.699	15.456	23.716	68.782	204.686	418.423
QAS	34887733	38296564	38459733	0.019	3.574	15.640	0.019	30.615	385.467

(b)

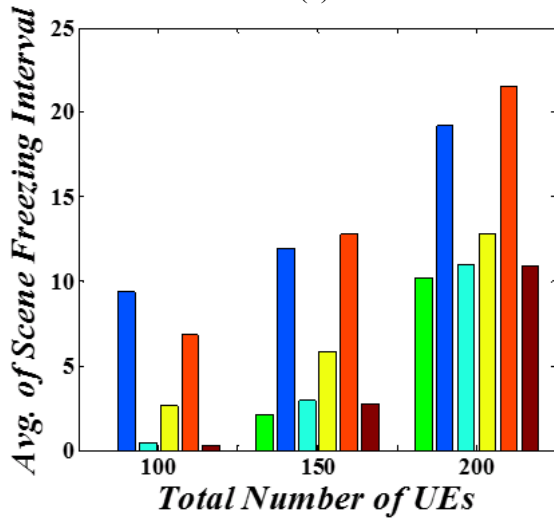




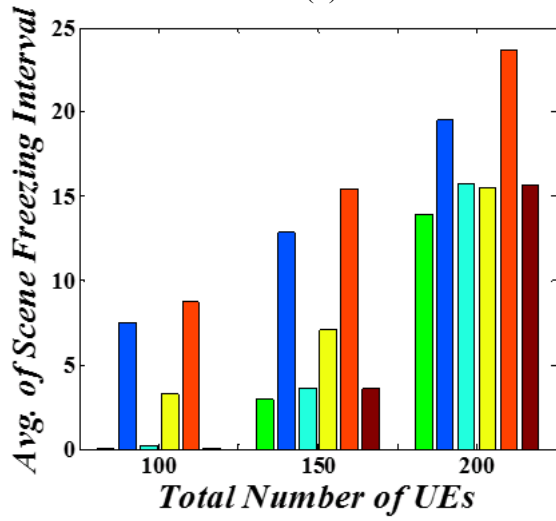
(a)



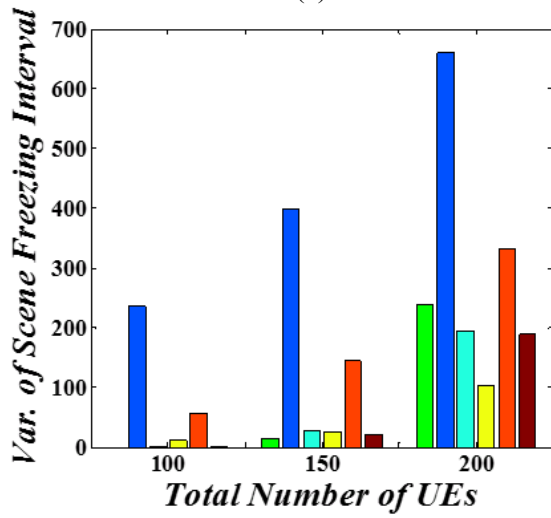
(b)



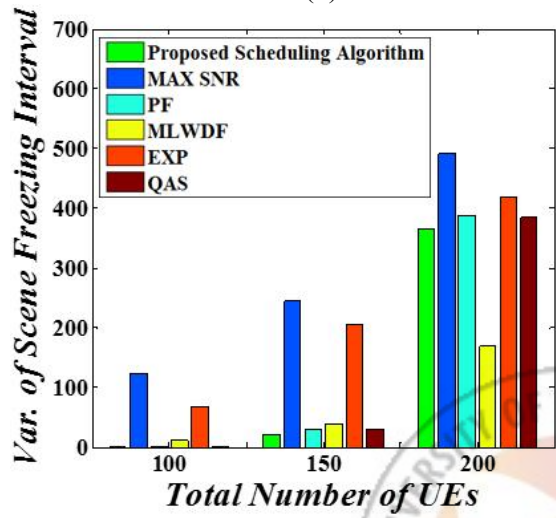
(c)



(d)



(e)



(f)

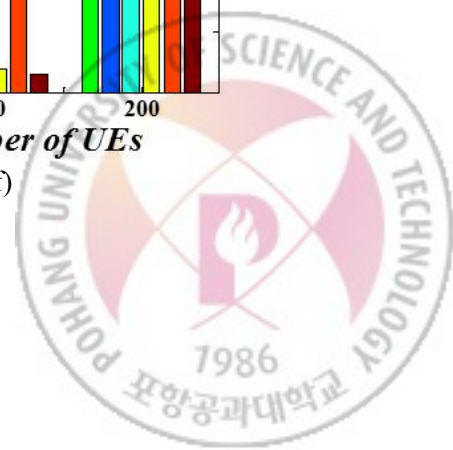
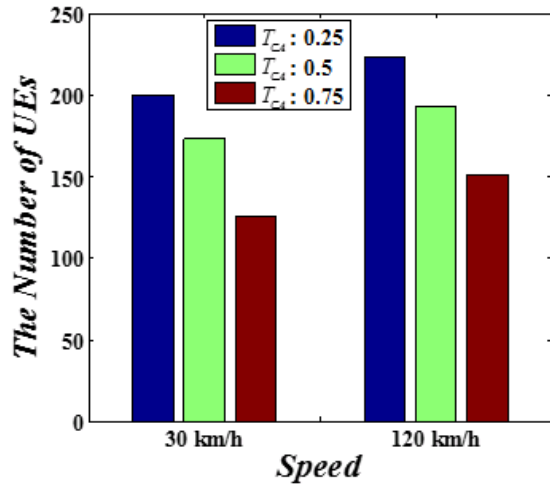


Figure 5-5 The performance comparison with existing methods according to the number of UEs in single cell : (a) average cell throughput when the speed is 30 km/h, (b) average cell throughput when the speed is 120 km/h, (c) average of scene freezing interval when the speed is 30 km/h, (d) average of scene freezing interval when the speed is 120 km/h, (e) variance of scene freezing interval when the speed is 30 km/h, and (f) variance of scene freezing interval when the speed is 120 km/h.

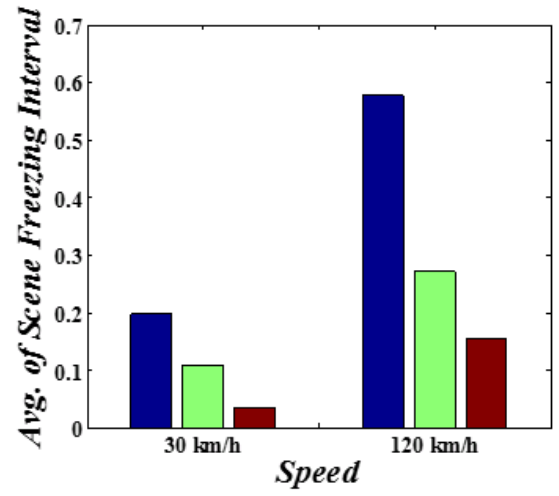
5.4.2 Performance Verification of the Proposed Call Admission Control and Handover Algorithms

First, we examine the performance of the proposed call admission control algorithm according to T_{CA} . Simulation results in terms of T_{CA} are presented in Figure 5-6. As T_{CA} becomes larger from 0.25 to 0.75, the proposed call admission control algorithm admits the smaller number of UEs because it accommodates a new call only when existing UEs have more buffered video frames. Hence, the QoE state in a cell tend to be improved as T_{CA} approaches to 1, that is, the average and the variance of scene freezing interval are decreased as shown in Figure 5-6 (b) and (c). It is also observed that more UEs are admitted at the cost of the increased average and variance of scene freezing interval as the mobility of UEs is increasing.

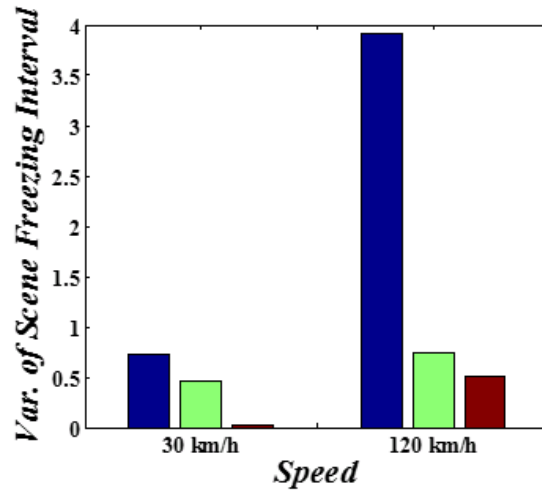




(a)



(b)



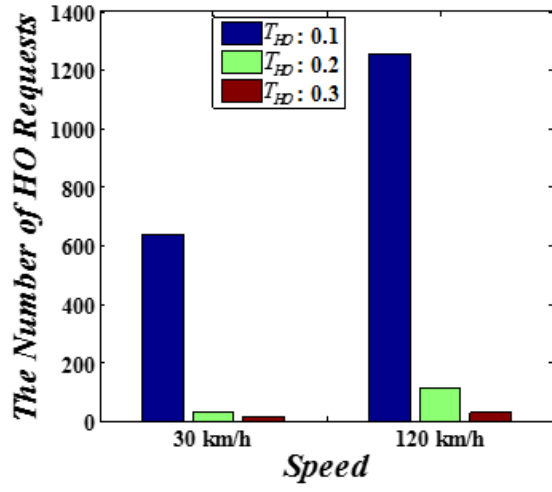
(c)

Figure 5-6 The performance comparison with respect to T_{CA} : (a) the number of UEs, (b) average of scene freezing interval, and (c) variance of scene freezing interval.

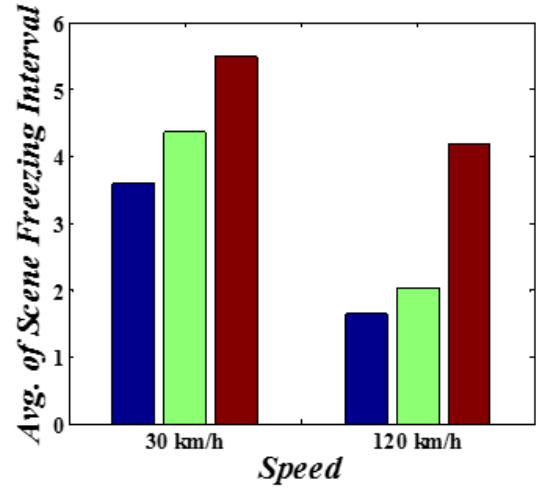


Secondly, the performance of the proposed handover algorithm is investigated. Figure 5-7 shows the performance of the proposed handover algorithm in terms of T_{HO} without call admission control. During this simulation, the number of UEs is set to 275 and T_{HO} is changing from 0.1 to 0.3. When T_{HO} is 0.1, the handover triggers occur very frequently as shown in Figure 5-7 (a) as a result of the ping-pong effect on the cell boundary. However, these frequent handover triggers on the cell boundary keep a balance of the QoE states among the adjacent cells. Thus, the average and the variance of scene freezing interval are decreased. On the other hand, as T_{HO} increases, the number of handover requests is reduced. However, the average and the variance of scene freezing interval become worse. When the speed is increasing to 120 km/h, the similar phenomenon is observed, i.e. both the average and the variance of scene freezing interval are decreased due to the effective load balancing caused by more frequent handover triggers.

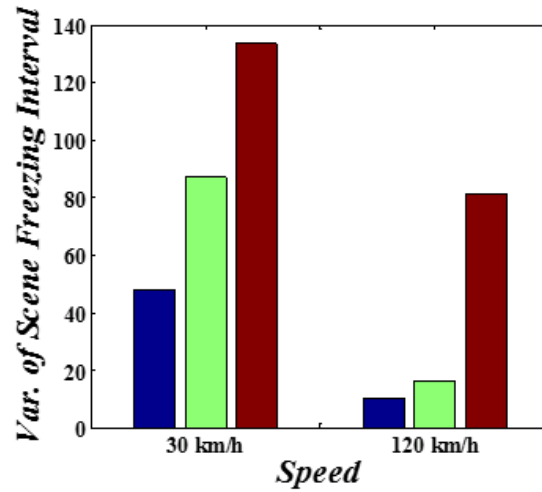




(a)



(b)



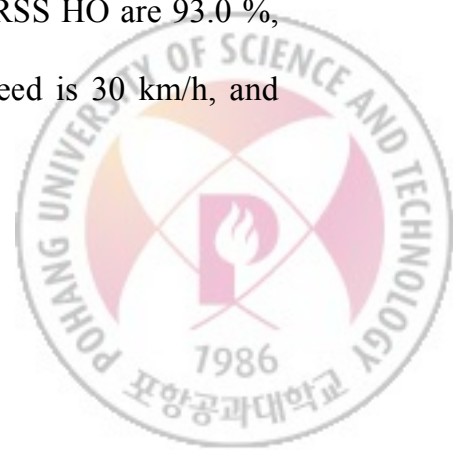
(c)

Figure 5-7 The performance comparison with respect to T_{HO} : (a) the number of handover requests, (b) average of scene freezing interval, and (c) variance of scene freezing interval.

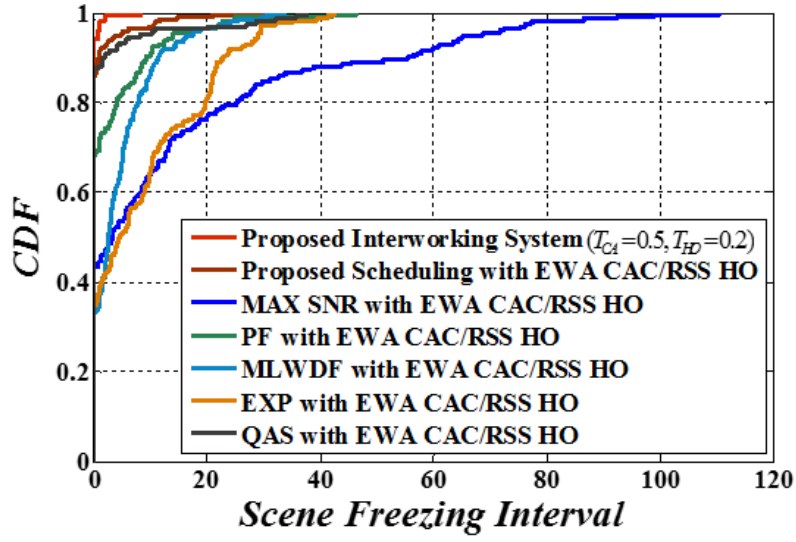


5.4.3 Performance Comparison with Existing Algorithms in Multiple Cells

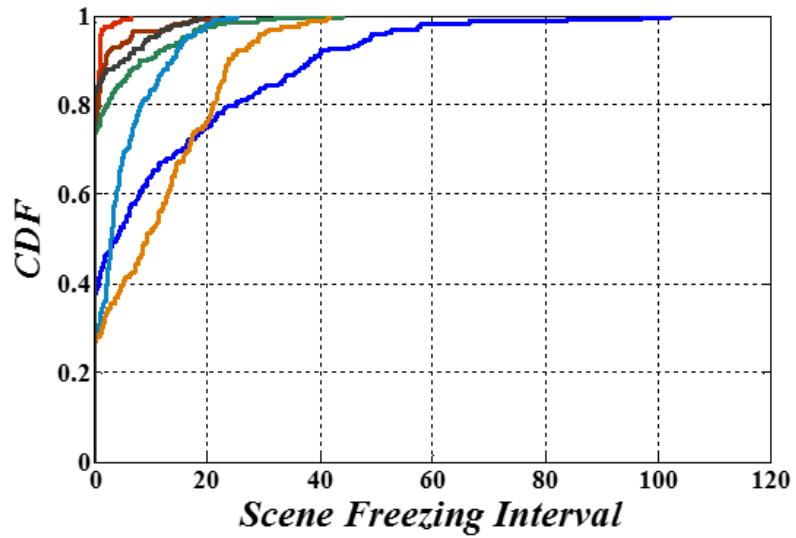
In this section, we compare the proposed interworking system with five other methods in terms of the average, the variance, and the maximum of scene freezing interval, average cell throughput, and the number of admitted UEs in multiple cells: ①MAX SNR with EWA CAC/RSS HO (i.e. call admission control algorithm admits a new call when the available cell capacity estimated from exponential weighted average is larger than the required cell capacity, handover algorithm conducts handover trigger when the received signal strength of target eNodeB is larger than one of current serving eNodeB), ②PF with EWA CAC/RSS HO, ③MLWDF with EWA CAC/RSS HO, ④EXP with EWA CAC/RSS HO, and ⑤QAS with EWA CAC/RSS HO. To compare the performance in multiple cells, T_{CA} and T_{HO} are set to 0.5 and 0.2, respectively. Figure 5-8 shows the cumulative distribution curves of the scene freezing interval. It is clearly observed in the figure that the proposed interworking system provides seamless video streaming services to more UEs compared to the other systems regardless of the mobility of UEs. The percentage of UEs not experiencing frozen scenes in cases of the proposed interworking system, the proposed scheduling with EWA CAC/ RSS HO, the MAX SNR with EWA CAC/ RSS HO, the PF with EWA CAC/ RSS HO, the MLWDF with EWA CAC/ RSS HO, the EXP with EWA CAC/ RSS HO, and the QAE with EWA CAC/ RSS HO are 93.0 %, 85.9 %, 43.4 %, 68.1 %, 33.0 %, 33.9 %, and 86.9 % when the speed is 30 km/h, and



decrease to 81.3 %, 76.0 %, 37.4 %, 73.4 %, 28.7 %, 27.2 %, and 82.8% when the speed is 120 km/h, respectively.

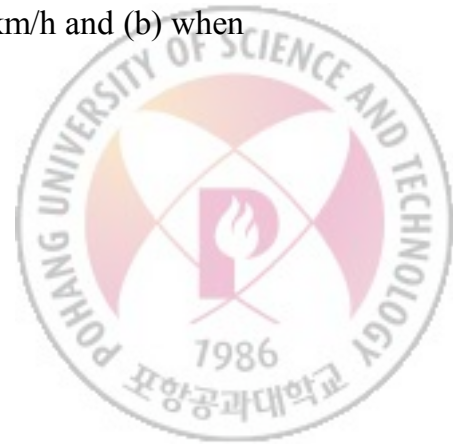


(a)



(b)

Figure 5-8 CDF of scene freezing interval: (a) when speed is 30 km/h and (b) when speed is 120 km/h.



The performance comparison is summarized in Table 5-2. The proposed interworking system significantly reduces the average, variance, and maximum of scene freezing interval while more UEs are accepted in the cells. To dynamically maintain QoE of all admitted UEs, average cell throughput is a little decreased compared to the MAX SNR with EWA CAC/RSS HO. The MAX SNR with EWA CAC/RSS HO shows the worst performance aspect of the scene freezing interval due to only considering wireless link states of UEs. In particular, the maximum of scene freezing interval is considerably large value caused by wireless resource starvation on UEs with worse wireless link states. However be caused by high average cell throughput, the number of admitted UEs is much bigger than other methods. Since the MLWDF with EWA CAC/RSS HO provides QoS fairness to all admitted UEs using the queueing delay in the eNodeB, the variance and maximum of scene freezing interval are smaller than those of the PF with EWA CAC/RSS HO. The QAS with EWA CAC/RSS HO achieves a substantially higher scene freezing interval than other existing methods, because this method directly considers QoE satisfaction of all admitted UEs.



Table 5-2 The summary of performance comparison with existing methods in multiple cells:

(a) when speed is 30 km/h and (b) when speed is 120 km/h.

<i>Method</i>	<i>Scene Freezing Interval</i> [sec]			<i>Avg. Cell Throughput</i> [Byte/sec]	# of Admitted UEs
	<i>Avg.</i>	<i>Var.</i>	<i>Max</i>		
Proposed Interworking System with $T_{CA} = 0.5$ and $T_{HO} = 0.2$	0.108	0.466	8.320	38723893	173
Proposed Scheduling with EWA CAC/RSS HO	0.776	10.963	31.080	36123128	192
MAX SNR with EWA CAC/RSS HO	14.125	501.861	110.342	44311893	235
PF with EWA CAC/RSS HO	2.792	41.937	46.337	38497724	198
MLWDF with EWA CAC/RSS HO	4.588	36.624	33.640	35347911	200
EXP with EWA CAC/RSS HO	8.737	104.213	42.280	30404124	174
QAS with EWA CAC/RSS HO	1.478	34.404	37.600	34303235	168

(a)



<i>Method</i>	<i>Scene Freezing Interval</i> [sec]			<i>Avg. Cell Throughput</i> [Byte/sec]	# of Admitted UEs
	<i>Avg.</i>	<i>Var.</i>	<i>Max</i>		
Proposed Interworking System with $T_{CA} = 0.5$ and $T_{HO} = 0.2$	0.272	0.747	6.480	43500693	193
Proposed Scheduling with EWA CAC/RSS HO	1.020	10.887	21.730	38413013	192
MAX SNR with EWA CAC/RSS HO	12.518	328.294	102.017	47937600	243
PF with EWA CAC/RSS HO	2.387	36.753	43.998	39431857	207
MLWDF with EWA CAC/RSS HO	4.790	30.646	25.290	37974168	205
EXP with EWA CAC/RSS HO	10.892	106.614	41.840	30385528	169
QAS with EWA CAC/RSS HO	1.242	12.640	19.178	36385955	186

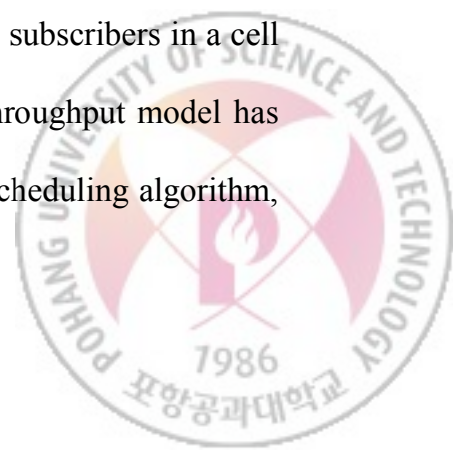
(b)



VI. Conclusions

In this dissertation, we proposed three cross-layer designed systems to improve quality of video streaming service over various wireless networks including MANETs, WiMAX network, and LTE network. First, we have proposed urgency-based joint working packet scheduling and routing algorithms that effectively support delay-sensitive data transmission over multi-rate MANETs. Basically, packet urgency, node urgency, and route urgency have been defined on the basis of the end-to-end delay requirement. Effective tightly coupled packet scheduling and routing algorithms have been designed based on these metrics. The experimental results have shown that the proposed joint working algorithms provide better service for delay-sensitive data transmission over multi-rate MANETs than the other methods, by distributing the traffic load over the entire network and effectively controlling the packets accumulated in the buffer of each node.

Second, we have proposed a novel joint working scheduling algorithm and call admission algorithm to provide stable video streaming service to more subscribers in a cell over WiMAX network. A measurement-based local linear network throughput model has been derived in terms of a control parameter of the proposed packet scheduling algorithm,



and it was demonstrated by simulation results that the proposed model can trace real network throughput accurately. Also we have shown that the proposed packet scheduling algorithm can satisfy the scene freezing rate constraint with the proposed λ adjustment algorithm. Finally, the proposed video streaming system has shown much better performance than other existing algorithms in terms of the average scene freezing rate and the number of supportable subscribers.

Third, we have proposed a QoE-based interworking packet scheduling, call admission control, and handover system to support smooth video streaming services over LET network. The proposed packet scheduling algorithm has designed in consideration of both the QoE states and the wireless link states of all admitted UEs. Based on the cell availability metric of the eNodeB, the call admission control algorithm and the handover algorithm determine a permission for new calls and a proper handover trigger, respectively. The experimental results have presented that the proposed interworking system is able to improve the QoE states of all admitted UEs and the network utilization in a cell simultaneously better than any other existing method in terms of scene freezing interval, cell throughput, and the number of admitted UEs.



요 약 문

무선 망에서 안정적인 영상 스트리밍 서비스를 위한 효과적인 크로스레이어 설계

무선 통신 기술은 다양한 모바일 데이터 서비스를 제공하기 위해 빠르게 발전되어 왔다. 셀룰러 링크의 속도는 광 대역에서의 동적인 스펙트럼 할당 정책을 이용하여 3G 망에서 2 Mbps 로 향상되었고, LTE 및 WiMAX 와 같은 4G 망에서는 최대 100 Mbps 를 제공한다. 이와 비슷하게 WiFi 망에서의 링크 속도 역시 300 Mbps 까지 향상되었다. 한편, iOS 및 안드로이드 기반의 스마트 디바이스의 증가에 따라 모바일 데이터 서비스는 폭넓게 이용되고 있으며, 모바일 영상 스트리밍 서비스는 전체 모바일 트래픽의 상당 부분을 차지하고 있다. 무선 통신 기술이 높은 데이터 전송 속도를 제공함에도 불구하고, 무선 망 환경에서 높은 품질의 모바일 데이터 서비스를 제공하는 것은 여전히 도전적인 과제이다. 특히, 다른 모바일 데이터 서비스에 비해 높은 데이터량을



요구하는 영상 스트리밍 서비스를 무선 망에서 끊김 없이 제공하는 것은 더 힘든 일이다. 게다가 영상 데이터가 가지는 엄격한 시간 제약 사항과 영상 압축에 따른 가변 데이터량은 상황을 더욱 악화시킨다.

본 학위 논문에서는 위와 같은 문제를 해결하기 위해 크로스레이어 기법을 적용하였다. WiFi, WiMAX, 및 LTE 와 같은 다양한 무선 환경에서 안정적인 영상 스트리밍 서비스를 제공하는 크로스레이어 설계를 제안한다. 첫 번째는 이동 애드 혹 네트워크상에서 지연에 민감한 영상 데이터를 효과적으로 전송하기 위한 크로스레이어 기반 패킷 스케줄링 및 라우팅 기법을 제안한다. 먼저 패킷 긴급도, 노드 긴급도, 및 경로 긴급도를 각 패킷의 종단 간 지연 요구사항을 고려하여 정의한다. 제안하는 기법은 긴급도 척도를 기반으로 MAC 계층에서의 패킷 스케줄링 기법과 네트워크 계층에서의 라우팅 기법이 긴밀하게 결합되어 이동 애드 혹 네트워크상에서 지연에 민감한 영상 전송 성능을 향상시킨다.

두 번째는 WiMAX 망에서 영상 스트리밍 서비스를 위한 패킷 스케줄링과 호 수락제어의 협력 연계 시스템을 제안한다. 패킷 스케줄링은 각 유저의 영상 버퍼 상태와 무선 링크의 신호세기를 고려하여 무선 자원을 할당하고, 셀의 이용률과 영상 서비스의 QoE 상태를 동시에 고려하여 제어 파라미터를 동적으로 결정한다. 호 수락제어에서는 패킷 스케줄링의 제어 파라미터를



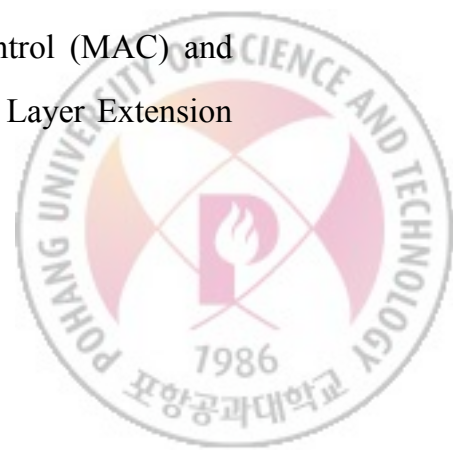
측정 기반 국소 선형 모델에 적용하여 WiMAX 셀의 이용 가능 용량을 예측하여 유저의 호 승인 여부를 결정한다.

마지막으로 멀티 셀 기반의 LTE 망에서 끊임 없는 영상 스트리밍 서비스 제공을 위해 QoE 상태 기반의 패킷 스케줄링, 호수락 제어, 및 핸드 오버 알고리즘의 상호 연동 시스템을 제안한다. 우선 UE QoE 상태, 셀 QoE 상태, 및 셀 가용성을 UE 들의 영상 버퍼 상태와 요구되는 QoE 제약 사항을 고려하여 정의 한다. 각 알고리즘은 QoE 상태 척도를 이용하여 상호 긴밀하게 연동되어 안정적으로 모든 UE 에게 영상 스트리밍 서비스를 원활하게 제공한다.



REFERENCES

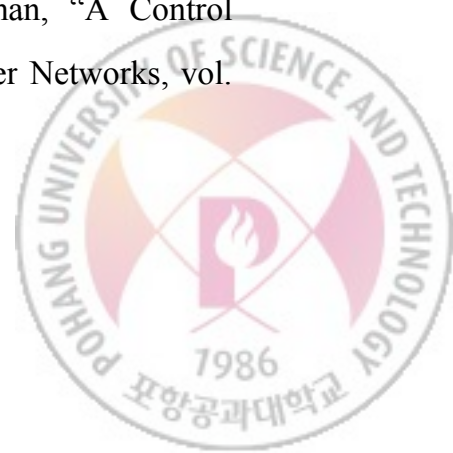
1. 3GPP TR 25.913, "Requirements for evolved UTRA (E-UTRA) and evolved UTRAN (E-UTRAN)," ver. 7.3.0.
2. 3GPP TS 36.300, "Evolved Universal Terrestrial Radio Access (E-UTRA) and Evolved Universal Terrestrial Radio Access Network (E-UTRAN); Overall Description; Stage 2", ver. 8.7.0, December 2008.
3. IEEE standard for local and metropolitan area networks part 16 (2004). Air interface for fixed broadband wireless access systems, IEEE Std 802.16-2004 (Revision of IEEE Std 802.16-2001).
4. D. Raychaudhuri and N. Mandayam, "Frontiers of Wireless and Mobile Communications," Proceedings of the IEEE, vol. 100, no. 4, pp. 824-840, April 2012.
5. Cisco Visual Networking Index: Global Mobile Data Traffic Forecast Update, 2012–2017.
6. 802.11a-1999 High-Speed Physical Layer in the 5 GHz Band, 1999.
7. IEEE 802.11g: Further Higher Data Rate Extension in the 2.4 GHz Band, 2003.
8. IEEE 802.11e-Amendment 8: Medium Access Control (MAC) Quality of Service Enhancements, 2005.
9. IEEE 802.11n-Amendment 5: Enhancements for Higher Throughput, 2009.
10. IEEE 802.11, Part 11: Wireless LAN Medium Access Control (MAC) and Physical Layer (PHY) Specifications, 1999.
11. IEEE 802.11b, Part 11: Wireless LAN Medium Access Control (MAC) and Physical Layer (PHY) Specifications: Higher-Speed Physical Layer Extension in the 2.4 GHz Band, 1999.



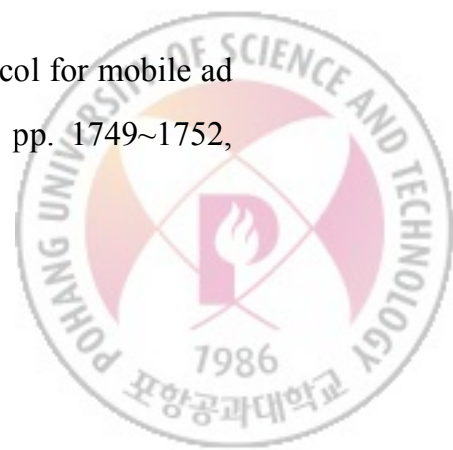
12. C. E. Perkins and P. Bhagwat, "Highly Dynamic Destination-Sequenced Distance-Vector Routing (DSDV) for Mobile Computers," *ACM SIGCOMM Computer Communication Review*, vol. 24, no. 4, pp. 234~244, October 1994.
13. T. Clausen, P. Jacquet, A. Laouiti, P. Minet, P. Muhlethaler, A. Qayyum, and L. Viennot "Optimized Link State Routing Protocol," *IETF Internet Draft*, draft-ietf-manet-olsr-07.txt, 2002.
14. C. C. Chiang, H. K. Wu, W. Liu, and M. Gerla, "Routing in Clustered Multihop Mobile Wireless Networks with Fading Channel," *IEEE Singapore International Conference on Networks (SICON)*, pp. 197~211, April 1997.
15. S. Murthy and J. J. Garcia-Luna-Aceves, "An Efficient Routing Protocol for Wireless Networks," *ACM/Baltzer Mobile Networks and Applications*, vol. 1, no. 2, pp. 183~197, 1996.
16. D. B. Johnson, D. A. Maltz, and J. Broch, "DSR: The Dynamic Source Routing Protocol for Multi-Hop Wireless Ad Hoc Networks in Ad Hoc Networking," *Addison-Wesley*, pp. 139~172, 2001.
17. C. Perkins, E. Belding-Royer, and S. Das, "Ad hoc On-demand Distance Vector (AODV) Routing," *IETF RFC 3561*, July 2002.
18. V. D. Park and M. S. Corson, "A Highly Adaptive Distributed Routing Algorithm for Mobile Wireless Networks," *IEEE International Conference on Computer Communications (INFOCOM)*, April 1997.
19. M. Jiang, J. Li, and Y. C. Tay, "Cluster Based Routing Protocol (CBRP)," *IETF MANET Working Group*, Internet-Draft, 1999.
20. M. R. Pearlman and Z. J. Hass, "Determining the Optimal Configuration for the Zone Routing Protocol," *IEEE Journal on Selected Areas in Communications*, vol. 17, no. 8, pp. 1395~1414, August 1999.



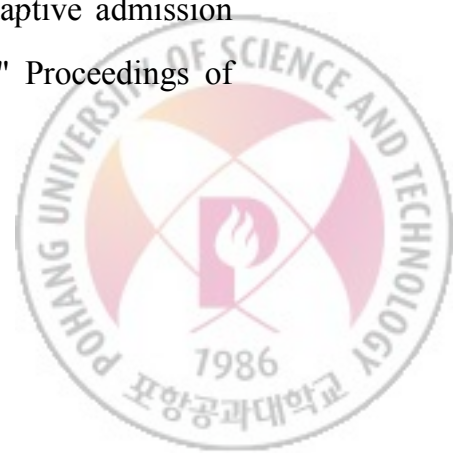
21. T. Chen, J. Walrand, and D. Messerschmitt, "Dynamic Priority Protocols for Packet Voice," *IEEE Journal on Selected Areas in Communications*, vol. 7, no. 5, pp. 632~643, June 1989.
22. C. Li and E. Knightly, "Coordinated Multihop Scheduling: A Framework for End-to-End Services," *IEEE/ACM Transactions on Networking*, vol. 10, no. 6, pp. 776~789, December 2002.
23. H. Lim, C. Lim, and J. C. Hou, "A Coordinate-Based Approach for Exploiting Temporal-Spatial Diversity in Wireless Mesh Networks," *ACM International Conference on Mobile Computing and Networking (MobiCom)*, pp. 14~25, September 2006.
24. G. Iannaccone, C. Brandauer, T. Ziegler, C. Diot, S. Fdida, and M. May, "Comparison of Tail Drop and Active Buffer Management Performance for Bulk-data and Web-like Internet Traffic," *IEEE Symposium on Computers and Communications (ISCC)*, pp. 122~129, July 2001.
25. S. Floyd and V. Jacobson, "Random Early Detection Gateways for Congestion Avoidance," *IEEE/ACM Transaction on Networking*, vol. 1, no. 4, pp. 397~413, August 1993.
26. W. Feng, K. G. Shin, D. Kandlur, and D. Saha, "The BLUE Active Buffer Management Algorithms," *IEEE/ACM Transactions on Networking*, vol. 10, no. 4, pp. 513~528, August 2002.
27. T. J. Ott, T. V. Lakshman, and L. H. Wong, "SRED: Stabilized RED," *IEEE International Conference on Computer Communications (INFOCOM)*, pp. 1346~1355, March 1999.
28. J. Aweya, M. Ouellette, D. Y. Montuno, and A. Chapman, "A Control Theoretic Approach to Active Buffer Management," *Computer Networks*, vol. 36, pp. 203~235, July 2001.



29. T. Elbatt and A. Ephremides, "Joint Scheduling and Power Control for Wireless Ad-hoc Networks," IEEE International Conference on Computer Communications (INFOCOM), pp. 976~984, 2002.
30. L. Chen and W. Heinzelman, "QoS-aware Routing Based on Bandwidth Estimation for Mobile Ad hoc Networks," IEEE Journal on Selected Areas in Communications, vol. 23, no. 3, pp. 561~572, March 2005.
31. B. Liang and M. Dong, "Packet Prioritization in Multi-hop Latency Aware Scheduling for Delay Constrained Communication," IEEE Journal on Selected Areas in Communications, vol. 25, no. 4, pp. 819~830, May 2007.
32. H. Wu, X. Wang, Y. Liu, Q. Zhang, and Z. Zhang, "SoftMAC: Layer 2.5 MAC for VoIP Support in Multi-hop Wireless Networks," IEEE Communications Society Conference on Sensor, Mesh and Ad Hoc Communications and Networks (SECON), September 2005.
33. G. Holland, N. Vaidya, and P. Bahl, "A Rate-Adaptive MAC Protocol for Multi-Hop Wireless Networks," ACM International Conference on Mobile Computing and Networking (MobiCom), July 2001.
34. B. Sadeghi, V. Kanodia, A. Sabharwal, and E. Knightly, "OAR: An Opportunistic Auto-Rate Media Access Protocol for Ad Hoc Networks," ACM International Conference on Mobile Computing and Networking (MobiCom), September 2002.
35. Z. Ji, Y. Yang, J. Zhou, M. Takai, and R. Bagrodia, "Exploiting Medium Access Diversity in Rate Adaptive Wireless LANs," ACM International Conference on Mobile Computing and Networking (MobiCom), pp. 345~359, September 2004.
36. Y. Seok, J. Park, and Y. Choi, "Multi-rate aware routing protocol for mobile ad hoc networks," In IEEE Vehicular Technology Conference, pp. 1749~1752, Spring 2003.



37. Z. Fan, "High throughput reactive routing in multi-rate ad hoc networks," *Electronics Letters*, vol. 40, issue. 25, pp. 1591~1592, 2004.
38. A. Jalali, R. Padovani R. and Pankaj, "Data throughput of CDMA-HDR a high efficiency-high data rate personal communication wireless system," *Proceedings of IEEE Vehicular Technology Conference*, March 2000.
39. M. Andrews, K. Kumaran, K. Ramanan, and A. Stolyar,, "Providing quality of service over a shared wireless link," *IEEE Communications Magazine*, vol. 39, no. 2, pp. 150~153, 2001.
40. S. Shakkottai and A.L. Stolyar, "Scheduling algorithms for a mixture of real-time and non-real-time data in HDR," *Bell Labs, Tech. Rep*, 2001.
41. C.G Kang, T.W. Kim, and J.H. Kim, "Adaptive delay threshold-based priority queueing scheme with opportunistic packet scheduling for integrated service in mobile broadband wireless access systems," *IEEE Communications Letters*, vol. 12, no. 4, pp. 241~243, 2008.
42. D. Niyato and E. Hossain, "Call admission control for QoS provisioning in 4G wireless networks: issues and approaches," *IEEE Network*, vol. 19, issue 5, pp. 5~11, September 2005.
43. D. Niyato and E. Hossain, "Connection admission control algorithms for OFDM wireless networks," *Proceedings of IEEE GLOBECOM*, November 2005.
44. S. S. Jeong, J.A. Han, and W.S. Jeon, "Adaptive connection admission control scheme for high data rate mobile networks," *Proceedings of IEEE Vehicular Technology Conference*, September 2005.
45. K. H. Sohn, J. Kim, T. S. Kim, Y. Young, and J. Seo, "Adaptive admission control algorithm for multiuser OFDMA wireless networks," *Proceedings of IEEE INFOCOM*, April 2006.



46. Y. Ge and G. S. Kuo, "An Efficient Admission Control Scheme for Adaptive Multimedia Services in IEEE 802.16e Networks," Proceedings of IEEE Vehicular Technology Conference, September 2006.
47. J. Y. Lee and K. B. Kim, "Statistical connection admission control for mobile WiMAX systems," Proceedings of IEEE Wireless Communications and Networking Conference, March 2008.
48. M. Qian, Y. Huang, J. Shi, Y. Yuan, and L. Tian, "A Novel Radio Admission Control Scheme for Multiclass Services in LTE Systems," Proceedings of IEEE GLOBECOM, November 2009.
49. D. Aziz and R. Sigle, "Improvement of LTE Handover Performance through Interference Coordination," Proceedings of Vehicular Technology Conference, April 2009.
50. T. Jansen, I.-M. Balan, I. Moerman, and T. Kurner, "Handover parameter optimization in LTE self-organizing networks," Proceedings of IEEE Vehicular Technology Conference, September 2010.
51. P. Legg, G. Hui, and J. Johansson, "A Simulation Study of LTE Intra-Frequency Handover Performance," Proceedings of Vehicular Technology Conference, September 2010.
52. K. Kitagawa, T. Komine, T. Yamamoto, and S. Konishi, "A handover optimization algorithm with mobility robustness for lte systems," Proceedings of Personal Indoor and Mobile Radio Communications, September 2011.
53. A. Lobinger, S. Stefanski, T. Jansen, and I. Balan, "Coordinating Handover Parameter Optimization and Load Balancing in LTE Self-Optimizing Networks," Proceedings of Vehicular Technology Conference, May 2011.
54. P. Munoz, R. Barco, and L. de la Bandera, "On the Potential of Handover Parameter Optimization for Self-Organizing Networks," IEEE Transactions on Vehicular Technology, vol. 62, issue 5, pp. 1895~1905, June 2013.



55. E. Haghani, S. Parekh, D. Calin, E. Kim, and N. Ansari, "A Quality-Driven Cross-Layer Solution for MPEG Video Streaming Over WiMAX Networks," *IEEE Transactions on Multimedia*, vol. 11, issue 6, pp. 1140~1147, October 2009.
56. S. Deb, S. Jaiswal, and K. Nagaraj, "Real-Time Video Multicast in WiMAX Networks," *IEEE INFOCOM*, pp. 13~18, April 2008.
57. W.S. Jeon and D.G. Jeong, "Combined Connection Admission Control and Packet Transmission Scheduling for Mobile Internet Services," *IEEE Transactions on Vehicular Technology*, vol. 55, no. 5, pp. 1582~1593, September 2006.
58. J. Navarro-Ortiz, P. Ameigeiras, J.M. Lopez-Soler, and J. Lorca-Hernando, "A QoE-Aware Scheduler for HTTP Progressive Video in OFDMA Systems," *IEEE Communications Letters*, vol. 17, no. 4, pp. 677~680, April 2013.
59. S. Karachontzitis, T. Dagiuklas, and L. Dounis, "Novel cross-layer scheme for video transmission over LTE-based wireless systems," *Proceedings of IEEE International Conference on Multimedia and Expo*, July 2011.
60. S. Ryu, B. Ryu, H. Seo, and M. Shin, "Urgency and Efficiency based Packet Scheduling Algorithm for OFDMA Wireless System," *IEEE International Conference on Communications (ICC)*, pp. 2779~2785, May 2005.
61. L. Huang and T. H. Lai, "On the Scalability of IEEE 802.11 Ad Hoc Networks," *ACM International Symposium on Mobile Ad Hoc Networking & Computing*, Lausanne, Switzerland, pp. 173~182, June 2002.
62. T. H. Lai and D. Zhou, "Efficient and scalable IEEE 802.11 Ad-Hoc-Mode Timing Synchronization Function," *International Conference on Advanced Information Networking and Applications*, pp. 318~323, March 2003.



63. J. P. Sheu, C. M. Chao, W. K. Hu, and C. W. Sun "A Clock Synchronization Algorithm for Multihop Wireless Ad Hoc," *Wireless Personal Communications*, vol. 43, no. 2, pp. 185~200, 2007.
64. G. Holland, N. Vaidya, and P. Bahl, "A rate-adaptive MAC protocol for multi-hop wireless networks," *International Conference on Mobile Computing and Networking*, pp. 236~251, August 2001.
65. G. Bianchi and I. Tinnirello, "Kalman filter estimation of the number of competing Terminals in an IEEE 802.11 network," *Annual Joint Conference of the IEEE Computer and Communications*, pp. 844~852, April 2003.
66. S. Ekelin, M. Nilsson, E. Hartikainen, A. Johnsson, J. E. Mangs, B. Melander, and M. Bjorkman, "Realtime measurement of end-to-end available bandwidth using Kalman filtering," *IEEE/IFIP Network Operations and Management Symposium (NOMS)*, pp.73~84, April 2006.
67. M. M. Carvalho, J. J. Garcia-Luna-Aceves. "Delay analysis IEEE 802.11 in single-hop networks," *IEEE International Conference on Network Protocols*, Atlanta, GA, USA, November 2003.
68. NS-2 [Online]. Available: <http://www.isi.edu/nsnam/ns/index.html/>.
69. Joint Video Team (JVT) reference software, version 15.1. [Online]. Available: <http://iphome.hhi.de/suehring/tml/>.
70. E.W. Knightly and H. Zhang, "D-BIND: An accurate smoothing algorithm model for providing QoS guarantee to VBR traffic," *IEEE/ACM Transactions on Networking*, vol. 5, no. 2, pp. 219~231, April 1997.
71. A.M. Adas, "Using adaptive linear prediction to support real-time VBR video under RCBR network service model," *IEEE/ACM Transactions on Networking*, vol. 6, no. 5, pp. 635~644, October 1998.



72. M.M. Krunz and A.M. Ramasamy, "The correlation structure for a class of scene-based video model and its impact on the dimensioning of video buffers," IEEE Transactions on Multimedia, vol. 2, no. 1, pp. 27~36, March 2000.
73. J. Beran, R. Sherman, M.S. Taqqu, and W. Willinger, "Long-range dependence in variable bit rate video traffic," IEEE Transactions on Communications, vol. 43, no. 2/3/4, pp. 1566~1579, February 1995.
74. H. Song, "A metadata-based video-on-demand transmission scheme over bandwidth renegotiating network," IEICE Transactions on Communications, vol. E87-B, no. 5, pp. 1373~1381, May 2004.
75. J. Chen, C.-C. Wang, F. C.-D. Tsai, C.-W. Chang, S.-S. Liu, J. Guo, W.-J. Lien, J.-H. Sum and C.-H. Hung, "The design and implementation of WiMAX module for ns-2 simulator," Workshop on ns-2: the IP network simulator, Pisa, Italy, October 2006.
76. The video trace file; <http://trace.eas.asu.edu/h264/>
77. V. Frost and B. Melamed, "Traffic modeling for telecommunications networks," IEEE Communications Magazine, vol. 32, no. 3, pp. 70~81, March 1994.
78. F. E. Bustamante and Y. Qiao, "Friendships that last: peer lifespan and its role in P2P protocols," International Workshop on Web Content Caching and Distribution, pp. 233~246, 2004.
79. G. Piro, L. A. Grieco, G. Boggia, F. Capozzi, and P. Camarda, "Simulating LTE Cellular Systems: an Open Source Framework," IEEE Transactions on Vehicular Technology, vol. 60, no. 2, pp. 498~513, February 2011.
80. T. Porter and X. Peng, "An objective approach for measuring video playback quality in lossy networks using TCP," IEEE Communication Letters, vol. 15, pp. 76~78, January 2011.



81. R. Mok, E. Chan, and R. Chang, "Measuring the quality of experience of HTTP video streaming," Proceedings of IFIP/IEEE International Symposium on Integrated Network Management, May 2011.
82. Inlet Media Corporation. FLVTool2 – flash video and meta data manipulation.
Available: <http://www.inlet-media.de/flvtool2/>.



Curriculum Vitae

Name: **Wan Kim**

Education

2003.3~2007.8	Department of Computer Science and Engineering, Hongik University (B.S.)
2008.3~2015.2	Department of Computer Science and Engineering, POSTECH (Ph.D.)



Involved Projects

March 2008 ~ February 2009

Research on Multimedia Transmission and Multiple Antenna Transmission Systems based on Cross-layer Design for Wireless Mobile Communications (무선 이동통신에서 cross-layer 디자인을 기반한 멀티미디어 전송 기술 및 다중 안테나 전송기법 개발), Korea Science and Engineering Foundation (한국과학재단), Republic of Korea.

March 2008 ~ February 2010

Research on Transmission Protocol for Wireless Multimedia Application (무선 멀티미디어 응용을 위한 전송 프로토콜 연구), KAIST and Ministry of Information and Communication (정보통신부), Republic of Korea.

July 2008 ~ December 2008

Implement on Simulation Model based on 802.15.4a for Location Tracking (802.15.4a 기반 위치인식을 위한 시뮬레이션 모델개발), Daegu Gyeongbuk Institute of Science & Technology (대구경북과학기술연구원), Republic of Korea.

July 2008 ~ December 2011

Next generation Network & Services research under CENNS (Center for Next generation Network & Services research) (차세대 네트워크 서비스 연구센터), Ministry of Knowledge Economy (지식경제부), Republic of Korea.



August 2008 ~ July 2009

The study of high-quality video phone service system (고화질 영상 전화 서비스 시스템에 대한 연구), LG Electronics Inc. (LG 전자), Republic of Korea.

December 2008 ~ August 2013

IT Convergence for Ubiquitous Autonomic Systems (유비쿼터스 오토노믹 시스템을 위한 IT 융합 연구) under World Class University (WCU), Ministry of Education, Science and Technology (교육과학기술부), Republic of Korea.

March 2009 ~ February 2012

PC-based Platform Development and its Operation for Dynamic Service Composition (동적 서비스제어를 위한 PC 기반 플랫폼 구축 및 운용 기술 개발): FIRST@PC (Future Internet Research for Sustainable Testbed based on PC), Ministry of Knowledge Economy (지식경제부) & Korea Communications Commission (방송통신위원회), Republic of Korea.

March 2010 ~ February 2011

Research of Fountain Code-based Video Transmission System over Wireless Networks (무선망에서 파운틴 코드 기반의 영상 전송 시스템에 관한 연구), POSTECH Information Research Laboratories (정보통신연구소), Republic of Korea.

July 2010 ~ November 2010

The research of the media transmission technology supporting QoS/QoE over convergence network (유무선 통합망 환경에서 QoS/QoE 를 지원하는 미디어 전송 기술 연구),



Electronics and Telecommunication Research Institute (한국전자통신연구원), Republic of Korea.

March 2011 ~ February 2012

Research of Combined System of Packet Scheduling and Call Admission Control and Video Streaming over WiMAX network (WiMAX 망에서 영상 전송을 위한 패킷 스케줄링과 호 수락 제어의 복합 시스템 연구), POSTECH Information Research Laboratories (정보통신연구소), Republic of Korea.

February 2011 ~ November 2011

Scalable Web Service Discovery (확장성을 고려한 웹 서비스 검색 기술 연구), SAMSUNG (삼성 전자), Republic of Korea.

July 2011 ~ November 2011

The development of AL-FEC protocol stack (AL-FEC 프로토콜 스택 개발), Electronics and Telecommunication Research Institute (한국전자통신연구원), Republic of Korea.

July 2011 ~ December 2011

The research of stable transmission technology for overlay multicast based on fountain codes (파운틴 코드 기반의 안정적인 오버레이 멀티캐스트 전송 기법 연구), Electronics and Telecommunication Research Institute (한국전자통신연구원), Republic of Korea.



April 2012 ~ November 2012

The research of the Systematic Fountain Code (Systematic Fountain Code 연구), Electronics and Telecommunication Research Institute (한국전자통신연구원), Republic of Korea.

June 2013 ~ December 2013

OpenFlow 기반 SDN 시험 인프라 확산 및 개선, National Information Society Agency (한국정보화진흥원), Republic of Korea.

June 2013 ~ May 2016

LTE 네트워크상에서 QoS 를 지원하는 모바일 동영상 스트리밍 트래픽의 스케일러블 오프로딩 시스템 설계 및 구현 방안 연구, National Research Foundation of Korea (한국연구재단), Republic of Korea.

April 2013 ~ April 2018

CCN 기반의 다차원 scalability 를 활용한 5G 이동통신 기술 연구 개발, Korea Communications Agency (한국방송통신전파진흥원), Republic of Korea.

July 2013 ~ December 2014

차세대 Mobile Cloud Infra 기반 기술 연구, SAMSUNG (삼성 전자), Republic of Korea

July 2014 ~ December 2014

OF@TEIN 기반 멀티 도메인 모바일 클라우드 네트워킹 플랫폼 구축 및 실험, National Information Society Agency (한국정보화진흥원), Republic of Korea.



Publications

A) International Journal Papers

- 1) **Wan Kim** and Hwangjun Song, "QoS-aware joint working packet scheduling and call admission control for video streaming service over WiMAX network," ACM/Springer Wireless Networks , Vol. 17, No. 4, pp. 1083-1094, May 2011.
- 2) **Wan Kim**, Hyunchul Joo, Ki Jin An, Inkyu Lee, and Hwangjun Song, "Urgency-based packet scheduling and routing algorithms for delay-sensitive data over MANETs," ACM/Springer Wireless Networks, Vol. 19, No. 7, pp. 1595-1609, Oct. 2013.
- 3) **Wan Kim** and Hwangjun Song, "QoE-based Interworking Packet Scheduling, Call Admission Control, and Handover System for Video Streaming Services over LTE networks," in revision.

B) International Conference Papers

- 1) Dai-Boong Lee, **Wan Kim**, and Hwangjun Song, "An effective mobile IPTV channel control algorithm over WiMAX network," IEEE Consumer Communications & Networking Conference (CCNC) 2010.
- 2) Dongju Lee, **Wan Kim**, and Hwangjun Song, "An effective packetization algorithm of LT codes for stable video streaming over wireless network," SPIE Applications of Digital Image Processing XXXIV 2011.



- 3) **Wan Kim**, Hyunchul Joo, Kijin An, and Hwangjun Song, "A novel packet urgency metric-based cross-layer design for video streaming over multi-rate MANETs," International Wireless Communication and Mobile Computing Conference (IWCMC) 2013.
- 4) **Wan Kim** and Hwangjun Song, "A novel combined packet scheduling and call admission control for video streaming service over WiMAX network," IEEE Globecom 2010 Workshop on Multimedia Communications and Services.
- 5) S. Min, Y. Choi, N. Kim, **W. Kim**, O. Kwon, B. Kim, J. Lee, D. Kim, J. Kim, Hwangjun Song, "Implementation of a programmable service composition network using NetFPGA-based OpenFlow switches," 1st Asia NetFPGA Developers Workshop 2010.
- 6) **Wan Kim** and Hwangjun Song, "Cross layer designed handover, call admission, and scheduling for video streaming over LTE networks," in preparation.

C) Domestic Journal Papers

- 1) 이경철, **김완**, 송황준, "다중 홉 이동 애드 혹 네트워크에서 크로스레이어 기반의 효과적인 멀티미디어 전송 알고리즘," 한국통신학회 논문지, Vol. 35, No.5, pp. 474-481, 2010.
- 2) **김완**, 안기진, 주현철, 이경철, 안진웅, 손명규, 양연모, 송황준, "UWB 채널 상에서 실내 위치인식을 위한 시뮬레이터," 한국통신학회논문지, Vol. 35, No. 7, pp. 1058-1065, 2010.



- 3) 이동주, 김완, 양연모, 송황준, "무선 네트워크 환경에서 효과적인 영상 스트리밍을 위한 And-Or 트리 기반의 LT 부호화 심볼 패킷화 알고리즘," 한국통신학회 논문지, Vol. 36, No.9, pp. 749-757, 2011.
- 4) 주현철, 김완, 송황준, "WiMAX 망에서 낮은 자원 사용량을 지원하는 안정적인 이동 IPTV 시스템," 정보과학회 논문지, Vol. 39, No.6, pp. 461-467, 2012.

D) Domestic Conference Papers

- 1) 김완, 송황준, "WiMAX 망에서 비디오 스트리밍을 위한 메타 데이터 기반 패킷 스케줄링 알고리즘" 한국통신학회 (KICS 2009)
- 2) 이경철, 안기진, 주현철, 김완, 송황준, 손명규, 안진웅, "802.15.4a 기반 위치인식을 위한 시뮬레이션 모델 개발 연구" 한국통신학회 (KICS 2009)
- 3) 김완, 송황준, "WiMAX 망에서 비디오 스트리밍을 위한 패킷 스케줄링과 호 수락제어의 새로운 연계 시스템" 한국통신학회 (KICS 2010)
- 4) 이대봉, 김완, 송황준, "WiMAX 망에서 모바일 IPTV 를 위한 효과적인 채널 제어 기법" 한국통신학회 (KICS 2011)
- 5) 주현철, 김완, 송황준, "WiMAX 망에서 파운틴 코드 기반의 모바일 IPTV 시스템" 한국정보과학회 한국컴퓨터종합학술대회 (KCC 2012) (우수 논문상 수상)



Patents

A) International Patents

- 1) JAPAN: "モバイル I P T V サービスを提供する方法及びこれのためのシステム"

Application Number: 2009-197250, Receipt Date: 27-Aug-2009.

Patent Number 5006917, Receipt Date: 1-June-2012.

- 2) USA: "Mobile IPTV System and Method of Providing Mobile IPTV Service"

Application Number: 12548370, Receipt Date: 26-Aug-2009.

Patent Number: 8,223,665, Date: 17-Jul-2012.

- 3) JAPAN: "符号化シンボルのパケット化方法及びこのような方法を使用する装置"

Application Number: 2011-248963, Receipt Date: 14-Nov-2011.

- 4) USA: "Methods of Packetizing Encoded Symbol and Apparatus for Using the Same"

Application Number: 13/297,071, Receipt Date: 15-Nov-2011.

- 5) USA: " Method of Providing Mobile IPTV Service and System using the Same"

Application Number: 14/125,007, Receipt Date: 09-DEC-2013.

- 6) EUROPE: "Method of Providing a Mobile IPTV Service, and System for Executing Same"

Application Number: 12835293.7, Receipt Date: 03-DEC-2013.



7) CHINA: "提供移動 IP 電視服的方法及其系統"

Application Number: 201280034038.X, Receipt Date: 06-JAN-2014.

8) JAPAN: "モバイル I P T V サービスの提供方法及びそれを実行するシステム"

Application Number: 2014-520148, Receipt Date: 09-JAN-2014.

B) Domestic Patents

1) "모바일 I P T V 서비스를 제공하는 방법 및 이를 위한 시스템,"

등록번호: 10-2009-0070337, 등록일: 2011 년 4 월 05 일.

2) "부호화 심볼의 패킷화 방법 및 이러한 방법을 사용하는 장치",

출원번호 10-2010-0120737, 출원일: 2010 년 11 월 30 일

3) "파운틴 코드 기반 비디오 스트리밍 시스템 및 그 방법",

출원번호 10-2011-0020086, 출원일: 2011 년 03 월 07 일

4) "모바일 I P T V 서비스 제공 방법 이를 실행하는 시스템",

출원번호 10-2011-0098243, 출원일: 2011 년 09 월 28 일

